Dissertation zur Erlangung des Doktorgrades der Fakultät für Chemie und Pharmazie der Ludwig-Maximilians-Universität München

Characterization of the Cyclin Dependent Kinase Complex Bur1-2 and its Interaction with RPA

Emanuel Clausing
aus München, Deutschland
2008

Erklärung

Diese Dissertation wurde im Sinne von § 13 Abs. 3 bzw. 4 der Promotionsordung vom 29. Januar 1998 von Herrn Prof. Dr. Ralf-Peter Jansen betreut.

Ehrenwörtliche Versicherung

Diese Dissertation wurde selbstständig, ohne unerlaubte Hilfe erarbeitet.

München, den 18. November 2008

Emanuel Clausing

Dissertation eingereicht am 18. November 2008
1. Gutachter: Prof. Dr. Ralf-Peter Jansen
2. Gutachter: Prof. Dr. Karl-Peter Hopfner
Mündliche Prüfung am 18. Dezember 2008

Table of Contents

Summary

Gene expression is highly regulated and interconnected to processes like mRNP processing, mRNA export as well as to DNA repair and replication. The first step of gene expression is the transcription of protein coding genes by RNA polymerase II. Transcription is controlled by general transcription factors, the phosphorylation of the C-terminal domain of Rpb1, the largest subunit of RNA polymerase II, and chromatin modifications that allow proper accessibility of the DNA. A major player in these coupling processes is the TREX complex, coupling transcription elongation to the nucleo-cytoplasmic export of the mRNP via the nuclear pore complex. Particularly, the THO subcomplex of TREX has functions in hyperrecombination, nucleotide excision repair and transcription coupled repair.

A genetic screen with TREX components, performed to identify genes involved in these processes, lead to the identification of the cyclin dependent kinase Bur1. Bur1 and its cyclin Bur2 are needed for efficient transcription elongation by RNA polymerase II by regulating the methylation of histone tails. Interestingly, Bur1 interacts *in vivo* with RPA, a single strand DNA binding protein essential for genome stability. This biochemical interaction raised the idea of a novel interconnection between transcription, chromatin modification and genome maintenance.

Mutations in the *BUR1* as well as in the *RFA1* gene lead to sensitivity to drugs that cause DNA damage and replication or transcription stress. Deletion of the C-terminus of Bur1, which is sufficient for the binding to RPA, also renders cells sensitive to those agents. This shows the functional significance of this protein-protein interaction in the cell upon stress induction.

However, attempts to identify the DNA repair pathway Bur1 is involved in showed that mutations in *BUR1* do not behave epistatic with deletions of specific pathways. This result points to a more general, maybe regulatory role of Bur1 in the response to DNA damage. It is interesting to note that mutations in *BUR1* lead to increased genomic instability as they show the appearance of a higher amount and longer persistence of nuclear foci, DNA repair “factories” that contain, among other proteins, Rfa1 and Rad52.

Furthermore, *RFA1* mutants show decreased levels of histone H3 alone as well as lower levels of histone H3 Lysine 4 trimethylation, a mark for transcription elongation, when combined with a mutation in *BUR1*. The *RFA1* mutant is also impaired in the

expression of a β-galactosidase reporter gene, pointing to a function of RPA in transcription.

Interestingly, combining *BUR1* and *RFA1* mutants leads to a lower susceptibility of cells to stress than one of the mutations alone. On the one hand, this could be elucidated by better growth of the double mutant strains upon stress compared to the single mutants. On the other hand, whole genome expression analysis shows that the double mutant strain clusters with the *bur1* mutant whereas the *rfa1* mutant does not, showing that its expression pattern is closer to the *bur1* mutant. Both results show that the protein complexes have antagonistic roles as the combination of both mutations leads to a suppression phenotype based on differential gene expression.

Taken together, a function of Bur1 in genome maintenance could be established, as well as an effect of RPA on transcription elongation and chromatin modification. The results provide a possibility to speculate about a coupling of transcription and genome stability mediated by the interaction of Bur1-2 with RPA.

1. Introduction

Many studies have revealed molecular details in the fields of transcription regulation and DNA repair over the last years. Both processes are regulated by a sophisticated network of factors that ensure the right timing and coordination. Especially, a tight interconnection of these processes with others, that were initially thought to be discrete, could be determined.

1.1. Transcription

All information needed by the cell to live is encoded in the DNA. The enzyme transcribing all protein coding genes is RNA Polymerase II (RNApolII).

Transcription is regulated in several ways. First, the assembly and binding of general transcription factors as well as the Mediator complex control transcription initiation. The phosphorylation of the C-terminal domain (CTD) of the largest subunit of RNApolII, Rpb1, provides a second level of regulation. The C-terminal domain (CTD) of RNApolII is comprised of a number of tandem YSPTSPS repeats. (Svejstrup, 2004) Those repeats are conserved through evolution but the number of repeats changes in different eukaryotic organisms ranging form 26-27 copies in yeast, 45 in flies to 52 copies in human (Corden, 1990). The tandem repeats of the CTD can be phosphorylated on Serine 2 (S2) and Serine 5 (S5). These phosphorylations are a major source of regulation. A third mechanism of transcription regulation is achieved by covalent histone modifications, mostly ubiquitination and methylation, and chromatin remodelling that leads to the necessary accessibility of the DNA. The great level of interconnectivity between those regulatory events will be discussed in greater detail below.

1.1.2 Regulation of transcription initiation by general transcription factors

Initiation of transcription in eukaryotes is achieved by the recognition of promoter elements that form a platform for the binding of general transcription factors. (Smale and Kadonaga, 2003).

The first step is the binding of TBP, a subunit of TFIID to the TATA box, the best characterized element of the core promoter. This leads to DNA bending and serves as a nucleation site for the following factors. Afterwards, TFIIA binds and stabilizes the DNA/TBP complex. Subsequently, TFIIB contacts this complex and recruits hypo-

phosphorylated RNApolII together with TFIIF. The final assembly of TFIIE and TFIIH forms the pre-initiation complex (PIC) (Van Dyke *et al.*, 1988). TFIIH regulates the initiation of transcription in two ways. First, it unwinds the DNA using energy from the hydrolysis of ATP leading to the formation of the so called open complex. In this complex the DNA is melted forming a "transcription bubble". Second, it phosphorylates the CTD of RNApolII on S5 with its kinase subunit Kin28 leading to the clearance of the promoter and transcription initiation. This subset of factors is required for the initiation of basal transcription *in vitro* from most promoters (Woychik and Hampsey, 2002).

Another protein complex identified to be necessary is the Mediator, functioning in co-activation as well as in co-repression. Mediator can bind to specific DNA sequences as well as to the unphosphorylated CTD and fulfils its function in transcription initiation, because it dissociates from RNApolII after the CTD is phosphorylated (Max *et al.*, 2007). The Mediator subunits Srb10/Srb11 can also phosphorylate S5 of the CTD already before the assembly of the PIC and thus hinders its formation. Due to this property it also has a repressive function (Hengartner *et al.*, 1998).

Some of the general transcription factors and the Mediator complex remain bound in a scaffold complex on the promoter to allow a rapid re-initiation of transcription on a given gene (Yudkovsky *et al.*, 2000). An overview of these steps in transcription initiation is shown in Figure 1.

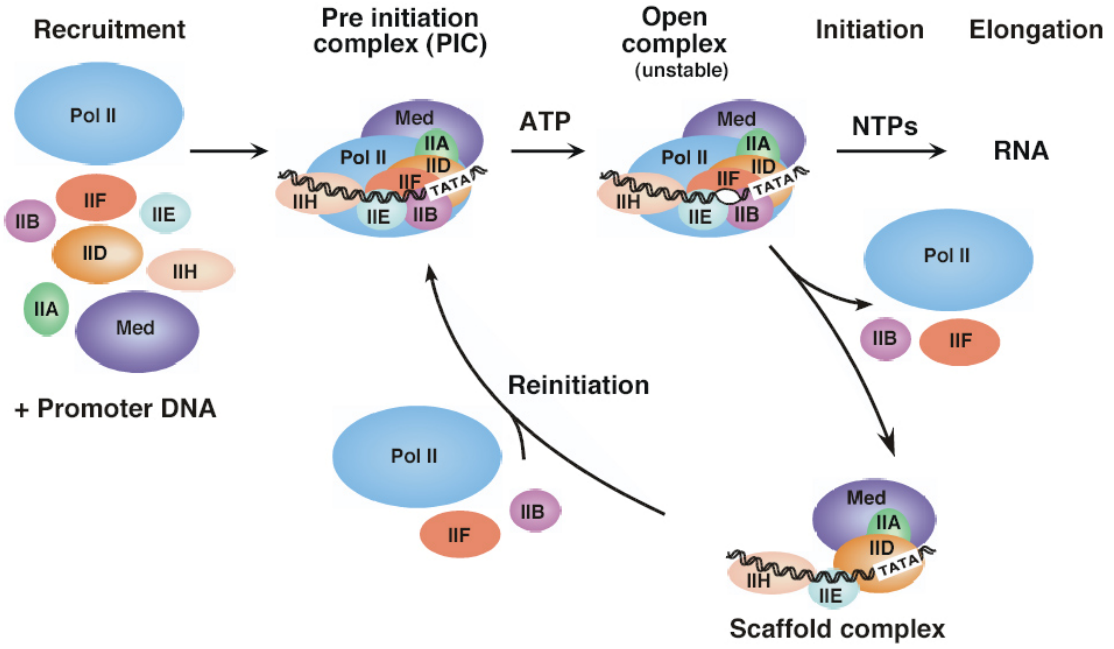

Figure 1: Transcription initiation and re-initiation by RNApolII (Hahn, 2004)

1.1.3 Transcription elongation and termination

The transition from initiation to productive elongation is facilitated by a shift from S5 to S2 phosphorylation on the CTD (Marshall *et al.*, 1996) and phosphorylation of Spt5 (Wada *et al.*, 1998), a component of the negative regulator DSIF. In human this is carried out by the positive transcription elongation factor b (P-TEFb), which consists of the cyclin dependent kinase Cdk9 and cyclin T.

Two putative Cdk9 homologs exist in *S. cerevisiae*. On the one hand the Ctk1 complex that is responsible for the S2 phosphorylation of RNApolII's CTD (Cho *et al.*, 2001) and on the other hand the Bur1-2 complex, which is most likely not involved in CTD phosphorylation but in the phosphorylation of Spt5 and regulation of chromatin modification. The phosphorylation of Spt5 is speculative and results from indirect experiments showing that Cdk9 from *S. pombe* is able to phosphorylate Spt5 and complements for the deletion of *BUR1* in *S. cerevisiae* (Pei and Shuman, 2003). The functions of the Bur1-2 complex will be discussed later in greater detail.

Despite of these proteins, other factors like TFIIS or the PAF complex are recruited to the ORF during transcription elongation (Pokholok *et al.*, 2002).

After transcription is terminated (Gilmour and Fan, 2008) the CTD becomes dephosphorylated on S2 by Fcp1 (Cho *et al.*, 2001; Hausmann and Shuman, 2002) and on S5 by Ssu72 (Dichtl *et al.*, 2002; Krishnamurthy *et al.*, 2004) and is recycled for another round of transcription.

Figure 2 gives an overview about the whole "transcription cycle" from initiation to elongation and termination as reviewed in (Egloff and Murphy, 2008; Prelich, 2002).

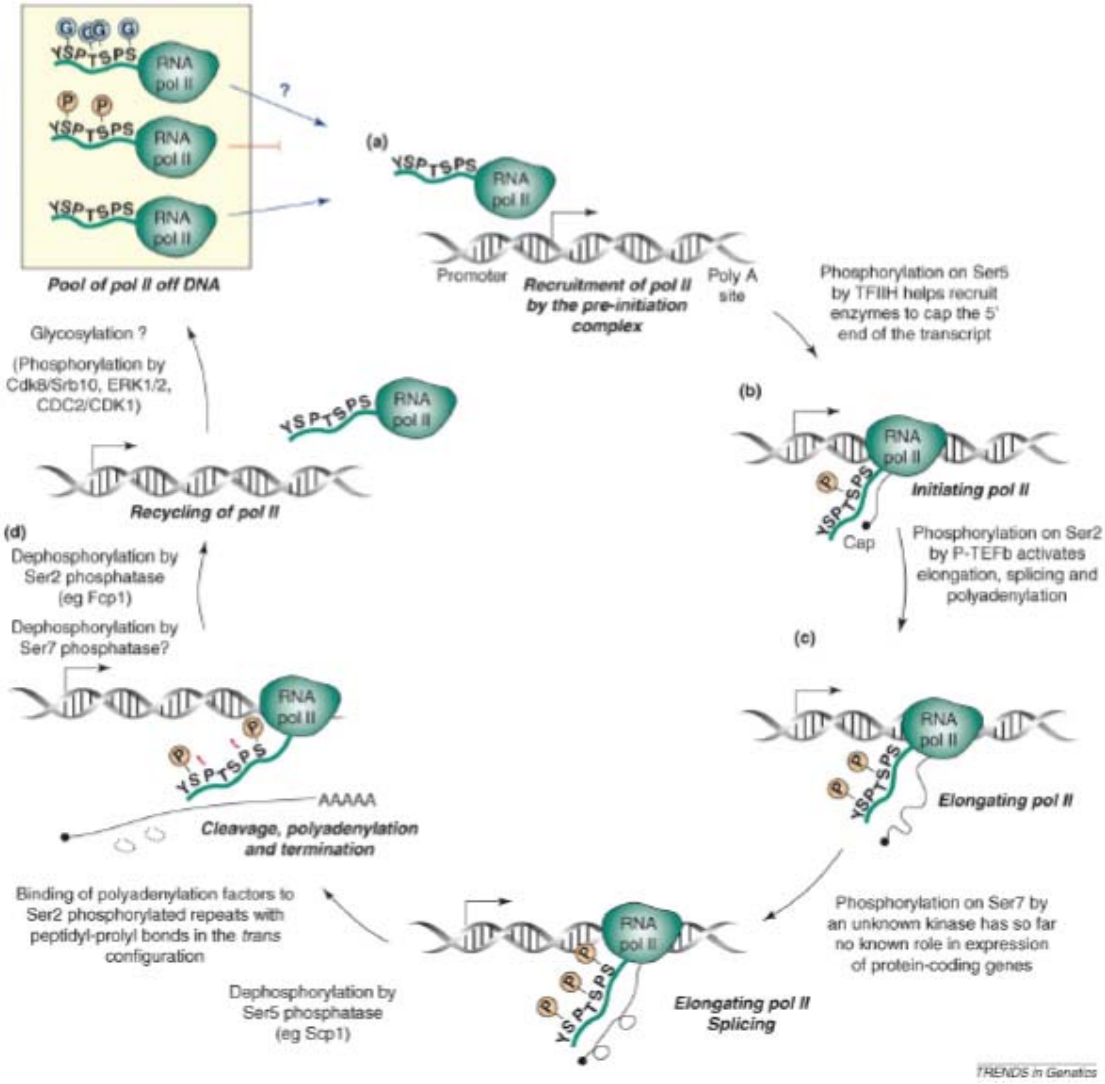

Figure 2: The eukaryotic mRNA transcription cycle and interconnection to other processes. (Egloff and Murphy, 2008)

1.1.4 Transcription associated chromatin modifications in yeast

Transcription, especially transcription elongation, is regulated by a defined landscape of histone modifications. This is most likely a consequence of RNApolII moving through the gene and recruiting various chromatin modifying enzymes. An overview of these modifications is shown in Figure 3.

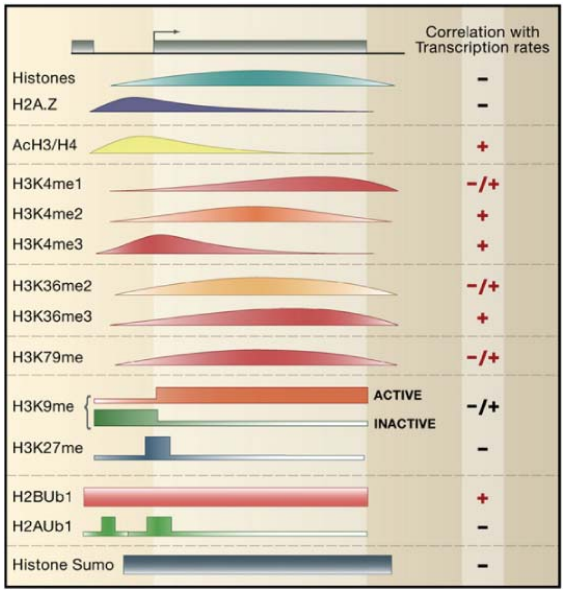

Figure 3: Distribution of histone modifications from a transcriptional point of view (Li *et al.*, 2007).

The curves represent the distribution based on genome-wide approaches. Except for H3K9me, H3K27me and H2Aub1, most data were obtained in yeast.

1.1.4.1 Histone H2B ubiquitination

Histone H2B monoubiquitination (H2Bub) is facilitated by Rad6 in *S. cerevisiae* on Serine 123 of histone H2B (Robzyk *et al.*, 2000). The E3 ubiquitin ligase Bre1, is associated with Rad6 to recruit it to the promoter of transcriptionally active genes. The deletion of *BRE1* also leads to elimination of H2Bub (Wood *et al.*, 2003). Additionally, the PAF complex, needed for transcription elongation, is important for the control of the ubiquitination. Deletions of *RTF1* and *PAF1* reduce the level of histone H2Bub, even though they are not needed for the recruitment of Rad6 (Wood *et al.*, 2003). Thus, it seems to regulate its activity. Deletion of *RTF1* leads to inability of Rad6 to travel with RNApolII into the open reading frame. Additional factors are also required, *e.g.* Bur1-2 when mutated, also reduce the level of ubiquitinated H2B (Laribee *et al.*, 2005). It is unclear if this is a direct effect or a consequence of the inability to recruit PAF. Kin28 loss and thus loss of S5 phosphorylation eliminates H2Bub, whereas loss of Ctk1 and thus loss of S2 has no effect. These data indicate that Rad6 and H2Bub are important in the initiation and early steps of transcription elongation.

The ubiquitination of histone H2B is a prerequisite for histone H3 methylation (Sun and Allis, 2002). Deletion of *RAD6* as well as mutation of histone H2B prevent the methylation of histone H3 on Lysine 4 and 79, catalyzed by the histone

methyltransferases Set1 and Dot1, respectively. This phenomenon is unidirectional as mutations that affect H3 modification have no effect on the ubiquitination of histone H2B. The methylation of Lysine 36 on histone H3 is not dependent on H2Bub (Briggs *et al.*, 2002).

Interestingly, there is much more histone methylation than ubiquitination in the cell. A possible explanation might be the different stability of those modifications. Methylation is supposed to be a very stable mark, whereas the ubiquitination has a very high turnover rate. This means that methylated histones most likely have been ubiquitinated before.

There are several possibilities how H2Bub facilitates the subsequent histone methylation. Either the ubiquitination leads to an unfolding of the chromatin making it possible for Set1 and Dot1 to bind, or the ubiquitination is directly recognized by these methyltransferases. Another model is based on the fact, that the PAF complex, besides its need for H2Bub, is also needed for the methylation of H3K4 and H3K79 (Krogan *et al.*, 2003a; Ng *et al.*, 2003). PAF is required for the recruitment of Set1 to the promoter which in turn leads to the H3K4 methylation. Set1 is not active until PAF activates Rad6-Bre1 to ubiquitinate H2B. H2Bub might then regulate the activity of the methyltransferases. This model would explain the identical phenotypes of *Δpaf1*, *Δrad6* and *htb1*-K123R. In the *Δpaf1* mutant H3K4 can not be methylated, because Set1 can not be recruited to chromatin, in *Δrad6* and *htb1*-K123R H3K4 can not be methylated because Set1 can not be activated.

The deubiquitination on *S. cerevisiae* is carried out by Ubp8, a component of the SAGA co-activator complex (Daniel *et al.*, 2004) Experiments have shown that a *Δubp8* mutant has elevated levels of H2Bub, both globally and at the *GAL1* promoter upon galactose activation. Ubp8 is required for the recruitment of Ctk1, the S2 phosphorylated CTD form of RNApolII and Set2 to the 5' end of the ORF (Wyce *et al.*, 2007). H2B monoubiquitination prevents Ctk1 recruitment to elongating RNApolII. This might indicate that the H2B ubiquitination serves as a checkpoint for early transcription elongation. The S2 phosphorylation also provides a binding site for Set2, the methyltransferase for H3K36, which is required for the subsequent steps in transcription elongation. As Rad6 and Ubp8 bind to elongating RNApolII there might be multiple rounds of H2B ubiquitination and deubiquitination occurring during transcription elongation (Fig. 4).

Besides the histone ubiquitination function, Rad6 has also acts in DNA repair and protein degradation pathways. Here, it makes use of different ubiquitin ligases like Rad18 (Jentsch *et al.*, 1987).

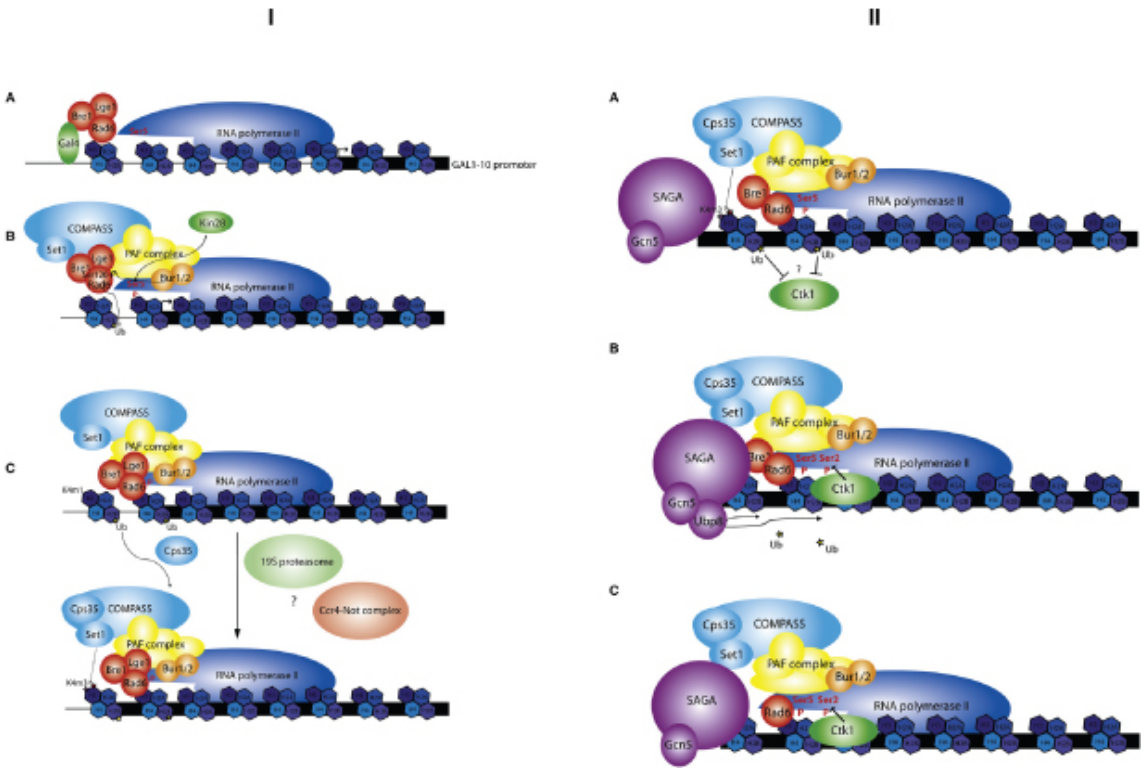

Figure 4: Histone H2B ubiquitination and deubiquitination in transcription elongation (Weake and Workman, 2008)

I. Ubiquitination of histone H2B is important for early steps in transcription initiation and elongation.

II. Deubiquitination of histone H2B is required for later steps in transcription elongation.

1.1.4.2 Histone H3 Lysine 4 methylation

One of the currently most studied histone modifications in transcription elongation is the methylation of histone H3 Lysine 4 (H3K4me). This reaction is accomplished by the Set1 (COMPASS in yeast, MLL in human) complex. The monomethylation (H3K4me) peaks to the end of the gene, the dimethylation (H3K4me2) in the middle and the trimethylation (H3K4me3) at the transcription start site (Pokholok *et al.*, 2005). Those three modifications depend on each other, meaning that the residue has to be monomethylated first before it can be di- and trimethylated. It seems like the monomethylation is achieved by the basal activity of Set1 and that the di- and trimethylation are depending on the recruitment of Set1 during transcription. Phosphorylation of S5 of RNApolII by Kin28 recruits Set1 to the 5' region of a gene

(Zhang *et al.*, 2005). As the Set1 complex is recruited mainly in the beginning of transcription the di- and trimethylation rise during early transcription elongation making monomethylation less frequent at this stage. Towards the end of the gene more monomethylation is present because it is not converted into di- or trimethylation. H2B ubiquitination specifically affects di- and trimethylation but does not eliminate monomethylation (Dehe *et al.*, 2005). Additionally, H3K4me2 and H3K4me3 depend on the association of the PAF complex with RNApolII. In a *Δpaf1* strain H3K4me2 and me3 are not detectable whereas H3K4me is. Another factor important especially for H3K4me3 is the cyclin dependent kinase Bur1. Mutations in *BUR1* reduce H2Bub but only affect H3K4me3 (Laribee *et al.*, 2005).

There are also indications that the Ccr4-Not mRNA processing complex has a function in the steps between H2B ubiquitination and H3 Lys4 methylation (Laribee *et al.*, 2007a). This complex participates both in mRNA degradation and transcription regulation as a repressive factor. Mutations in some of the components reduce trimethylation of H3 Lys4 but do not affect mono- or dimethylation or H3K79 methylation. The Not4 component has a RING domain that is required for H3K4me3 and might thus be an E3 ubiquitin ligase (Laribee *et al.*, 2007b).

Interestingly, there seems to be no direct effect of the H3K4 methylation on transcription. *In vitro*, there is no measurable impact of this modification and Set1 does not affect the processivity of RNApolII and is not essential. Thus, the function is most likely to recruit other chromatin remodelling factors but the mechanism will be a task for future research.

1.1.4.3 Histone H3 Lysine 36 methylation

The methylation of Lysine 36 on histone H3 (H3K36me) is mediated by the histone methyltransferase Set2. It associates with S2 phosphorylated RNApolII in the body of actively transcribed genes (Krogan *et al.*, 2003b). This histone mark seems to serve as a binding site for the Rpd3 complex. Rpd3 is a histone deacetylase in *S. cerevisiae* that functions as a transcriptional co-repressor via interaction with the DNA binding factor UME6 (Kadosh and Struhl, 1997, , 1998). Acetylation and deacetylation of lysine residues on histones are linked to transcriptional activation and repression, respectively. Eaf3 is a subunit of the Rpd3 complex and deletion strains show an increase in acetylation in coding regions, sometimes with a bias to the 3' end. This acetylation shows an inverted distribution to the H3K36 methylation levels. Deletions *EAF3* and *SET2* have strikingly similar phenotypes, leading to the

conclusion that H3K36 dictates the global levels of histone acetylation related to Eaf3 (Joshi and Struhl, 2005).

1.1.4.4 Histone H3 Lysine 79 methylation

Methylation of Lysine 79 is mediated by Dot1 and important for the regulation of transcriptional silencing (Ng *et al.*, 2002). On telomeres and other heterochromatin-like regions H3K79 is hypomethylated whereas it is hypermethylated in actively transcribed regions.

1.1.5 Interconnection of transcription with other processes

The process of transcription is intimately coupled to other processes in gene expression like mRNA processing and export as well as to DNA replication, recombination and repair (Orphanides and Reinberg, 2002). These processes, except for the DNA repair associated ones, are controlled by the recruitment of different factors dependent on the phosphorylation pattern of the CTD. The CTD stimulates capping, splicing and 3'-processing which is facilitated by different regions of the CTD (Fong and Bentley, 2001). The phosphorylation of S5 is required for recruiting the capping apparatus whereas 3'-end processing and splicing depend on phosphorylation of S2 (Ahn *et al.*, 2004).

Components of the TREX complex couple TRanscription to mRNA EXport (Strasser *et al.*, 2002). The TREX complex is needed for efficient transcription elongation (Chavez and Aguilera, 1997; Chavez *et al.*, 2000) (Rondon *et al.*, 2003), splicing (Kim *et al.*, 1997), and genome stability (Jimeno *et al.*, 2002). The coupling of transcription and mRNA export is mediated by the interaction of THO and Yra1 which in turn binds to the mRNA export factor Mex67-Mtr2 to transport the mature mRNP to the cytoplasm via interaction with nuclear pore proteins (Strasser and Hurt, 2000). Yra1 has also been shown to be required for S-phase entry (Swaminathan *et al.*, 2007). THO components were shown to be defective in NER (Gonzalez-Barrera *et al.*, 2002) and TCR (Gaillard *et al.*, 2007) and cause the formation of R-loops, DNA:RNA hybrids, that lead to transcription impairment and transcription associated recombination (Huertas and Aguilera, 2003; Piruat and Aguilera, 1998) (Fig. 5).

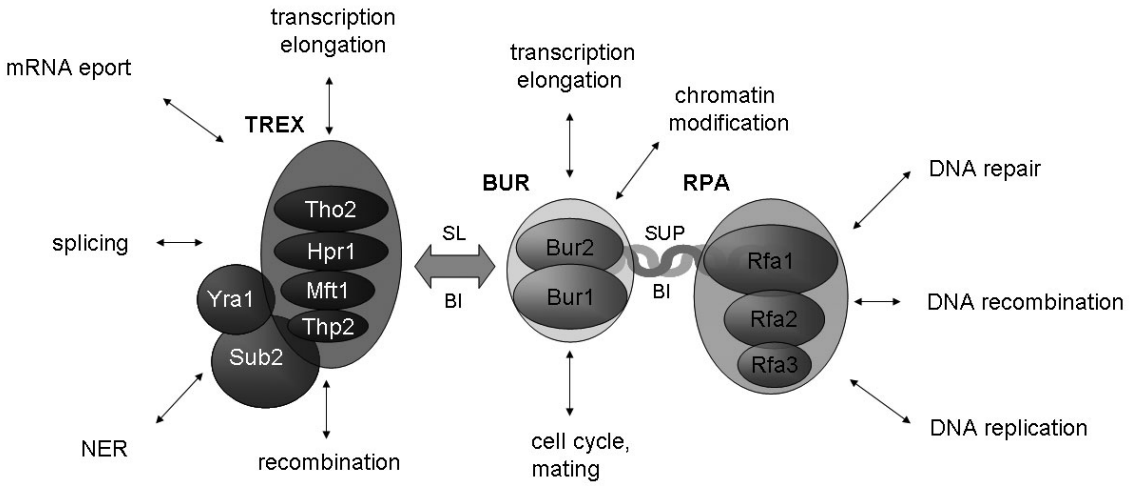

Figure 5: Interconnections and functions of TREX, BUR and RPA

The TREX complex couples transcription to mRNA export. Mutations in TREX components show phenotypes in various cellular processes like transcription elongation, mRNA export, splicing, nucleotide excision repair (NER) and transcription associated recombination. The cyclin dependent kinase/cyclin complex Bur1-2 was found to interact genetically (SL; synthetic lethality) as well as biochemically (BI; biochemical interaction) with TREX (Sträßer, unpublished data). The major function of the BUR complex is regulation of transcription elongation, most likely due to histone modification. A biochemical interaction of Bur1-2 and RPA could be established in our lab. RPA, consisting of Rfa1, Rfa2 and Rfa3, is a single strand DNA binding protein with functions in DNA repair, recombination and replication. *BUR1* and *RFA1* additionally interact genetically (SUP; suppression) pointing to antagonistic roles in the process they are involved in. These Interactions might provide a molecular explanation how these processes are coupled.

1.2. The function of Bur1-Bur2

1.2.1 Identification of Bur1-Bur2

BUR1 was first identified as a protein with an unspecific function in the release from α-factor induced G1 arrest where it suppresses the supersensitivity of a *GPA1* mutation, a heterotrimeric G-protein that binds to pheromone receptors. Due to the suppression it was called *SGV1* (suppressor of *GPA*1v50). A mutation rendering the G1 cyclin Cln3 hyperactive was able to rescue the deletion of *BUR1* indicating that it may act downstream of *BUR1* (Irie *et al.*, 1991).

The now commonly used name *BUR1* comes from a screen performed in the Prelich lab using *SUC2* deleted of its upstream activating sequence (UAS) as a reporter gene. This mutation causes cells to die on sucrose as a carbon source. Mutations able to rescue the phenotype were called the BUR genes (bypass UAS requirement).

The genes identified here are involved transcription. For example RNAPolII, general transcription factors like TBP and chromatin genes like histone H3.
Later, Bur1 was shown to be a cyclin dependent kinase and Bur2 as the corresponding cyclin (Yao *et al.*, 2000)

1.2.2 Function of Bur1-Bur2 in transcription elongation

Bur1 was shown to phosphorylate the CTD of RNApolII *in vitro* (Murray *et al.*, 2001) but *in vivo* the CTD phosphorylation does not change dependent on *BUR1,* still it is needed for efficient transcription elongation (Keogh *et al.*, 2003). It was shown that Bur1 copurifies with Ser5 phosphorylated RNApolII indicating that it binds to initiating RNApolII. It is synthetic lethal with *CTK1*, *SPT4* and *SPT5*, temperature sensitive with *DST1* and 6'-AU sensitive. All these data point to a function in transcription (Lindstrom and Hartzog, 2001; Murray *et al.*, 2001).
Bur1 itself is phosphorylated by *CAK1* (Yao and Prelich, 2002) as it is the case for other transcription associated kinases like Kin28 (Espinoza *et al.*, 1998) or Ctk1 (Ostapenko and Solomon, 2005).
Deeper insight into the function of BUR in transcription elongation comes from more recent publications showing that *Δbur2* shows a specific impairment in histone H3 Lys4 trimethylation (H3K4me3) and histone H2B ubiquitination (H2Bub) but had no effect on histone H3 Lys79 methylation (Laribee *et al.*, 2005). (This paper was the first one showing an uncoupling of the histone H3 Lys4 from the Lys79 methylation.) Rad6, an E2-ubiquitin conjugating enzyme needed for the ubiquitination of histone H2B, was identified as an *in vitro* substrate of Bur1. Mutation of the phosphorylated site on Rad6 impairs H2Bub to the same extend as deletion of *BUR2 (Wood et al., 2005)*.
As Rad6 is not fully inactivated by this mutation, the phosphorylation might just enhance its catalytic activity. Rad6 is still recruited to the promoter without *BUR2* whereas the PAF complex, which is needed for the activity of Rad6, is not. It is thus not completely clear if the impairment in H2Bub and H3K4me3 comes directly from the Bur1 complex and its phosphorylation of Rad6 or indirectly due to a failure in recruiting the PAF complex (Wood *et al.*, 2005).
The deletion of *BUR1* is suppressed by the deletion of the methyltransferase activity of Set2 or by mutation of Serine 36 on histone H3. Set2 deletion did not rescue all *BUR1* phenotypes pointing to Set2 and Bur1 having partly antagonistic but non overlapping roles. Bur1-2 is needed for transcription associated histone H3 Lys36

trimethylation. Deletions of *CHD1*, a chromodomain containing chromatin remodeler, and *EAF3*, a component of the Rpd3S deacetylation complex also containing a chromodomain, suppress the growth defect of *Δbur1* but act downstream of the H3K36 methylation showing a new connection of Bur1 and histone methylation. It seems as ifs the complete abolishment of H3K36 methylation is less harmful for the cell than a missregulation (Chu *et al.*, 2006). Also *Δrtf1* appears to suppress *Δbur1* and it was also shown that deletion of those factors restored the recruitment of RNApolII to the gene that is lowered in *Δbur2* (Keogh *et al.*, 2005). The suppression of *Δbur1* by deletion of *CHD1* and *EAF3* as well as other genes involved in this pathway was also pointed out in this publication.

Proteins containing a JmjC domain are able to reverse the di- and trimethylation of histone H3K36 and act as transcriptional repressors. H3K36 methylation in yeast acts as a docking site for Eaf3, a subunit of Rpd3S. This histone deacetylation inhibits transcription initiation on cryptic start sites within the gene. Set2/Rpd3S inhibits PolII elongation and counteracts Bur1. Jhd1 and Rph1, both containing a JmjC domain, have been shown to specifically demethylate Lys36. Both promote PolII transcription through repressive chromatin generated by Set2/Rpd3S. Overexpression of both of these proteins suppress *Δbur1* thus bypassing the requirement for Bur1 by removing the repressive Lys36 methylation. Rph1 was originally isolated as a transcriptional repressor of photolyase and is phosphorylated by Rad53 upon DNA damage suggesting that histone methylation/demethylation might somehow be linked to DNA repair (Kim and Buratowski, 2007).

1.4. DNA repair

Cells are constantly challenged with agents that lead to DNA damage. This can either be extrinsic factors, like UV irradiation, or intrinsic factors, like reactive oxygen species. It is estimated that a human cell repairs about 10000 DNA damages per cell per day. Compared to this, the actual mutation frequency is extremely low due to highly sophisticated and interconnected DNA repair mechanisms. The pathway choice is dependent on the specific kind of DNA damage.

DNA repair pathways can be divided into two major classes. The excision repair pathways and the double strand break repair pathways.

All excision repair pathways share the same principle. The first step is the recognition of the damage followed by a dual incision of the DNA backbone. The damaged site is

excised from the DNA and a new strain is synthesized on the basis of the non-damaged strand by a DNA polymerase which is then ligated again.

The nucleotide excision repair (NER) pathway is needed for the removal of damages that distort the DNA helix, *e.g.* CPDs. The NER pathway is not essential for survival but leads to several illnesses like Cockayne's syndrome or xeroderma pigmentosum (Thoma, 1999). It can be subdivided into global genomic repair (GGR) which is responsible for generally repairing the genome and transcription coupled repair (TCR), specifically repairing damage in the transcribed strand of a gene. It has been shown that UV damage is repaired faster in the transcribed strand than in the non-transcribed one (Sweder and Hanawalt, 1992). Most of the proteins needed for both of the pathways are the same just the recognition is facilitated by different proteins. Damage recognition in GGR is fulfilled by the Rad16-Rad7 complex (Guzder *et al.*, 1997) whereas Rad26 and the RNApolII subunit Rpb9 are responsible for TCR (Li and Smerdon, 2002).

Damaged bases that do not distort the DNA structure like oxidation and alkylation are repaired by the base excision repair pathway (BER). The damage is recognized by specific glycosylases like Mag1 and processed by AP endonucleases like Apn1 (Memisoglu and Samson, 2000). The glycosylase cleaves the N-glycosylic bond between the base and the sugar, producing an abasic site. Here, the backbone is cleaved and the correct base is inserted by a DNA polymerase. One can distinguish between short-path BER when only one base is excited and long-path BER where usually two to six bases are excited.

Mismatch repair (MMR) targets mismatches that either come from DNA replication, homologous recombination or alkylating agents. It is thus considered as a damage avoidance and replication fidelity pathway (Marra and Schar, 1999).

The most hazardous DNA damages for the cell are DNA double strand breaks (DBS). Two different pathways exist to repair this kind of damage: homologous recombination (HR), which is the major DSB repair pathway in yeast and non-homologous end joining (NHEJ), which is the more important one in human. The HR branch is always preferred by the cell as it always leads to error free repair. NHEJ just uses short homologies for guiding repair and joins DNA ends, which might in turn result in loss of nucleotides.

HR requires the genes of the RAD52 epistasis group (Krogh and Symington, 2004). The first event upon a DSB is phosphorylation of histone H2A (metazoan histone

H2AX) (Fillingham *et al.*, 2006). The broken ends are recognized and processed by the Mre11/Rad50/Xrs2 exonuclease complex producing a 3' ssDNA overhang which is subsequently bound by RPA. Rad52 facilitates the displacement of RPA by Rad51 which leads to a filament searching for homologous sequences. Rad55 and Rad57 initiate the strand exchange, which leads to replication of the homologous strand by a DNA polymerase and subsequent ligation.

NHEJ in yeast requires the DNA end binding proteins Ku70/Ku80 and the MRX complex. These two complexes recruit Lig4/Lif1 which in turn ligates the broken DNA ends (Shrivastav *et al.*, 2008).

1.5 Replication Protein A (RPA)

RPA has been discovered 20 years ago and the multiple functions and domains have been extensively studied until today (Iftode *et al.*, 1999; Wold, 1997).

RPA is a heterotrimeric protein complex. The subunits are named RPA1, 2, 3 or RPA70, RPA32 (sometimes also RPA34 which might be due to different migration behaviour of the middle subunit due to phosphorylation) and RPA14 in higher eukaryotes. (The yeast counterparts are called Rfa1, 2 and 3 because the abbreviation RPA was already assigned to the subunits of RNA Polymerase I). RPA binds single stranded DNA (ssDNA) with high affinity but is also able to bind double stranded DNA (dsDNA) and RNA but with approximately three orders of magnitude lower affinity. Homologous heterotrimeric ssDNA binding proteins have been found in all eukaryotes that were examined. RPA was originally shown to be essential for SV40 virus replication (Wold and Kelly, 1988) and was subsequently called "Replication Protein A" even though it has functions in DNA replication, recombination and repair and thus the "R" could also stand for recombination or repair. RPA becomes phosphorylated in the cell on its middle subunit when bound to ssDNA. It was also shown for RPA that it might have a function in transcription by binding to specific dsDNA regulatory sequences (Luche *et al.*, 1993; Singh and Samson, 1995; Tang *et al.*, 1996). The complex is very abundant and seems to be the most abundant ssDNA binding protein (estimated $3 \times 10^4 - 5 \times 10^5$ molecules per human cell). Additionally, this protein complex is very stable, *e.g.* in urea up to 6 M or guanidinium-HCL up to 2 M. The subunits are only soluble when expressed together. RPA1 alone is insoluble, RPA2 and RPA3 are soluble when expressed together.

They might form a pre-complex that is necessary for the folding of the complete complex.

1.5.1 Expression and localization

The mRNA expression of RPA peaks at the G1/S transition but the protein half-life is very long (>12 h in human cells). The cellular localization changes during the cell cycle: During G1 and G2 phase RPA is diffusely localized to the nucleus with RPA3 also detectable in the nucleolus. RPA70 seems to be associated with dsDNA in G1. During S-phase, chromosomal DNA replication occurs in a punctuate pattern, also termed replication foci or replication centers, in which 300-1000 DNA molecules and multiple proteins are aggregating to form replication factories. RPA becomes recruited to those foci before the initiation of replication and stays there also during DNA synthesis. After the completion it dissociates from chromosomes. During M-phase only RPA2 is found to associate with chromosomes, RPA3 is selectively localized to the cytoplasm. The overall ratio of all subunits stays constant during the cell cycle.

1.5.2 DNA binding

Binding of RPA to DNA under physiological conditions needs a length of 30 nucleotides. However, an 8 nucleotide binding mode has also been observed. According to the current model RPA binds first to 8 nucleotides with DNA binding domains A and B (Fig. 5) and has a more globular shape. Using additional contacts with the secondary binding domains C and D it forms an elongated conformation and binds 30 nucleotides. RPA can bind to bubbles of dsDNA as small as 4 nucleotides and yeast RPA was shown to bind up to 90-100 nucleotides building nucleosome like structures. Probably due to those two binding modes, RPA confers a helicase activity that is independent of ATP. It has been found to bind to damaged DNA, most likely due to the helix disturbance, and prefers polypyrimidines (T/C) over polypurines (A/G).

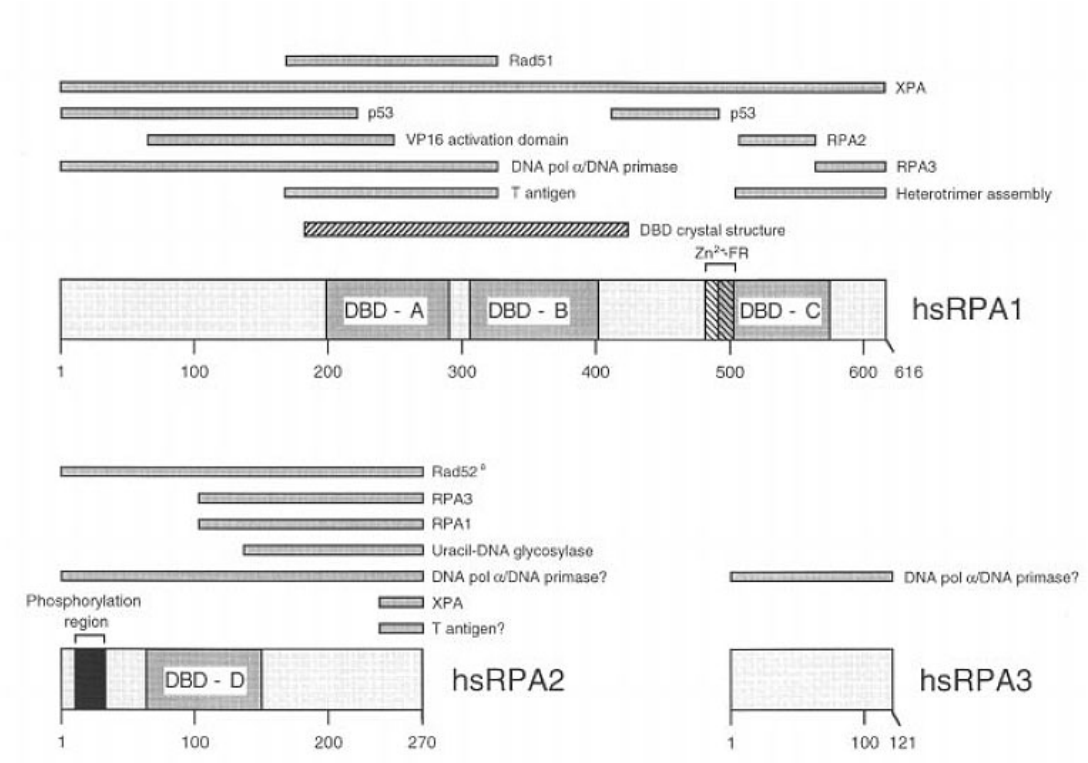

Figure 6: RPA domains and interactions with other proteins (Iftode *et al.*, 1999).

1.5.3 The RPA subunits

The biggest subunit, RPA70, has several functions. It has an intrinsic DNA binding activity, binds to numerous proteins and is essential for DNA replication, recombination and repair. Studies in yeast have shown that all residues except of the N-terminal 10 amino acids are essential. RPA70 undergoes a conformational change upon DNA binding. In the human protein the center domain contains the DNA binding domains, the N-terminal domain is needed for complex formation and the C-terminal domain is needed for protein-protein interactions (Fig. 6). The DNA binding domains are interchangeable in yeast and the domains of the human protein can substitute for the yeast counterpart, showing a high level of conservation. RPA70 contains a Zink finger domain, but its function is unknown and it is also unknown if it really binds Zink. The middle subunit, RPA32, has three domains. A secondary DNA binding domain, located in the center, phosphorylation sites that become phosphorylated in a cell cycle dependent manner but are not essential, and the C-terminus, needed for protein-protein interactions and complex assembly (Fig. 6). The phosphorylation

occurs from the G1/S transition to late mitosis. Human RPA is phosphorylated by the cyclin dependent kinase cdk2 when it is in complex with the G1 cyclins A and B but not with the G2 cyclin E. It becomes additionally hyperphosphorylated *in vivo* in response to DNA damage. Another kinase, DNA-PK, needs DNA for phosphorylating RPA32. Phosphorylation can also be achieved by the checkpoint kinase ATM and the yeast counterpart Mec1. Thus, at sites of DNA damage, recombination and during DNA repair the phosphorylation might serve to recruit other factors needed for the respective process.

The function of RPA14, besides RPA complex formation, is still mostly unknown but it seems to be important for efficient DNA binding and correct positioning of the complex (Weisshart *et al.*, 2004). Cells with a deletion of the N-terminal 70 (of 122) amino acids are still viable but temperature sensitive.

1.5.4 Functions in replication, recombination and repair

The RPA complex has roles in several DNA associated cellular processes. In DNA replication it could be involved in polymerase switching because it is involved in the synthesis of a small primer by DNA polymerase α (Pol α) before the switch to DNA polymerase δ (Pol δ). In viral DNA replication it binds to the viral origin and helps in denaturation together with the T antigen. Those factors then recruit Pol α. The stimulatory role of RPA on Pol α requires the ssDNA binding activity of RPA.

In DNA recombination and DSB repair RPA might have a function due to the binding of Rad51 and Rad52 to the RPA32 subunit. In yeast the interaction with Rad52 seems to be mediated via the whole protein with the strongest affinity to Rfa1. This function was deeply analysed and lead to a model in which a DNA DSB is first recessed to generate a 3‘-ssDNA tail that is subsequently bound by RPA. Rad52 then acts to displace RPA and facilitates binding of Rad51, leading to the formation of a filament that is able to search for homologous sequences for recombination. *In vivo,* this is thought to be much more complex because of the need for numerous other factors for foci formation (Lisby et al., 2004).

In addition, DNA repair pathways require RPA. Mismatch repair can be stopped by adding antibodies directed against RPA and adding back RPA restores it. The mechanism is still unknown (Guo *et al.*, 2006).

A function in base excision repair (BER) has been established due to the interaction with UNG (uracil-DNA-glycosylase). RPA has been shown to be stimulatory for long

patch BER by facilitating gap filling by DNA polymerase (DeMott *et al.*, 1998). Additionally, a lot of RPA mutants are MMS sensitive.

RPA is essential for nucleotide excision repair (NER). In the early stage it interacts with XPA (Rad14 in yeast), a DNA damage recognition factor, and stimulates its activity to bind to the damaged DNA. Afterwards the XPG ERCC1-XPF (Rad2, Rad10 and Rad1 in yeast) endonuclease complex is recruited to the damaged site. RPA also interacts with XPG. Finally, RPA participates in the gap filling reaction together with PCNA and DNA polymerases δ and ε.

RPA has moreover been shown to act in transcription-coupled repair. A mutant of *rfa1*, that was completely defective in GG-NER was still able to repair the transcribed strand, even though with reduced activity (Teng et al., 1998).

Additionally, RPA functions in cell cycle and checkpoint regulation due to interaction with p53.

1.5.5 Function in transcription

RPA might also have a role in regulating transcription. It has been published to bind to the URS1 sequence in yeast, a sequence that negatively regulates the activity of several metabolically regulated genes (Luche *et al.*, 1993), as well as the MAG locus, which has a repressive effect on DNA repair and metabolism genes (Singh and Samson, 1995). In other organism like sea urchin or human RPA was found to bind to the P10 site, regulating expression in early development, and the promoter of metallothionein, respectively. In the case of the metallothionein promoter it was demonstrated that higher expression of RPA inhibits its expression (Tang *et al.*, 1996).

Two recent publications (Elmayan *et al.*, 2005; Kapoor *et al.*, 2005) highlight that mutations in *RPA2* release the silencing induced by mutations in the DNA glucosylase/lyase *ROS1*. RPA and *ROS1* interact both genetically and physically. This RPA mutation furthermore leads to enhanced expression of some transposons. Neither DNA methylation nor siRNA expression is blocked by this mutation but histone H3 Lys4 trimethylation is increased whereas the Lys9 methylation is decreased in the double mutant in comparison to the *ros1* mutant, depicting a role for RPA in the maintenance of gene silencing at specific loci.

Thus, a possible role of RPA in transcription could be revealed, even though a mechanism remains elusive.

1.6. Aim of this work

Genome expression and maintenance are among the most important processes in the cell. A key player in gene expression is the TREX complex, important for transcription and the coupling to the transport of the mature mRNP to the cytoplasm. Furthermore, subunits of TREX, *HPR1* and *THO2*, function in genome maintenance. A synthetic lethal screen with TREX lead to the identification of the cyclin dependent kinase Bur1, indicating a functional overlap with the TREX complex. Bur1 is an essential protein regulating transcription by the methylation of histone tails. This kinase interacts with RPA, a protein that is essential for DNA repair, replication and recombination. This interaction might provide a molecular explanation how these processes are coupled.

Therefore, the aim of this work was the analysis of the interaction of the Bur1-2 complex with RPA and the functional characterization of both protein complexes in the cellular processes mentioned before. First, the genetic and biochemical interaction of both complexes should be investigated. One of the aims, in addition to the characterisation of the complex, was to create a Bur1 mutant unable to bind to RPA without changing the other properties of the protein, like the ability to fulfil its kinase function and to interact with other proteins. Second, a function of Bur1 in DNA repair, replication and recombination events should be identified, specifically with the aim to find the DNA repair pathway *BUR1* might be involved in. Additionally, finding a phosphorylation target of Bur1 kinase was a matter of particular interest. Third, a putative role for the RPA complex in transcription and histone methylation should be determined.

The results of this study should allow deeper insight into new functions of the Bur1-2 and RPA complexes as well as a speculation about a coupling of transcription elongation, chromatin modification and genome maintenance by a previously unknown mechanism.

2. Results

2.1. The kinase Bur1 interacts genetically with TREX

The TREX complex was shown to couple transcription to mRNA export (Strasser *et al.*, 2002). In order to identify genes with overlapping functions to TREX, a synthetic lethal (SL) screen was performed (Sträßer, unpublished data). One of the candidates indentified in the screen was the cyclin dependent kinase *BUR1*. It was found in screens with *Δhpr1* and *Δmft1*, both deletions of components of the THO complex. As the genetic interactions of BUR and TREX were not focus of this work only an example of the synthetic lethality is shown here. For testing the SL relationship of *BUR1* and *YRA1* strains that were deleted of both genes and transformed with plasmids coding for the wild type genes with addition of promoter and terminator sequences and containing a *URA3* marker. As both, *BUR1* and *YRA1*, are essential genes, this strain was subsequently transformed with plasmids carrying mutations in both, or only one of the genes as control, respectively. The wild type *URA3*-containing plasmids can be shuffled out of the cells by restreaking them on plates containing 5'-FOA and the growth behaviour caused by the mutant alleles is subsequently determined. If strains containing either wild type copies of the genes examined or single mutations grow but cells containing mutations in both of the genes die they are synthetic lethal. This phenotype can hint to a physical or functional interaction of the genes examined as the cell can compensate for mutation in one of the genes but not in both. Combination of *bur1* temperature sensitive (ts) mutants with ts mutants of *yra1* showed a SL phenotype (Fig. 7). Thus, the SL relationship of *BUR1* could be extended to another component of the TREX complex.

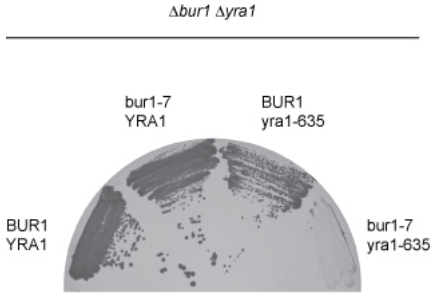

Figure 7: *BUR1* is synthetic lethal with *YRA1*

The *BUR1 YRA1* shuffle strain was transformed with plasmids coding for either wild type copies of *BUR1* or *YRA1* or mutations in one of the genes or both. Transformants were restreaked on plates containing 5'-FOA and grown for 4 days. No growth in the double mutant strains shows a synthetic lethal interaction of these *bur1* and *yra1* alleles.

2.2. Bur1-2 and RPA interact biochemically

To obtain deeper insight of the function of the Bur1-2 cyclin dependent kinase/cyclin complex, tandem affinity purifications (TAP) of Bur1-TAP and Bur2-TAP were performed to find *in vivo* interaction partners.

2.2.1 Interaction of Bur1-2 with RPA

Eluates of TAP purifications of Bur1-TAP and Bur2-TAP were analyzed by SDS PAGE, stained with Coomassie and the copurifying bands were analyzed by mass spectrometry. A stoichiometric Bur1 and Bur2 complex was obtained in both purifications. Substoichiometrically Rfa1, Rfa2 and Rfa3 as well as Rad52 could be identified as major interactors (Fig. 8 A and Sträßer, unpublished data) indicating that the Bur1-2 complex might also have a function in processes RPA is involved in. These processes could be DNA replication, recombination or repair. To also test if RPA is able to bind the BUR complex, Rfa1-TAP was purified. The untagged wt strain serves as a control for unspecific binding. Prt1 is a protein with a function in an unrelated process. It is part of the translation initiation factor eIF3 and as well serves as a control for unspecific protein binding. As the relative amount of RPA in the cell is much higher than the amount of BUR (about ten fold based on microscopy fluorescence intensity data, data not shown), only a small fraction of bound BUR complex was expected in the Rfa1-TAP purification. The BUR complex is not visible in the Coomassie staining but Western blot analysis using an antibody specific for Bur1 shows that it binds specifically to Rfa1 but is not detectable in control purifications. The second higher molecular weight band in the Rfa1- and Prt1-TAP cell extracts corresponds to the cross reaction of the secondary antibody with protein A from the TAP tag which is cleaved of for elution (Fig. 8 B).

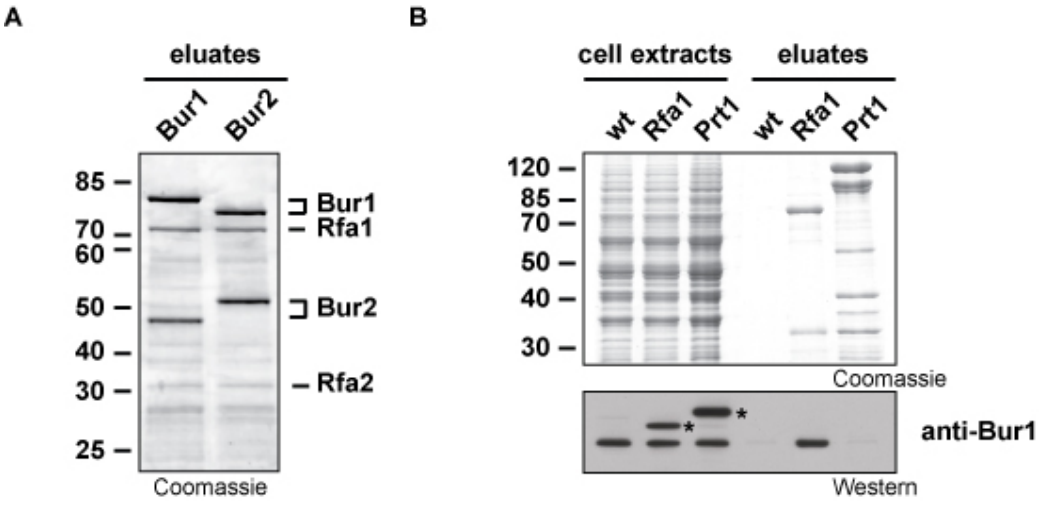

Figure 8: Bur1-2 interact biochemically with RPA

(A) Tandem affinity purifications of Bur1 and Bur2 from *S. cerevisiae*. Eluates were separated by 10% SDS PAGE and co-purifying proteins were analyzed by mass spectrometry. Bur1 and Bur2 bands are shifted to a higher molecular weight in the respective purification due to the tag. Rfa1 and Rfa2 were identified to interact with the BUR complex.

(B) TAP purification of an untagged wt strain, Rfa1-TAP and Prt1-TAP. Cell extracts and eluates were separated by 12% SDS-PAGE, blotted and probed with an antibody directed against Bur1. Bur1 copurifies specifically with Rfa1 but not with control purifications. (* The higher molecular weigh band in the cell extracts corresponds to the cross reaction of the secondary antibody with the TAP tag.)

2.2.2 The C-terminus of Bur1 is unstructured and sufficient for binding to RPA

Being interested in the interaction of the Bur1-2 and RPA complexes, the interaction was investigated in more detail. Secondary structure predictions of the Bur1 C-terminus using PSIPRED (McGuffin *et al.*, 2000) show that there is no predictable secondary structure in this part of Bur1 (Fig. 9 B). The N-terminal part of Bur1 shows homology to kinases, especially with cyclin dependent kinases (amino acids 1-365). This fragment of the protein will be referred to Bur1 kinase domain, whereas amino acids 365-657 will be referred to as Bur1 C-terminus. TAP purifications of the Bur1 kinase domain did not result in Coomassie stainable amounts of protein and Western blot analysis shows that this part of the protein is much less expressed than the C-terminal construct or full length Bur1 (data not shown). However, the C-terminus was TAP tagged, purified and shows interaction with Rfa1 and thus probably with the whole RPA complex, which was confirmed by mass spectrometry (Fig. 9 C). As expected the C-terminus did not bind to Bur2 which is consistent with other studies

showing that in cyclin dependent kinases the cyclin binds to the kinase domain to activate it (Baumli *et al.*, 2008).

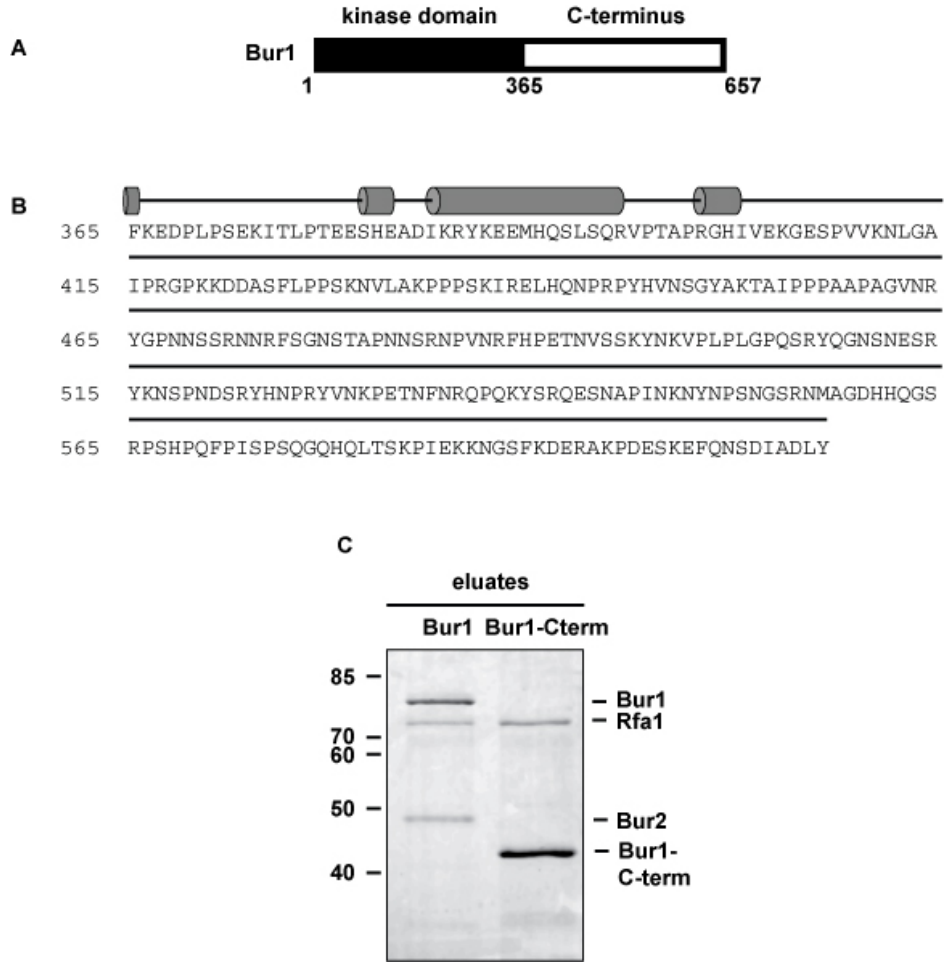

Figure 9: Analysis of the Bur1 C-terminus.

(A) Schematic showing the domain structure of Bur1. The N-terminal part shows homology to cyclin dependent kinases, the C-terminus does not show any significant homology. (B) Secondary structure prediction using PSIPRED. Starting form amino acid 400 no secondary structure can be predicted. (C) TAP purifications of full length Bur1 and the Bur1 C-terminus. The Bur1 C-terminus is sufficient for binding to Rfa1 and does not bind to Bur2.

2.2.3 Mapping of the Bur1 and Rfa1 interaction site

The aim of these experiments was to map the Bur1-RPA interaction site to generate a full length protein just containing a point mutation which inhibits the binding to RPA. This construct could then be used for further characterizing the functional significance of the interaction of both protein complexes *in vivo*.

2.2.3.1 Interaction site mapping using a GST Pulldown approach

As no secondary structure for the C-terminus of Bur1 was predictable, a GST pulldown approach to identify possible binding sites was performed. To obtain first indications of the position of this binding sites, GST-tagged truncations of the Bur1 C-terminus were expressed recombinantly in *E. coli*, purified with GSH sepharose and subjected to a binding assay using high salt washed TAP purified RPA from *S.cerevisiea* (Fig. 10). GST was used as a negative control for unspecific binding.

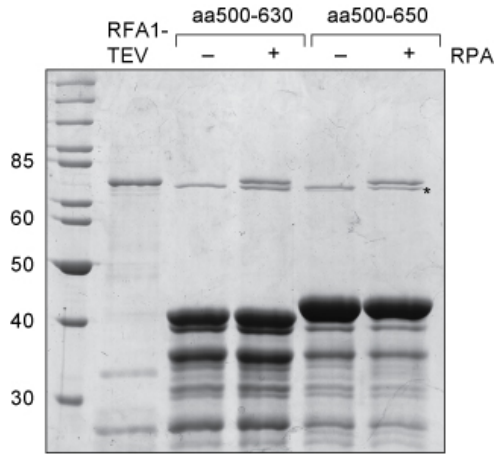

Figure 10: Example of the GST Pulldown based Bur1-RPA binding assay

Coomassie stained SDS-PAGE gel of the Bur1-RPA binding assay. GST tagged truncations of the Bur1 C-terminus were expressed in *E. coli* and purified using GSH sepharose. RPA was purified from *S. cerevisiae* using TAP tagged Rfa1 (lane 2). RPA was added (lane 4 and 6) or not, as negative control (lane 3 and 5), to the GST-bound Bur1 truncations. This figure shows fragments form amino acids 500-630 and 500-650. Both fragments were able to bind RPA. The asterisk (*) marks an unspecific protein originating from the *E. coli* expression.

The first constructs (Fig. 11) expressed were truncated 50 amino acids from the C-terminus (365-657, 365-600, 365-550, 365-500, 365-450, 365-400). The longest constructs bound RPA. The last construct that was still able to bind was ranging from amino acids 365-500 and the first construct not able to bind anymore was spanning amino acids 365-450. Thus, the binding site should be between amino acids 450 and 500. To further narrow down this region new constructs were generated that were shortened by 10 amino acids in this region (365-490, 480, 470, 460). The longest one was able to bind weakly, the other ones were not able to bind, leading to the conclusion that the binding site is between amino acids 480 and 500. In addition, as control experiments, also N-terminal truncations were generated starting at amino

acids 460, 470, 480, 490 and 500 until 657. Surprisingly, all those constructs were still able to bind to RPA indicating that there is a second binding site in the more C-terminal half of this domain.

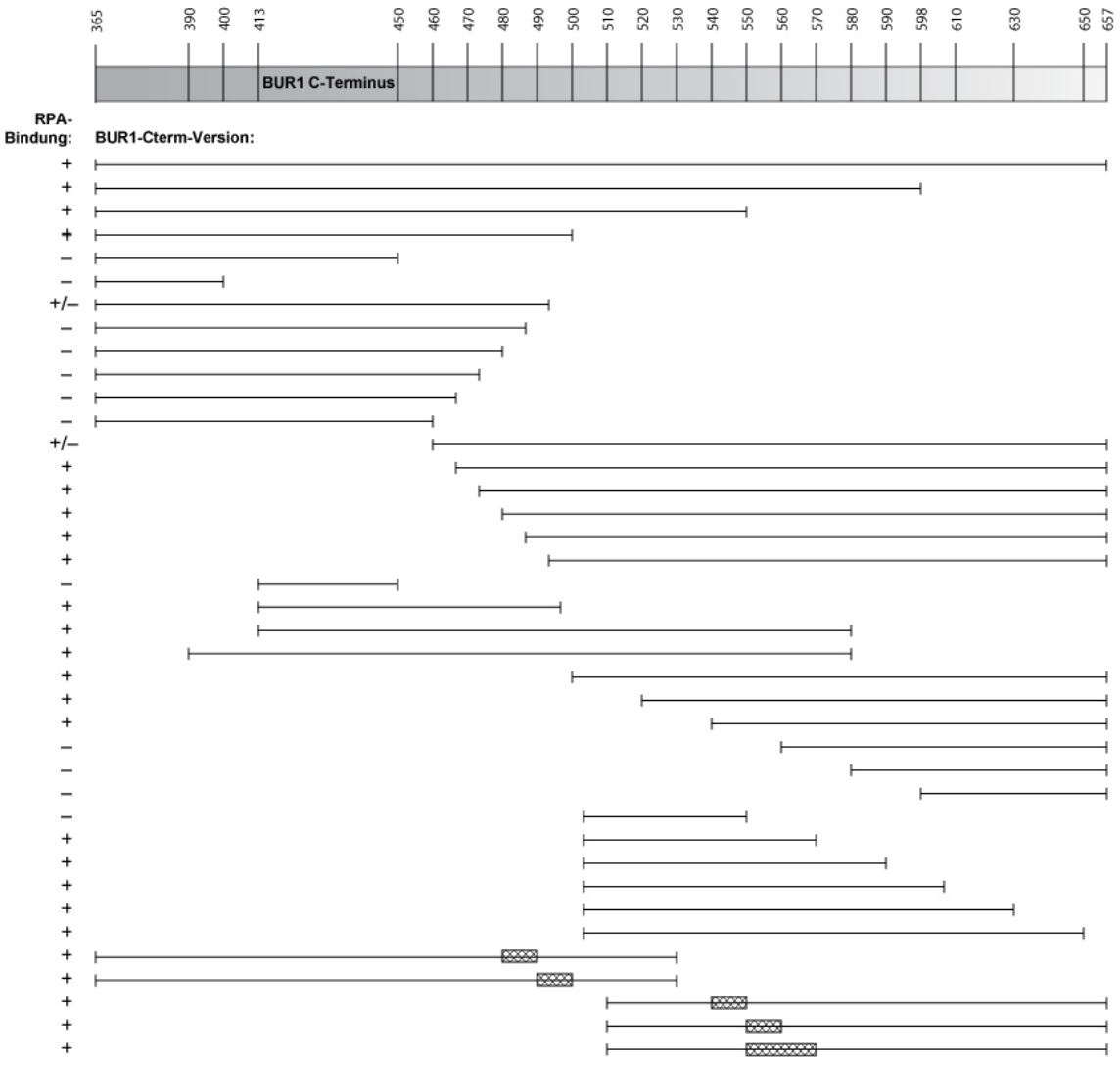

Figure 11: Summary of the binding abilities of fragments of the Bur1 C-terminus to RPA

Shown is a schematic of the Bur1 C-terminus from amino acids 365-657. The lines below depict the recombinantly expressed parts of the Bur1 C-terminus from *E. coli* and their ability to bind to TAP purified RPA from *S.cerevisiea*. Two putative binding sites could be identified in initial experiments ranging from amino acids 480 to 500 as well as from amino acids 540-560. But when those sites were deleted the fragments were still able to bind. The smallest fragments sufficient for binding to RPA reach from amino acids 413-500 and from 500-570.

This second binding site could then also be narrowed down to 20 amino acids spanning an area between amino acids 540 and 560. Those two binding sites should then be verified using constructs to express only one part of the protein where one of the binding sites mapped and this binding site was deleted. For the first binding site the construct was ranging from amino acids 365-530 and either amino acids 480-490 or 490-500 were deleted. Surprisingly, those constructs were again able to bind to RPA. The same approach was used for the second binding site. Constructs spanning from amino acids 510-657 missing either amino acids 540-550, 550-560 or 550-570 were tested for the binding ability and were also able to bind. The smallest constructs that were still able to bind were ranging from amino acids 413-500 and from amino acids 500-570. There might thus be weaker binding sites or a specific folding of the C-terminal domain of Bur1 induced by the binding to RPA that are sufficient for the binding to RPA (Fig. 11). The results of this study were part of the Diploma thesis of Barbara Müller.

2.2.3.2 Interaction site mapping using a peptide mapping approach

As a second approach for detecting the interaction site of the Bur1 C-terminus with RPA, a peptide array was generated. Here, fifteen amino acid long peptides spanning the Bur1 C-terminus from amino acids 365-657 were synthesized, in collaboration with Georg Arnold, with an overlap of 12 amino acids so there was a shift of three amino acids between each peptide. Those peptides were immobilized on a cellulose membrane using the SPOT approach (Frank, 2002; Hilpert *et al.*, 2007).

Purified RPA from *S. cerevisiae* could then be used to bind to this membrane and can subsequently be detected with an antibody to indentify the peptides necessary for binding.

To have a detectable epitope for antibody binding after the purification, a TAP tag was generated consisting of Protein A and a Flag tag with a TEV cleavage site in between. Using this tag it is possible to purify a protein with those tags and detect the eluted protein afterwards using an α-Flag antibody (Fig. 12). (It can also be used to natively elute the protein after the two step purification natively by competition with the Flag peptide in a smaller volume than with the usual TAP protocol and thus achieving a higher concentration.)

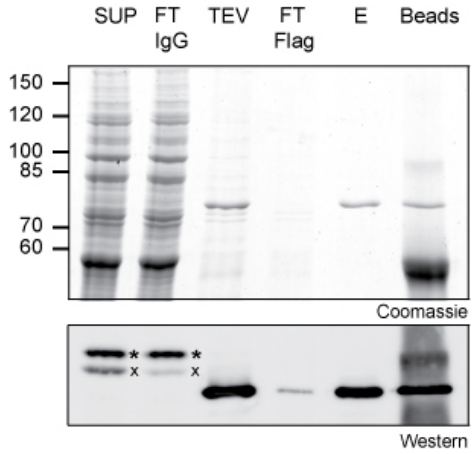

Figure 12: Rfa1 TAP purification using a TAP tag consisting of Protein A and Flag.
Rfa1 was C-terminally tagged with Protein A, a TEV cleavage site and a Flag epitope for eluting the native protein with a small tag for detection when bound to a peptide mapping membrane. The single purification steps were separated by SDS PAGE and stained with Coomassie. Additionally, they were subjected to Western blot analysis to test the detection with the α-Flag antibody. (* unspecific band, ^{x} Rfa1-FLAG-Protein A)

The purified, Flag-tagged RPA complex from *S. cerevisiae* (high salt washed TEV eluate) was incubated for binding on the peptide array, detected with an antibody against the Flag-tag and a secondary antibody carrying a HRPO enzyme for detection using ECL. This approach lead to a low signal to noise ratio, indicating that the interaction of the Bur1 C-terminus with RPA is relatively weak (Fig.13 B). The possible binding sites ranged from amino acids 396-443, 498-524 and 594-650 (Fig.14 D).

A second approach that is normally used for the detection of discontinuous epitopes when mapping a binding site for an antibody with the peptide array was also used. Here, the purified RPA complex was first incubated with the peptide mapping membrane, washed and immobilized on a PVDF membrane by three subsequent blotting steps. The advantage of the immobilization is that also lower amounts of the protein can be detected by a Western blot like approach afterwards because Rfa1 bound to the cellulose membrane is efficiently transferred and tightly bound to the PVDF membrane. This lead to a better signal to noise ratio than the “Far Western approach” (Fig.13 C). Here RPA bound almost the whole C-terminus of Bur1 (Fig.14 E). The possible binding sites are ranging from amino acids 383-473 and 501-650.

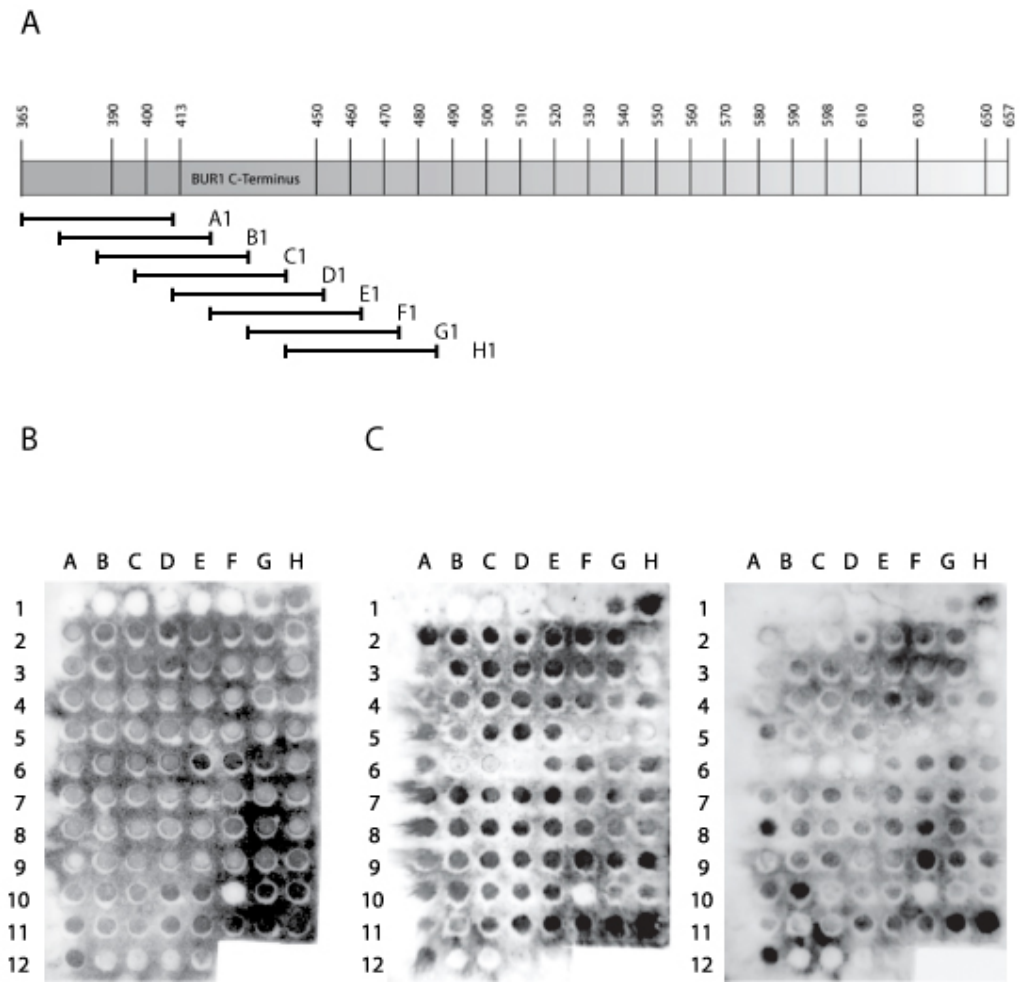

Figure 13: Peptide mapping for Bur1--Cterminus/RPA interaction site mapping

A peptide mapping approach was performed to map the interaction site of the Bur1 C-terminus with RPA. (A) Schematic representation of the peptides spotted onto the membrane. Peptides with a size of 15 amino acids were synthesized with a shift of 3 amino acids and spotted onto a cellulose membrane. (B) The membrane was incubated with Protein A-TEV purified, flag-tagged RPA directly and detected afterwards using antibodies against the Flag epitope and a secondary HRPO conaining antibody. The signal-to-noise ratio is relatively low. (C) For obtaining a better signal-to-noise ratio and detection of weaker interactions, the peptide mapping membrane was first incubated with RPA and blotted several times afterwards to transfer the bound protein to a PVDF membrane and immobilize it there. Detection with the corresponding antibodies is stronger and thus it is possible to detect weaker interactions. The two blots were done after each other. The fist one contains more protein but might also have more unspecific binding, the second one shows a more stringent representation.

2.2.3.2 Comparison of the interaction site mapping approaches

A comparison of the two methods used for the mapping of the Bur1 and RPA interaction sites was performed (Fig. 14). The smallest constructs that were still able to bind were ranging from amino acids 413-500 and from amino acids 500-570

(Fig.14 B). The GST pulldown based assay identified two binding sites ranging from amino acids 480 to 490 and from amino acids 540 to 560 (Fig.14 C). However, deletions of those sites in the Bur1 C-terminus were still able to bind to RPA. It seems likely that there are more, and probably weaker, binding sites that could not be detected using this assay. Using a peptide array approach most of the C-terminus was able to bind to RPA. The possible binding sites were ranging from amino acids 396-443, 498-524 and 594-650 (Fig. 14 D), in the case of the direct “Far Western” approach and from amino acids 383-473 and 501-650 after blotting (Fig. 14 E). These results hint to the existence of several short binding sites that cooperate in binding. Surprisingly, those sites do not overlap in the different approaches. Thus, it is not possible to generate a non RPA-binding mutant of Bur1 that just contains a point mutation or small deletion without deleting the whole C-terminus.

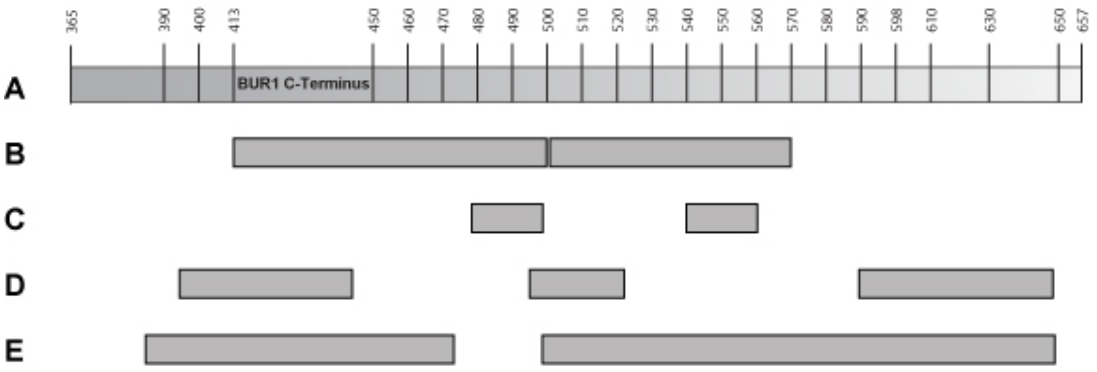

Figure 14: Comparison of the Bur1-RPA binding sites identified using the two approaches

(A) Schematic representation of the Bur1 C-terminus ranging from amino acid 365-657.

(B) The smallest fragments found in the GST pulldown approach that were sufficient for binding to RPA (amino acids 410-500 and 500-570).

(C) Binding sites indentified in the GST pulldown (amino acids 480-500 and 540-560).

(D) Binding sites indentified in the “Far Western” peptide mapping approach without blotting (amino acids 396-443, 498-524 and 594-650).

(E) Binding sites indentified in the blot based peptide mapping approach (amino acids 383-473 and 501-650).

2.2.4 Deletion of the Bur1 C-terminus leads to sensitivity to DNA damage as well as to replication and transcription stress

The C-terminus of Bur1 does not show homology to any other protein and is sufficient for binding to RPA. To further investigate the *in vivo* function of this domain, the Bur1

N-terminus, containing the kinase domain and the C-terminus were expressed in *S. cerevisiae*.

The ability to complement for the Bur1 knock-out was tested using these constructs. The N-terminus alone carrying the kinase domain was sufficient for complementing *Δbur1* with negligible growth impairment. The unstructured C-terminus was not able to rescue the deletion of *BUR1* and is lethal, as well as the complete knock-out (Fig. 15 A). However, it is interesting that deletion of the C-terminus and thus non-binding of RPA results in sensitivity of the cells to HU, 6'AU an MMS (Fig. 15 B), showing that the interaction of the BUR complex with RPA is needed for stress response.

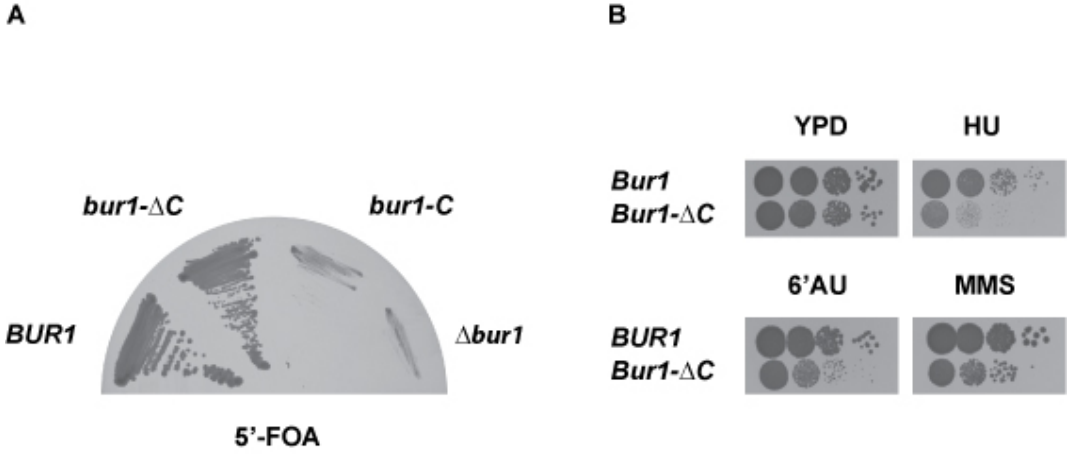

Figure 15: Deletion of the Bur1 C-terminus can complement for *Δbur1* but leads to sensitivity to stress.

(A) Complementation studies of the deletion of *BUR1*. Full length plasmid encoded *BUR1* as well as the kinase domain lacking the C-terminus can complement for *Δbur1*. The Bur1 C-terminus alone as well as an empty plasmid can not. (B) Deletion of the Bur1 C-terminus leads to sensitivity of the cells to HU (100 mM), 6'AU (100 µg/ml) and MMS (0.035%).

2.3. The interaction of Bur1 and RPA is most likely not conserved in human

2.3.1 Cdk9 and RPA do not co-immunoprecipitate

As *S. cerevisiae* Bur1 and RPA interact, experiments were performed to test if the human homolog, Cdk9, interacts with RPA. As a fist experiment, stably integrated, GFP-tagged Cdk9 (Röther, unpublished data) was purified from HeLa cells using a GFP binder matrix (Rothbauer *et al.*, 2008). The eluate was subjected to SDS-PAGE and stained with Coomassie. Copurifying bands were analysed by mass spectrometry (Fig.16 A). Cdk9 was identified, showing that the purification worked. Most of the other proteins copurifying were heat shock proteins (HS90A, HS90B,

HSP7C). Neither RPA nor the corresponding cyclins could be identified. To have a more sensitive method to examine the interaction, Cdk9-GFP was purified and the fractions of the purification were subjected to Western analysis using antibodies directed against Cdk9 as control and against RPA32 to elucidate a putative interaction. Mock purification of wild type cells serves as a control for unspecific binding. Both proteins could be detected in the cell extracts and the flow-through of the purifications. However, in the Cdk9-GFP eluate only Cdk9 was detected and not RPA32 showing that the proteins most likely do not interact (Fig.16 B). This could be either due to non binding of the proteins or because RPA32 binds to a different isoform of Cdk9, Cdk9-55 (Shore *et al.*, 2003). To test this, a reverse tagging strategy was used by purifying RPA32-GFP.

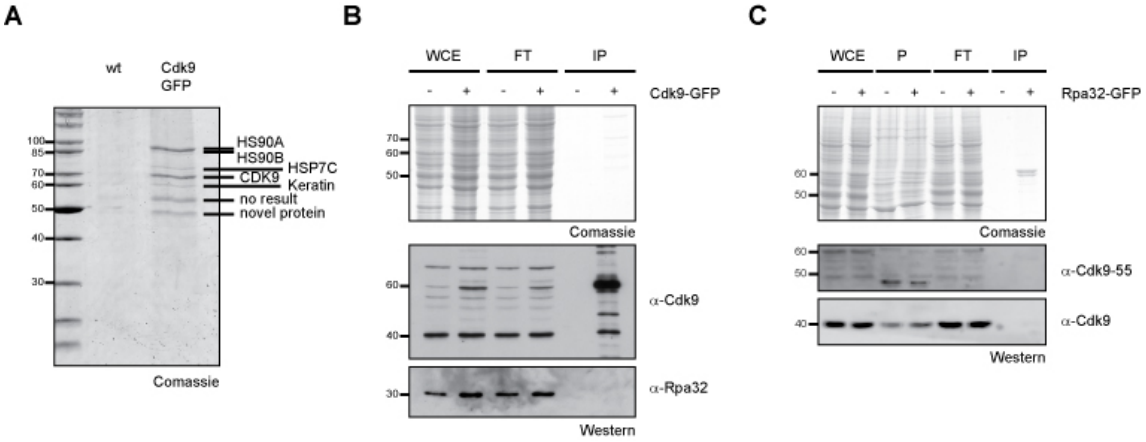

Figure 16: Human Cdk9 and Cdk9-55 do not interact biochemically with RPA

(A) Purification of GFP tagged Cdk9 from HeLa cells using GFP binder. Coomassie stained gel of the purification. Co-purifying bands were analyzed by mass spectrometry. Cdk9 itself could be indentified but not the corresponding cyclins. The other copurifiers are either heat shock proteins or unknown. (B) Pulldown of Cdk9-GFP using GFP binder. The different steps of the purification, whole cell extracts (WCE), Flow through (FT) and eluates (IP) were separated by SDS-PAGE and either Coomassie stained or subjected to western blotting and detection with a α-Cdk9 or an α-Rpa32 antibody. A clear enrichment of Cdk9 can be seen in the purification but Rpa32 can not be detected in the purification done under the same conditions as the yeast TAP purifications, in which Bur1 and RPA interact. (C) Purification of transiently expressed Rpa32-GFP using GFP binder. Here, also the insoluble fraction is shown (P). Rpa32 can be significantly enriched in the purification but no interaction with either Cdk9-55 or Cdk9 can be detected by Western blotting.

It was shown that when RPA is immunoprecipitated with a α-RPA32 antibody the complex shows a constant ratio of the three subunits (Din SU and Stillman, Gendev 1990). According to this, an affinity purification strategy using transiently expressed GFP tagged RPA32 was used to purify human RPA and test the association with Cdk9 or the Cdk9-55 isoform. The different steps of the purification, whole cell extracts (WCE), the insoluble pellet (P), flow-through (FT) and the eluate (IP) were subjected to SDS-PAGE and either Coomassie stained or analyzed by Western blotting. The Coomassie stain shows an enrichment of RPA32 in the eluate. Western blots, using antibodies directed against Cdk9-55 or Cdk9 show that the proteins are present in the different purification steps but not in the eluate (Fig. 16 C). Thus, neither Cdk9 nor Cdk9-55 was able to bind to human RPA.

2.3.2 Cdk9 and RPA do not colocalize

Another, independent approach, to test if Cdk9 and RPA bind was to examine the proteins by fluorescence microscopy in collaboration with Oliver Mortusewicz from the Leonhardt lab. It has been shown that hRPA forms foci in S-Phase (Coverley and Laskey, 1994) as well as after induction of DNA damage. HeLa cells expressing GFP-Cdk9 were treated with NCS or HU for four hours. The cells were fixed and co-localisation of Cdk9 with RPA examined. RPA forms foci after the treatment whereas GFP-Cdk9 stays diffuse in the nucleus and thus does not colocalize. Colocalisation of Cdk9 with the repair histone variant γ-H2AX as well as with microirradiation sites of DNA damage was also not detectable (data not shown).

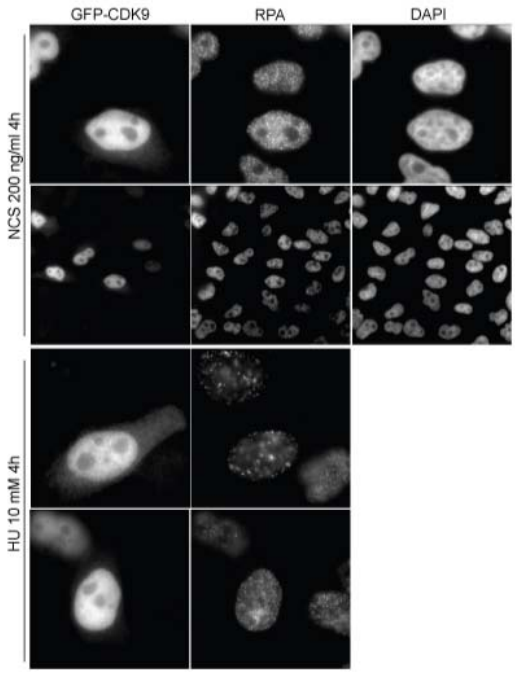

Figure 17: Cdk9-GFP and Rpa32-RFP do not colocalize after DNA damage or replication stress
HeLa cells expressing stably integrated Cdk9-GFP were treated with Neokarzinostatin to induce DSBs or with HU for inducing single or double strand breaks during DNA replication. Fixed cells were analyzed by fluorescence microscopy. RPA shows a punctuate staining after the treatment whereas Cdk9 stays diffuse showing no specific interaction of both proteins.

2.4. *BUR1* and *RFA1* interact genetically

2.4.1 Generation of *BUR1* and *RFA1* temperature sensitive mutants

To have a tool for a conditional knockout and for allele specific genetics, temperature sensitive mutants of *BUR1* (Sträßer, unpublished data) and *RFA1* were generated by hydroxylamine mutagenesis. As can be seen in Fig.18, those mutants grow like wild type when incubated at 30°C just *bur1-24 and rfa1-249* are already slightly impaired in growth. When grown at 37°C the mutations become lethal.

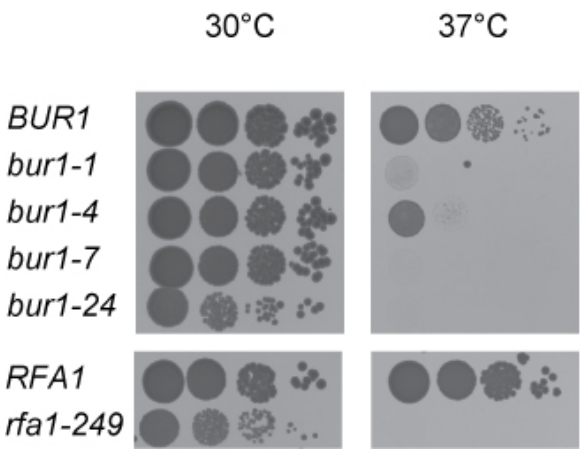

Figure 18: *BUR1* and *RFA1* temperature sensitive mutants

Growth of temperature sensitive mutants of *BUR1* and *RFA1* generated by random mutagenesis. The growth of those mutants is not or only slightly impaired at 30°C. Upon shift to the restrictive temperature of 37°C mutants show no growth anymore.

To see if the stability and expression of the mutants generated was still comparable to the wild type, Western blots of whole cell extracts from either wild type cells or cells that contain the mutant allele were performed using an antibody generated against the C-terminus of Bur1. The expression of the *bur1-1*, *bur1-4* and *bur1-7* mutants is the same compared to the wild type, just *bur1-24* that contains a premature stop codon, is expressed at lower levels or has a size of about 15 kDa that is not resolved on this gel. This protein would be non functional as the kinase domain is only partly expressed. Still, it seems to have basal activity as the cells survive at 30°C. The wild type protein shows a double band most likely corresponding to the phosphorylated form of the protein modified by CAK1 (Yao and Prelich, 2002) that is absent in the temperature sensitive mutants. The expression levels do not change upon shift to 37°C for 3 hours. Pgk1 serves as the loading control (Fig. 19).

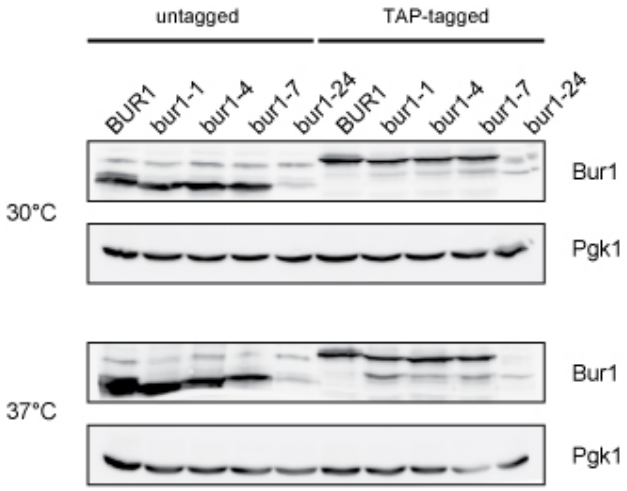

Figure 19: Expression and stability of Bur1 non- and TAP tagged temperature sensitive mutants

Expression of the *bur1* ts mutants was determined with western blots using an antibody directed against Bur1. The ts mutants are expressed to the same level as wt expression, except for *bur1-24* which is expressed in much lower amounts or much smaller. The temperature shift to 37°C was performed for 3 hours. Notably, the *bur1* mutants do not show the second higher molecular weight band which most likely corresponds to the phosphorylated form of Bur1 modified by CAK1 (Yao and Prelich, 2002). Pgk1 is used as a loading control.

Also the expression of *the rfa1-249* mutant was tested by Western blotting, using an antibody against Rfa1 (Brill and Stillman, 1991). It is the same as in the wild type (Fig. 20). Expression at 37°C was not determined, but the expression does not change upon treatment with MMS (data not shown).

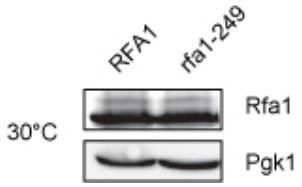

Figure 20: Expression and stability of the *rfa1-249* temperature sensitive mutant

Expression of the *rfa1-249* mutant was assayed by Western blotting using an antibody directed against Rfa1 (Brill and Stillman, 1991).The expression and stability is comparable to the wild type level. Pgk1 serves as the loading control.

2.4.2 *bur1* mutants are sensitive to DNA damage and to replication and transcription stress

Knowing that BUR and RPA interact biochemically lead to the idea of a function of the BUR complex in DNA replication, recombination and repair. To further investigate a function in one of these processes *bur1* mutants were subjected to drugs inducing

DNA damage (MMS) or replication stress (HU) or to an agent impairing transcription elongation (6'AU) (Fig. 21). Mutations in *BUR1* lead to sensitivity to replication stress induced by hydroxyurea when grown at semi permissive temperature of 33°C. The *bur1-1* and *bur1-4* mutations are only slightly sensitive whereas the *bur1-7* and *bur1-24* can not survive at a concentration of 100 mM and thus show a strong phenotype. The same phenotype can be seen for MMS at a concentration of 0.035%, a drug that causes DNA damage, indicating that *BUR1* might have a function in DNA repair. Other transcription elongation factors like *DST1* do not show this phenotype (data not shown). It is interesting to note that these *BUR1* mutants, except for *bur1-24*, are only slightly sensitive to 100 µg/ml 6'-Azauracil, a drug that impairs transcription elongation (Fig.21 6'AU).

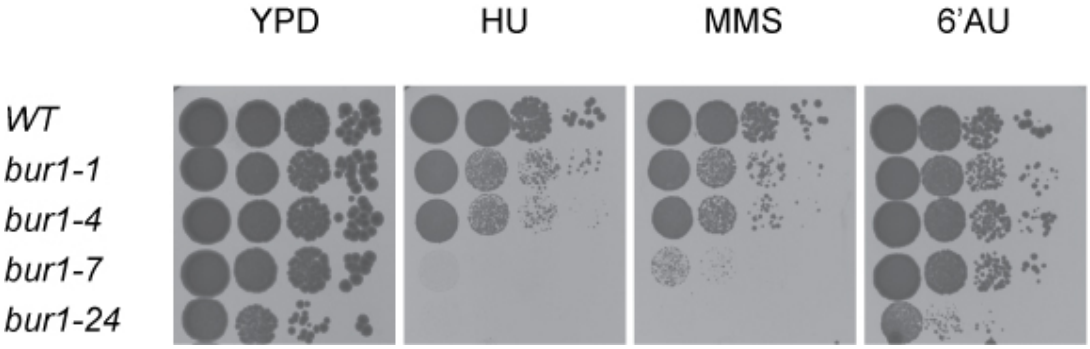

Figure 21: *BUR1* mutants are sensitive to replication stress, DNA damage and impairment of transcription elongation.

BUR1 mutants are sensitive to drugs that induce replication stress (100 mM HU) or DNA damage (0.035% MMS) as well as transcription impairment (100 µg/ml 6'AU). The *bur1-1* and *bur1-4* mutations show only a slight impairment. The *bur1-7* and *bur1-24* are strongly impaired by HU and MMS and can not compensate for replication stress and DNA damage. The *bur1-24* mutation is also strongly sensitive to 6'AU. It is interesting to note that the other three *BUR1* mutant are not or only slightly sensitive to the transcription elongation impairment.

2.4.3 A *rfa1* mutant is sensitive to drugs impairing transcription elongation

The interaction of Bur1 and RPA also suggests a function of RPA in transcription. To get first indications for this, *RFA1* mutants were subjected to drugs inducing DNA damage (MMS) or replication stress (HU) or to an agent impairing transcription elongation (6'AU). A mutation, *rfa1-249*, in the *RFA1* gene, the biggest subunit of RPA, shows growth impairment on replication stress (100mM HU) and DNA damage (0.01% MMS) as well as on transcription impairment (100 µg/ml) showing that this

mutant might have a function in DNA replication, DNA repair and most interestingly in transcription elongation (Fig.22).

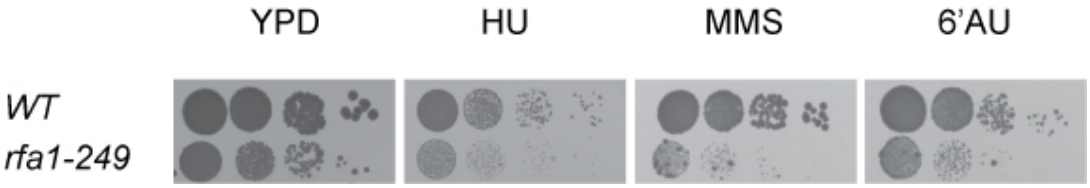

Figure 22: A *rfa1* mutant is sensitive to replication stress, DNA damage and impairment of transcription elongation.

The *rfa1-249* mutant is sensitive to drugs that induce replication stress (100 mM HU) or DNA damage (0.01% MMS) and most interestingly to transcription impairment (100 µg/ml 6'AU).

2.4.4 Mutations in *bur1* suppress the sensitivity of *rfa1* mutants

Bur1 and RPA interact biochemically and mutations in both of the genes lead to sensitivity of the cells to replication stress, DNA damage and impairment of transcription elongation. Due to these findings the genetic interaction of *bur1* mutants and *rfa1* mutants was examined. A *BUR1 RFA1* shuffle strain was created and transformed with plasmids that encode for either, *BUR1* wild type or a *bur1* mutation as well as a *RFA1* wild type or a *rfa1* mutation, respectively, to create strains having either wild type genes, mutations in one gene or double mutants. The *URA3* wt plasmids were shuffled out by restreaking transformants on plates containing 5'-FOA. The resulting yeast strains were spotted on plates with full media or full media containing Hydroxyurea (50 mM HU), Methylmethanesulfonate (0.005% MMS) or 6'-Azauracil (10 µg/ml 6'AU). Growth was analyzed after three days at 30°C. The single mutant strains show sensitivity to these drugs but interestingly, strains that had both mutations were growing better showing that the mutants suppress each other and hinting to antagonistic roles of the *BUR1* and *RFA1* genes (Fig. 23).

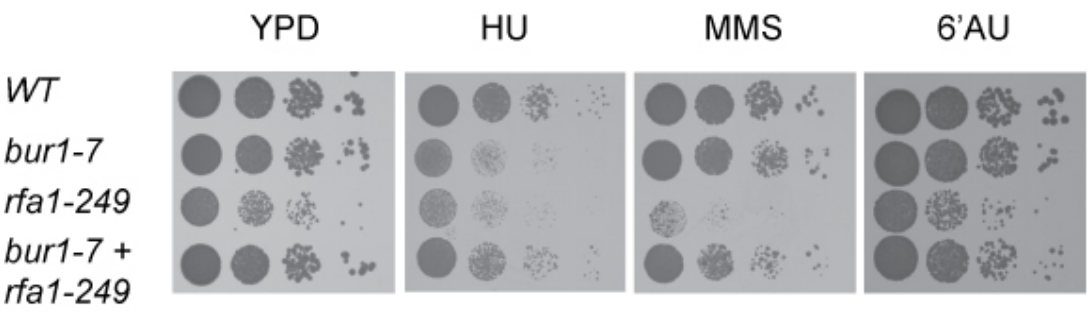

Figure 23: Suppression of *rfa1* mutant phenotype by mutation of *bur1*

Growth impairment of both, the *rfa1* and the *bur1* mutant is detectable on plates containing drugs that induce replication stress (50 mM HU) or DNA damage (0.005% MMS) as well as to transcription stress (10 µg/ml 6'AU). The *rfa1* mutant shows a stronger sensitivity than the *bur1* mutant. Noteworthy, combination of both mutants leads to better growth, showing that these cells can compensate for the stress and indicating a specific *in vivo* interaction of both proteins. As mutations compensate for each other we conclude that *BUR1* and *RFA1* might have antagonistic functions.

2.5 Role of *BUR1* in DNA repair

2.5.1 Epistasis and SL of *BUR1* with mutants in DNA repair pathways

As there were indications for Bur1-2 having a role in DNA repair, an epistasis analysis was performed, with the aim to identify the pathway the BUR complex is involved in.

Epistasis is an interaction between two genes. In the case of DNA repair, one would expect that upon the knockout of a specific pathway, deletion or mutation of an additional gene in the same pathway would not lead to an increased sensitivity to DNA damage as this pathway is already not functioning. If an additional impairment is visible, the conclusion is that another DNA repair pathway is affected and the sensitivities add up from the first and the second pathway.

For this analysis, double shuffle strains with deletions of distinct non-essential DNA repair pathway genes and *BUR1* were created. These strains were transformed with *bur1* mutants and either the repair pathway deletion was covered with the wild type plasmid as control experiment or not. The cells carrying combinations of a *bur1* mutation and a repair pathway deletion were subjected to DNA damage, for example by UV irradiation or MMS. UV irradiation leads to CC dimers, a bulky lesion, and MMS alkylates DNA. The sensitivity of these strains to DNA damage was determined either by 10-fold serial dilutions of cells on plates containing the damage inducing

compound or quantified by counting cells which were plated out in a defined amount and subjected to different concentrations of MMS or different doses of UV irradiation.
If *BUR1* had a function in a specific pathway one would expect to see that the double mutant grows like the deletion of this pathway as this specific pathway is not functional anymore and thus the *bur1* mutation can not have an additional effect. If the double mutant strain grows worse than the deletion of the specific DNA repair pathway one can conclude that the additive effect of this specific pathway deletion and *bur1* argues for an additional effect of *bur1* from a different pathway than the one examined.
Several non essential deletions of DNA repair pathways have been chosen for the analysis: *RAD52*, needed for homologous recombination (Krogh and Symington, 2004), *MSH6* functions in MMR and is involved in the recognition of mismatches (Bowers *et al.*, 1999), *POL4* is involved in DSB break repair via NHEJ (Tseng and Tomkinson, 2004), *RAD16* forms a complex with *RAD7* and is involved in the DNA damage recognition in NER (Guzder *et al.*, 1997), *RAD26* is responsible for TCR (Li and Smerdon, 2002). *RAD16* and *RAD26* functions partly overlap in both pathways, NER and TCR (Verhage *et al.*, 1996). *XRS2* is part of the MRX complex needed for DSB break repair (Assenmacher and Hopfner, 2004), *MAG1* is a glycosylase needed for damage recognition in BER and *APN1* an endunclease also functioning in BER (Memisoglu and Samson, 2000). *RNR1* is a subunit of ribonucleotide-diphosphate reductase, catalyzing dNTP synthesis and regulating DNA replication and damage checkpoint pathways (Yao *et al.*, 2003).

2.5.1.1 *BUR1* is synthetic sick with *RAD52* but not epistatic

Epistasis of *bur1* mutants was tested with *RAD52*. *RAD52* is known to have a function in double strand break (DSB) repair by homologous recombination (Fig.23).
The analysis of *BUR1* and *RAD52* shows two phenomena. On the one hand *bur1* mutants are already impaired in growth with the additional deletion of *RAD52* without the subjection to DNA damage. This can be seen slightly at 30°C and becomes stronger at 33°C. This synthetic sickness leads to the conclusion that *BUR1* and *RAD52* have a functional overlap without DNA damage and thus might act in the same pathway, *e.g.* in telomere maintenance. On the other hand as soon as the cells are challenged with DNA damage the double mutant strains grow significantly slower excluding the homologous recombination branch of DSB repair as the pathway *BUR1* functions in (Fig. 24).

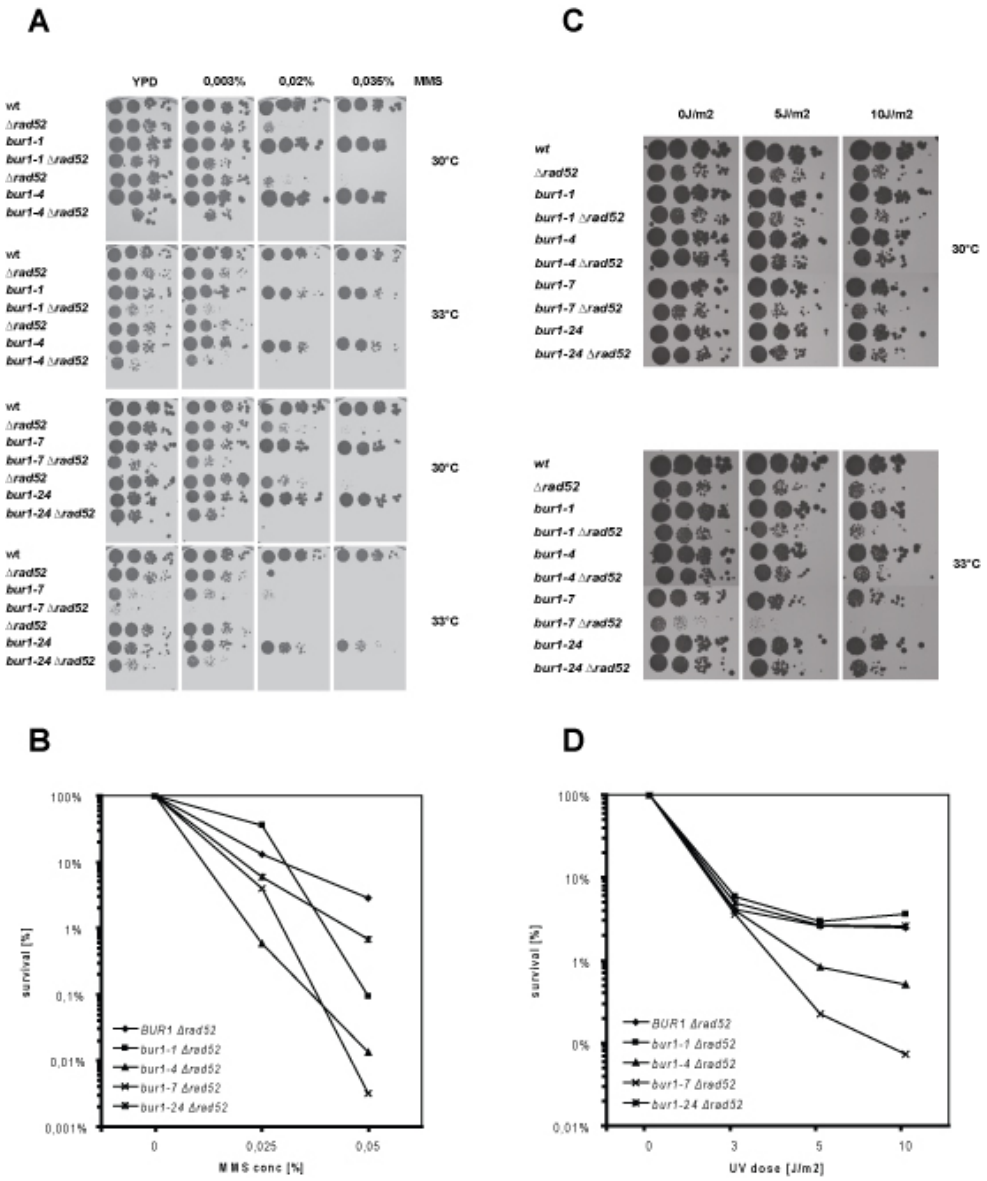

Figure 24: *BUR1* is not epistatic with *RAD52* but synthetic sick

(A) Ten-fold serial dilutions of strains carrying *bur1* mutations and a deletion of *RAD52* either covered with a wild type or empty plasmid were spotted on plates containing no drug or MMS. The *bur1* mutants are only slightly sensitive when subjected to MMS at 30°C and show higher sensitivity at 33°C. Interestingly, the *bur1* mutants are synthetic sick with *Δrad52* without DNA damage. After induction of damage by MMS the double mutants are much sicker than the single ones, excluding DSB repair by homologous recombination as the pathway *BUR1* acts in. (B) Quantification of the MMS sensitivity. At 0.05% MMS the double mutants becomes more sensitive than the deletion of *RAD52*. (C) Ten-fold serial dilutions of the strains also show higher sensitivity of the double mutant strains to UV irradiation. This can be seen especially with the *bur1-7* mutation at 33°C. (D) Quantification of the UV survival rates also shows that combination of *bur1-7* or *bur1-24* with the deletion of *RAD52* leads to a stronger sensitivity than deletion of *RAD52* alone. This indicates that *BUR1* does not have a specific function in DSB repair but in another DNA repair pathway and thus gives an additive effect to the deletion of *RAD52*.

2.5.1.2 *BUR1* is not epistatic with *MSH6*

To investigate the function of *BUR1* in mismatch repair (MMR) epistasis was tested between *BUR1* and *MSH6* (Fig. 25). The *bur1* mutants, especially *bur1-7* and *bur1-24* are more sensitive that the deletion of *MSH6*. Also the double mutants grow worse than *Δmsh6,* giving an additional effect of *bur1* mutations to the deletion of *MSH6.* Consequently, a function of *BUR1* in mismatch repair was excluded.

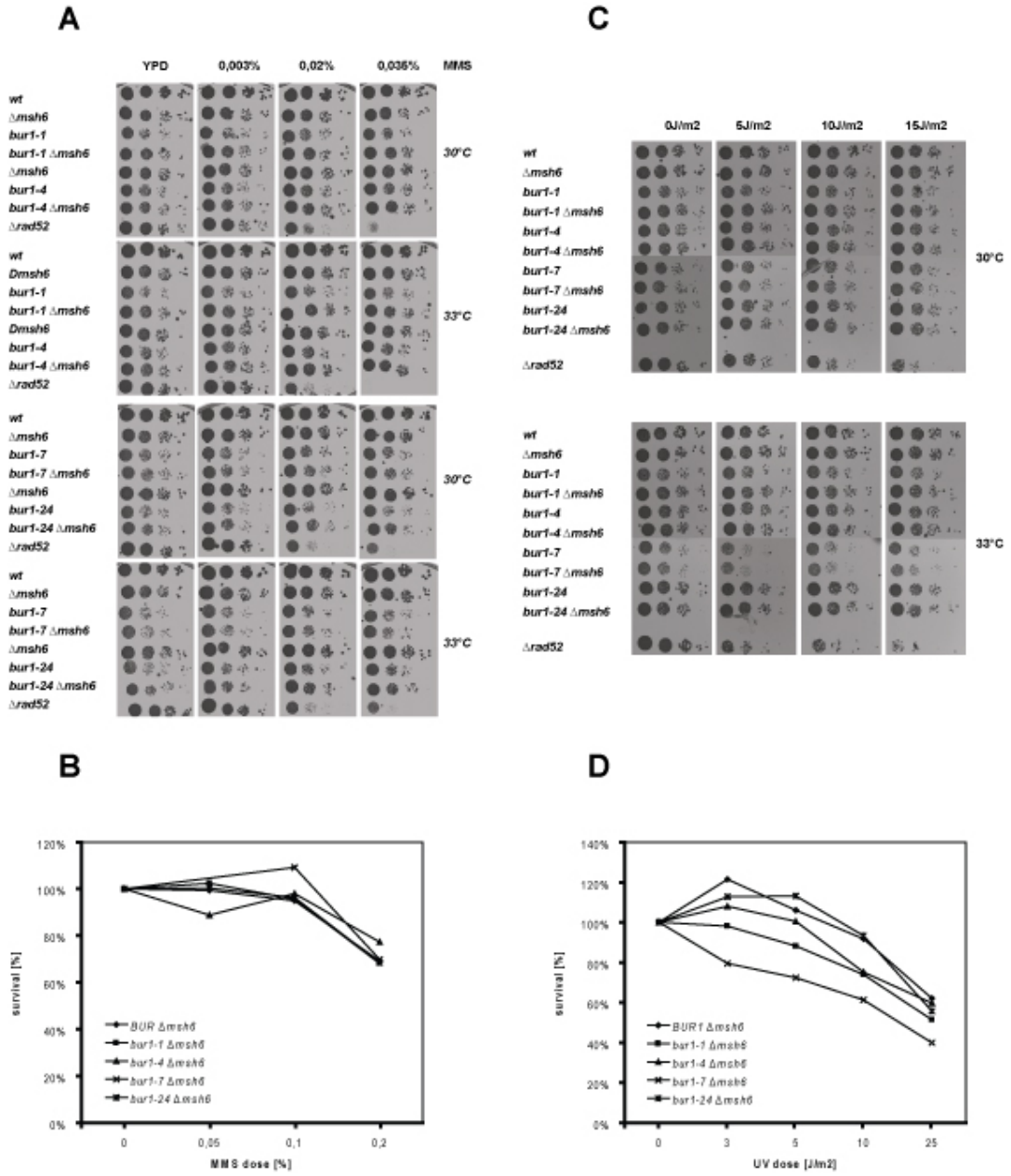

Figure 25: *BUR1* is not epistatic with *MSH6*

(A) Ten-fold serial dilutions of strains carrying a *bur1* mutation and a deletion of *MSH6* were spotted on plates containing no drug or MMS. After induction of damage by MMS the double mutants and the *bur1* mutants are sicker than the deletion of *MSH6*. Thus *bur1* mutants are more sensitive to DNA

damage than the deletion of the mismatch repair component *MSH6* excluding a function of *BUR1* in mismatch repair. (B) Quantification of the MMS sensitivity. At 0.2% MMS the double mutants becomes more sensitive than the deletion of *MSH6* alone. This effect is only slightly visible and is more pronounced at higher concentrations of MMS. (C) Ten-fold serial dilutions of the strains also show higher sensitivity of the double mutant and *bur1* mutant strains to UV irradiation. This can be seen especially with the *bur1-7* mutation at 33°C. (D) Quantification of this effect also shows that the combination of *bur1-7* with the deletion of *MSH6* is much more sensitive than deletion of *MSH6*. This indicates that *BUR1* does not have a specific function in mismatch repair but in another DNA repair pathway and thus gives an additive effect to the deletion of *MSH6*.

2.5.1.3 *BUR1* is not epistatic with *POL4*

The genetic interaction of *BUR1* mutants with *POL4* was also determined. *POL4* mediates DSB repair by the non-homologous end joining (NHEJ) pathway (Fig. 26). The sensitivity of the *BUR1* mutants, especially of the *bur1-7* mutant, as well as the *bur1-7 Δpol4* double mutant show stronger sensitivity than the deletion of *POL4,* indicating that the effect of *BUR1* is different from the one from *POL4* and thus excludes NHEJ as the process the BUR complex functions in.

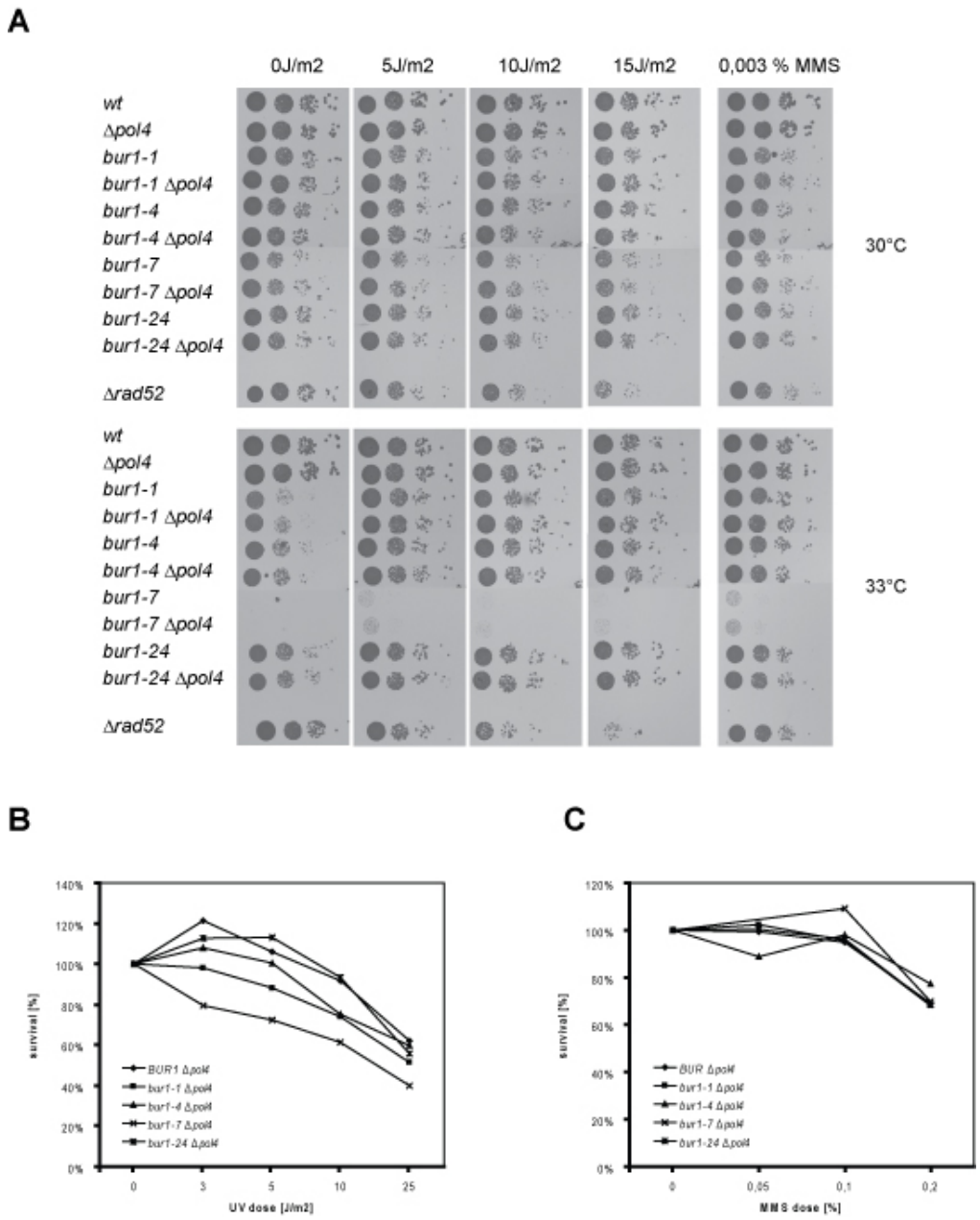

Figure 26: *BUR1* is not epistatic with *POL4*

(A) Ten-fold serial dilutions of strains carrying *bur1* mutants and a deletion of *POL4* that was transformed either with a plasmid coding for the wild type gene or an empty plasmid, were spotted on plates containing no drug, MMS or were irradiated with UV. After induction of damage by MMS or UV the double mutants and the *bur1* mutants are much sicker than the deletion of *POL4*. Thus *bur1* mutants are more sensitive to DNA damage than the deletion of the non-homologous end joining deletion *POL4* excluding a function of *BUR1* in NHEJ. (B) Quantification of the UV sensitivity. Already at 3J/m2 the double mutants becomes more sensitive than the deletion of *POL4*. The strongest phenotype is visible in the *bur1-7* mutant. (C) Quantification of the MMS sensitivity also shows that the combination of the *bur1* mutants with the deletion of *POL4* are more sensitive than deletion of *POL4* at 0.2% MMS. This indicates that *BUR1* does not have a specific function in DSB repair b NHEJ but in another DNA repair pathway and thus gives an additive effect to the deletion of *POL4*.

2.5.1.4 *BUR1* is not epistatic with *RAD16*

To examine a possible function of *BUR1* in nucleotide excision repair (NER) strains were created with a deletion of *BUR1* and *RAD16* (Fig. 27).

Mutations in the *BUR1* gene are as sensitive as deletion of the *RAD16* gene upon treatment with MMS or HU at 30°C. When grown at 33°C the *bur1-7* mutant and also the double mutants become more sensitive than *Δrad16*. The same phenotype can be seen when cells are UV irradiated. The *bur1-7* mutation is more sensitive than the deletion of *RAD16*. In the quantification only *bur1-7* shows high sensitivity but not the *bur1-7 Δrad16* mutation. This is not expected and most likely due to revertants in this strain that are then behave like the wild type. The results from the dot spot analysis shows that the function of *BUR1* is in a pathway different from NER. Additionally, as the *bur1-7* mutant is more sensitive to UV irradiation than *Δrad16* the same conclusion can be drawn from the quantification.

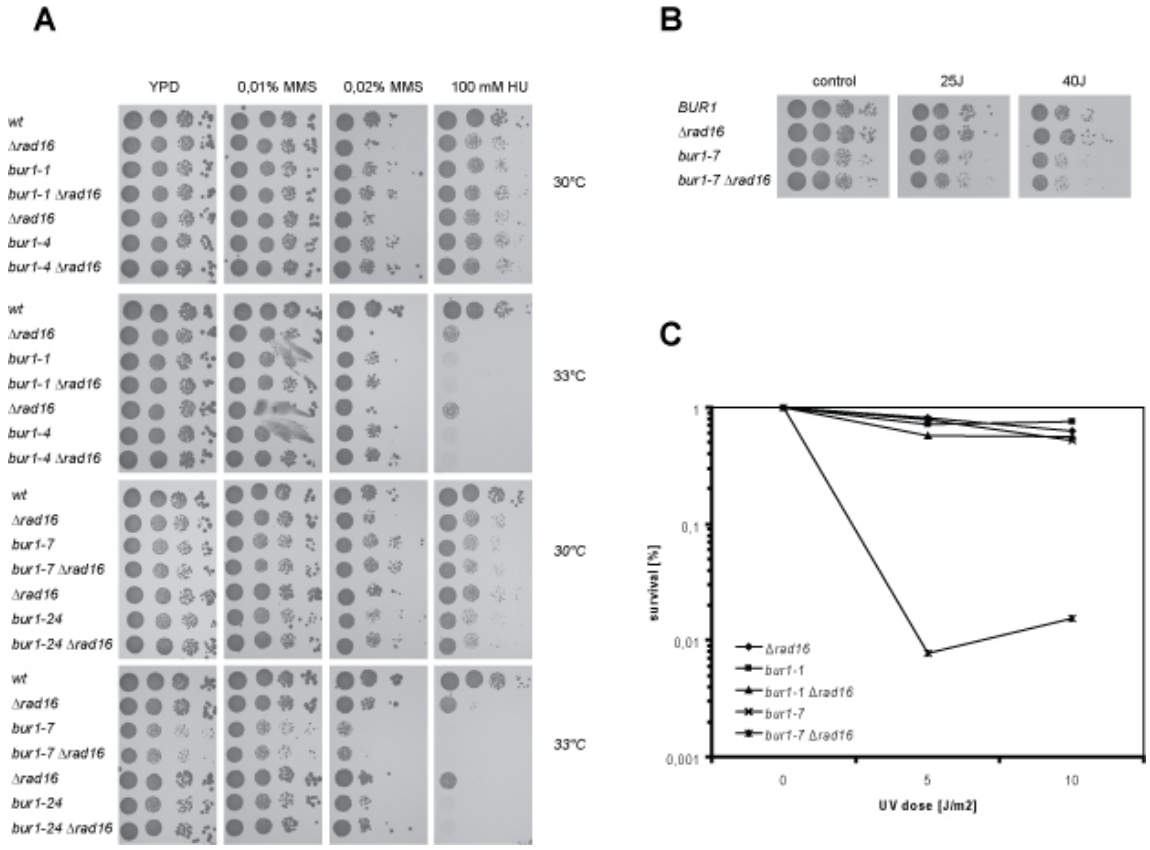

Figure 27: *BUR1* is not epistatic with *RAD16*

(A) Ten-fold serial dilutions of strains containing *bur1* mutations and a deletion of *RAD16* either covered with a wild type *RAD16* containing or empty plasmid were spotted on plates containing no drug, MMS or HU. The *bur1* mutants are sensitive when subjected to MMS at 30°C and show higher sensitivity at 33°C. Especially on 33°C the *bur1* mutants and the double mutants show a stronger sensitivity that the deletion of *RAD16*. After induction of damage by MMS or HU the double mutants

are much sicker than the single ones thus excluding NER as the pathway *BUR1* acts in specifically. (B) Ten-fold serial dilutions of the strains also show higher sensitivity of the *BUR1* and double mutant strains to UV irradiation. (C) Quantification of this effect also shows that especially the *bur1-7* mutant is very sensitive to UV irradiation. As it is more sensitive than the deletion of *RAD16* a specific function of *BUR1* in NER was excluded.

2.5.1.5 *BUR1* is not epistatic with *RAD26*

The *RAD26* gene was identified in yeast for having a role in transcription coupled repair (TCR). To elucidate a possible function of *BUR1* in this process, double mutants were generated and tested for their epistatic behaviour (Fig. 28).

The deletion of *RAD26* is not sensitive to MMS or HU. Compared to this the *bur1-7* and *bur1-24* mutants used in this assay, are far more sensitive than the deletion of *RAD26*. Also the double mutant strain behaves as the *bur1* mutant. No or only slight differences in strains carrying those mutations were detected after UV irradiation. As the *bur1* mutations show a higher sensitivity than the deletion of *RAD26*, *BUR1* is most likely not involved in TCR.

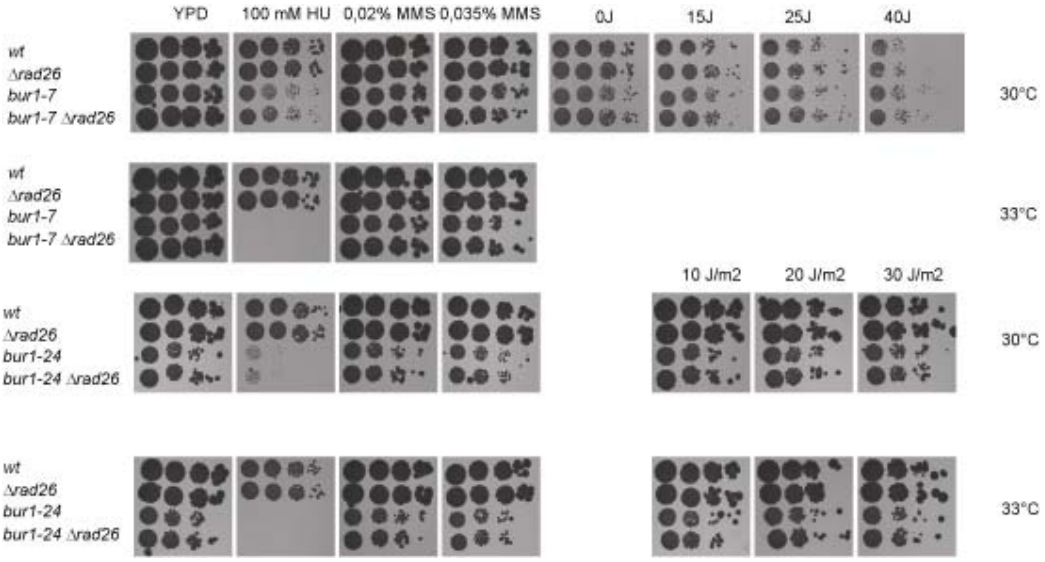

Figure 28: *BUR1* is not epistatic with *RAD26*

Ten-fold serial dilutions of strains containing *bur1* mutations and a deletion of *RAD26* either covered with a wild type *RAD26* containing or empty plasmid were spotted on plates containing no drug, HU, MMS or were irradiated with different doses of UV. Here, only *bur1-7* and *bur1-24* were tested as they show the strongest sensitivity. The *bur1* mutants are sensitive when subjected to HU and show only slight sensitivity to MMS and UV irradiation at 30°C but it is enhanced at 33°C. Especially on 33°C the *bur1* mutants and the double mutants show a stronger sensitivity that the deletion of *RAD26*. As the *bur1* mutants and the double mutants are sicker than the deletion of *RAD26,* TCR was excluded as the pathway *BUR1* acts in.

2.5.1.6 *BUR1* is not epistatic with *RAD16* and *RAD26* double mutants

It has also been shown that additional deletion of *RAD16* to the deletion of *RAD26* makes cells more sensitive to UV irradiation when the TCR pathway is knocked-out in addition to the NER pathway (Verhage *et al.*, 1996). To see the impact of a deletion of both pathways also *Δrad16 Δrad26* cells were tested for their epistatic behaviour with *BUR1* (Fig. 29).

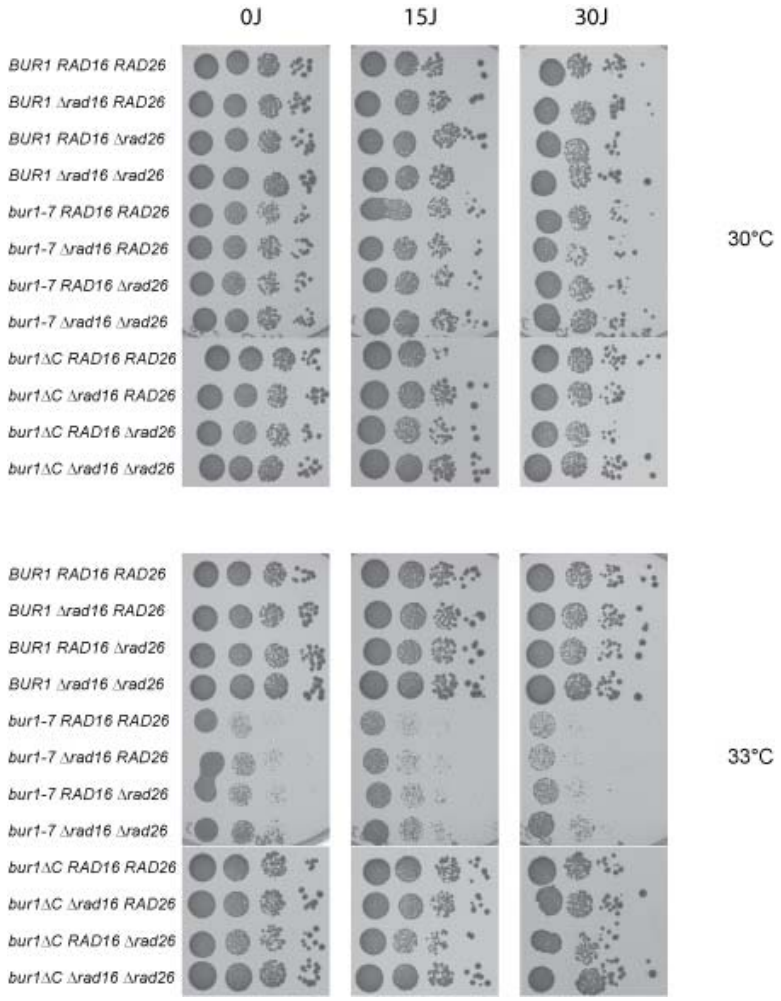

Figure 29: *BUR1* is not epistatic with a *RAD16 RAD26* double deletion

Ten-fold serial dilutions of strains that were deleted of *BUR1*, *RAD16* and *RAD26 and* transformed with combinations of plasmids encoding either wild type *BUR1* of *bur1-7*, *RAD16*, *RAD26* to cover the deletion or an empty plasmid to see the phenotype of the knockout, were subjected to UV irradiation. The additional deletion of a NER component in the *RAD26* deletion strain is supposed to show a stronger phenotype than the deletion of *RAD26* alone. Here both strains do not show sensitivity to UV irradiation but the combination of those deletions with *bur1-7*, especially at 33°C, shows a stronger sensitivity to UV damage. We conclude that *BUR1* does not act specifically in TCR because it gives an additive effect to the *RAD16* and *RAD26* knockouts pointing to an additional impairment in a different DNA repair pathway.

No additional UV sensitivity could be observed in the *Δrad16 Δrad26* double mutant strains compared to the wild type in dot spot analysis, even though it was shown in quantifications of the UV survival (Verhage *et al.*, 1996). At 30 °C all strains behave the same way in regard to the survival upon UV irradiation. When grown at 33°, semipermissive temperature, a clear impairment is visible when the *bur1-7* mutation is introduced. Cells grow already slower without irradiation but there is no difference in growth when either plasmid encoded *RAD16* of *RAD26* or both were reintroduced into the cells. Those strains also show sensitivity to UV irradiation compared to the untreated cells. As the *bur1* mutant shows a stronger sensitivity to UV irradiation than the *Δrad16*, *Δrad26* single and double mutation, a function of *BUR1* in TCR was excluded also when NER is impaired.

2.5.1.7 *BUR1* is not epistatic with *XRS2*

XRS2 is a component of the Mre11-Rad50-Xrs2 complex needed for DSB repair.
MMS sensitivities of genomically integrated *bur1-7* and *Δxrs2* as well as the double mutant were compared (Fig. 30). The deletion of *XRS2* has a strong impairment in compensation of DNA damage. Compared to this the *bur1-7* mutation is much less sensitive. But the double mutants are more sensitive than the deletion of *XRS2* alone showing that *BUR1* is not involved in DSB repair. It shows a stronger sensitivity and thus an additive effect arguing for impairment in a different repair pathway that is hit by the *bur1-7* mutation.

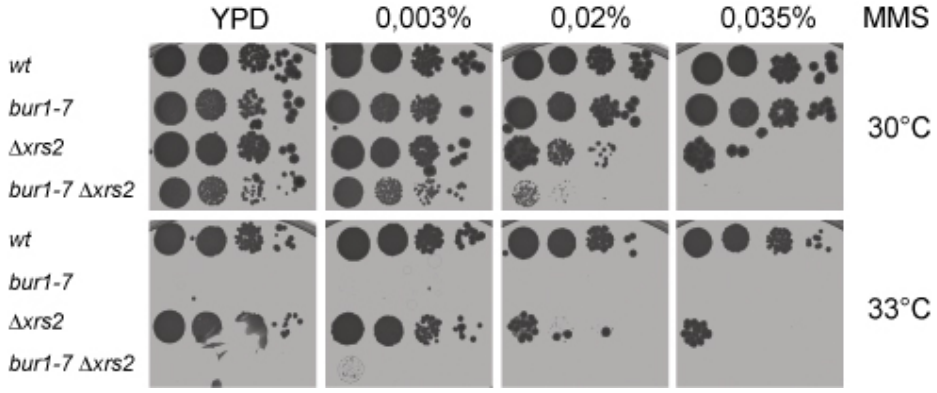

Figure 30: *BUR1* is not epistatic with *XRS2*

Ten-fold serial dilutions of strains carrying the *bur1-7* allele genomically integrated and a deletion of *XRS2,* either covered with a wild type *XRS2* encoding or empty plasmid were spotted on plates containing no drug or different concentrations of MMS. Here only *bur1-7* was tested because it shows the strongest sensitivity. The *bur1-7* mutant is sensitive when subjected to MMS already at 30°C and more severely affected at 33°C. The *bur1-7 Δxrs2* double mutant is clearly more sensitive than the single mutants showing that *BUR1* does not function in DSB repair.

2.5.1.8 *BUR1* is not epistatic with *APN1*

To elucidate a possible function of *BUR1* in base excision repair (BER), strains were created with a deletion of *BUR1* and *APN1* (Fig. 31).

The *bur1* mutants and *APN1* deletion showed no sensitivity upon MMS treatment at 30°C. However, as soon as the cells were grown at semipermissive temperature the *bur1-7* mutant and slightly also the *bur1-1* mutant as well as the corresponding double mutant strains are more sensitive than the deletion of *APN1* (Fig. 31 A). No sensitivity of the strains was visible in the quantification upon UV irradiation (Fig. 31 B). This is most likely due to a too low irradiation dose. At a higher dose the differences should be visible. The *bur1-7* and *bur1-24* mutants also show a higher sensitivity to HU at 30°C and 33°C than the *APN1* deletion. Additionally, *bur1-7* shows a slight sensitivity to Camptothecin, a drug that inhibits nucleic acid synthesis and induces DNA strand breaks, (Hsiang *et al.*, 1985) at 33°C (Fig. 31 C). Quantification of the MMS sensitivity also shows that *bur1-7 Δapn1* double mutants are more sensitive then the deletion of *APN1* (Fig. 31 D). This additive phenotype excludes a function of *BUR1* in BER.

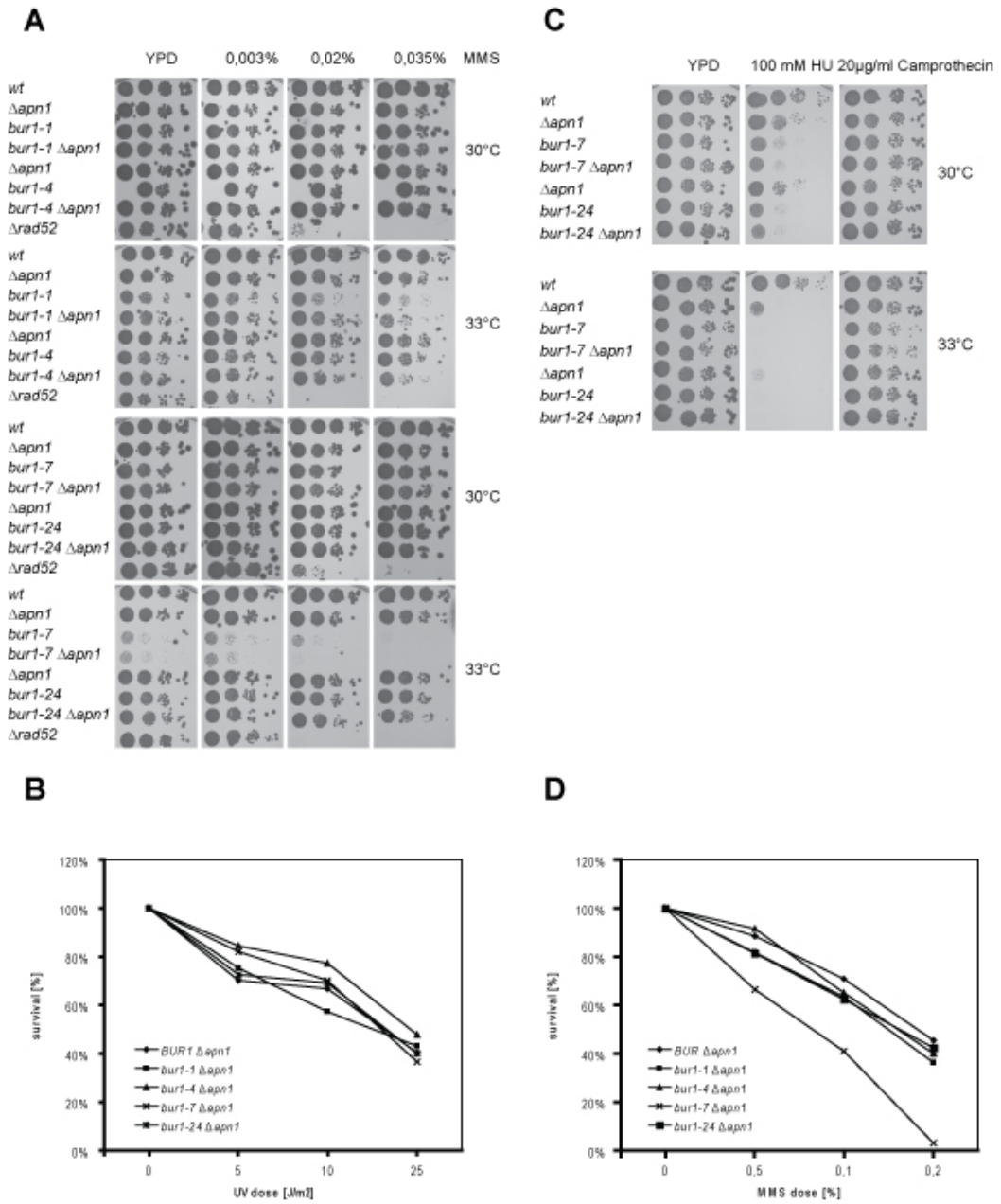

Figure 31: *BUR1* is not epistatic with *APN1*

(A) Ten-fold serial dilutions of strains carrying *bur1* mutations and a deletion of *APN1* were spotted on plates containing no drug or MMS. After induction of damage by MMS the double mutants and the *bur1* mutants are sicker than the deletion of *APN1*. Thus, *bur1* mutants are more sensitive to DNA damage than the deletion of the base excision repair gene *APN1,* excluding a function of *BUR1* in BER. (B) Quantification of the UV sensitivity. No difference could be observed in the sensitivity to UV irradiation between *bur1 Δapn1* and *Δapn1*. This is most likely due to a too low UV dose. Phenotypes could thus only be observed at higher doses. (C) Ten-fold serial dilutions of the *bur1-7* and *bur1-24* mutants with deletion of *APN1*. The *bur1* mutants, as well as the double mutants are more sensitive than the deletion of *APN1*. (D) Quantification of the MMS sensitivity. At 0.2% MMS the *bur1-7 Δapn1* double mutant becomes more sensitive than the deletion of *APN1*. These additive sensitivities exclude a function of *BUR1* in BER.

2.5.1.9 *BUR1* is not epistatic with *MAG1*

To investigate a function of *BUR1* in direct reversal of the alkylated site, strains were created with a deletion of *BUR1* and *MAG1*.

Growth of those strains on plates containing MMS shows that the *bur1-7* mutant and the *bur1-7 Δmag1* double mutant show a stronger sensitivity than the deletion of *MAG1* at 33°C and slightly on 30°C (Fig.32 A). Quantification of the UV sensitivity also shows a stronger effect for the *bur1-4 Δmag1* and *bur1-7 Δmag1* double mutants than deleting only *MAG1* (Fig.32 B). These additive effects exclude a function for *BUR1* in the direct reversal of alkylated sites.

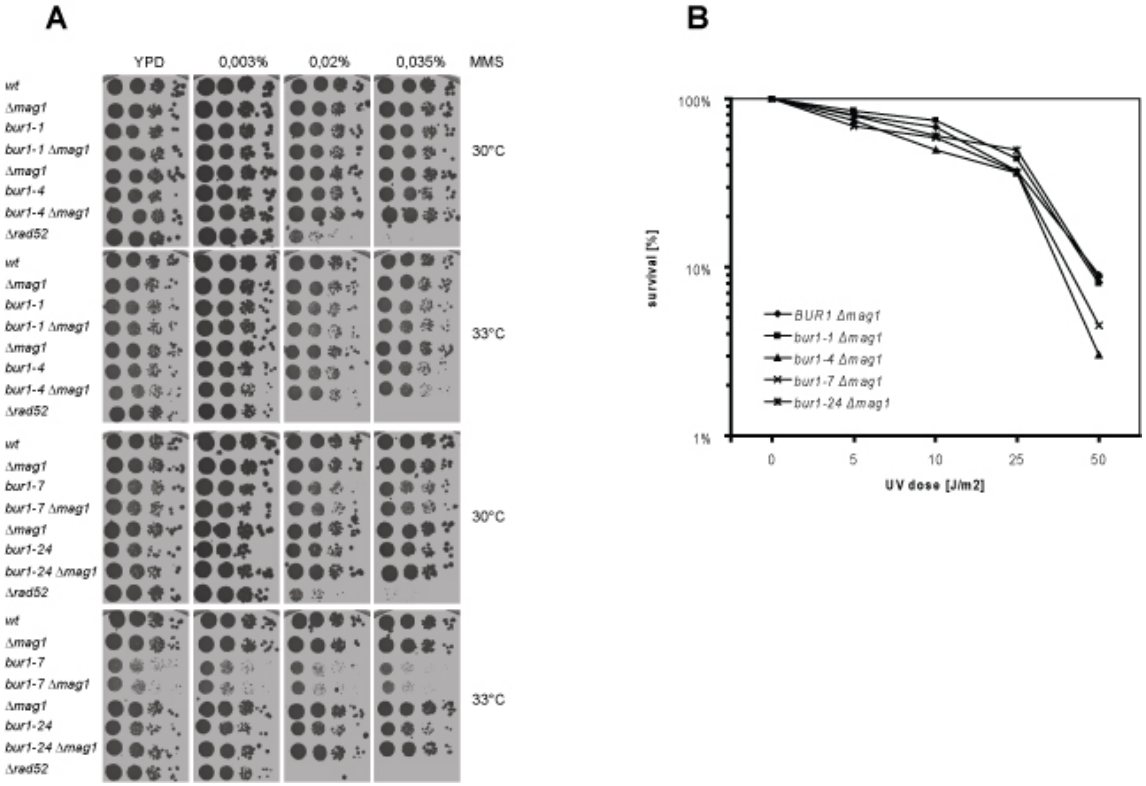

Figure 32: *BUR1* is not epistatic with *MAG1*

(A) Ten-fold serial dilutions of strains containing *bur1* mutations and a deletion of *MAG1* that was transformed either with a plasmid encoding for the wild type gene or an empty plasmid were spotted on plates containing different concentrations of MMS. After induction of damage by MMS the *bur1-7* and *bur1-7 Δmag1* double mutants are sicker than the deletion of *MAG1*. This phenotype is stronger at 33°C. (B) Quantification of the UV sensitivity. At 50 J/m2 the *bur1-4* and *bur1-7* double mutants become more sensitive than the deletion of *MAG1* alone. Thus *bur1* mutants are more sensitive to DNA damage than the deletion of the base excision repair factor *MAG1,* excluding a function of *BUR1* in BER.

2.5.1.10 *BUR1* is not epistatic with *RNR1*

To investigate a possible function of *BUR1* in DNA replication, epistasis was tested with *RNR1*.

The deletion of *RNR1* does not show sensitivity to MMS, HU and Camptothecin. In comparison, the *bur1-7* and *bur1-24* as well as the double mutants with *Δrnr1* show a stronger sensitivity to MMS and especially to HU. The phenotype on plates containing MMS is visible at 33°C, semipermissive temperature, whereas on HU the stains containing a mutation in *BUR1* show the sensitivity already at 30°C. No sensitivity of these strains could be observed on Camptothecin (Fig. 33 A). Quantification of the UV sensitivity shows, that combination of *bur1* mutants with the deletion of *RNR1* leads to an increased sensitivity of UV irradiation (Fig. 33 B). The quantification of the MMS sensitivity shows an additive effect for the *bur1-1* and *bur1-7* mutant when combined with *Δrnr1*, *bur1-24* was not determined (Fig. 33 C). The additive effect between *BUR1* and *RNR1* excludes a function in DNA replication.

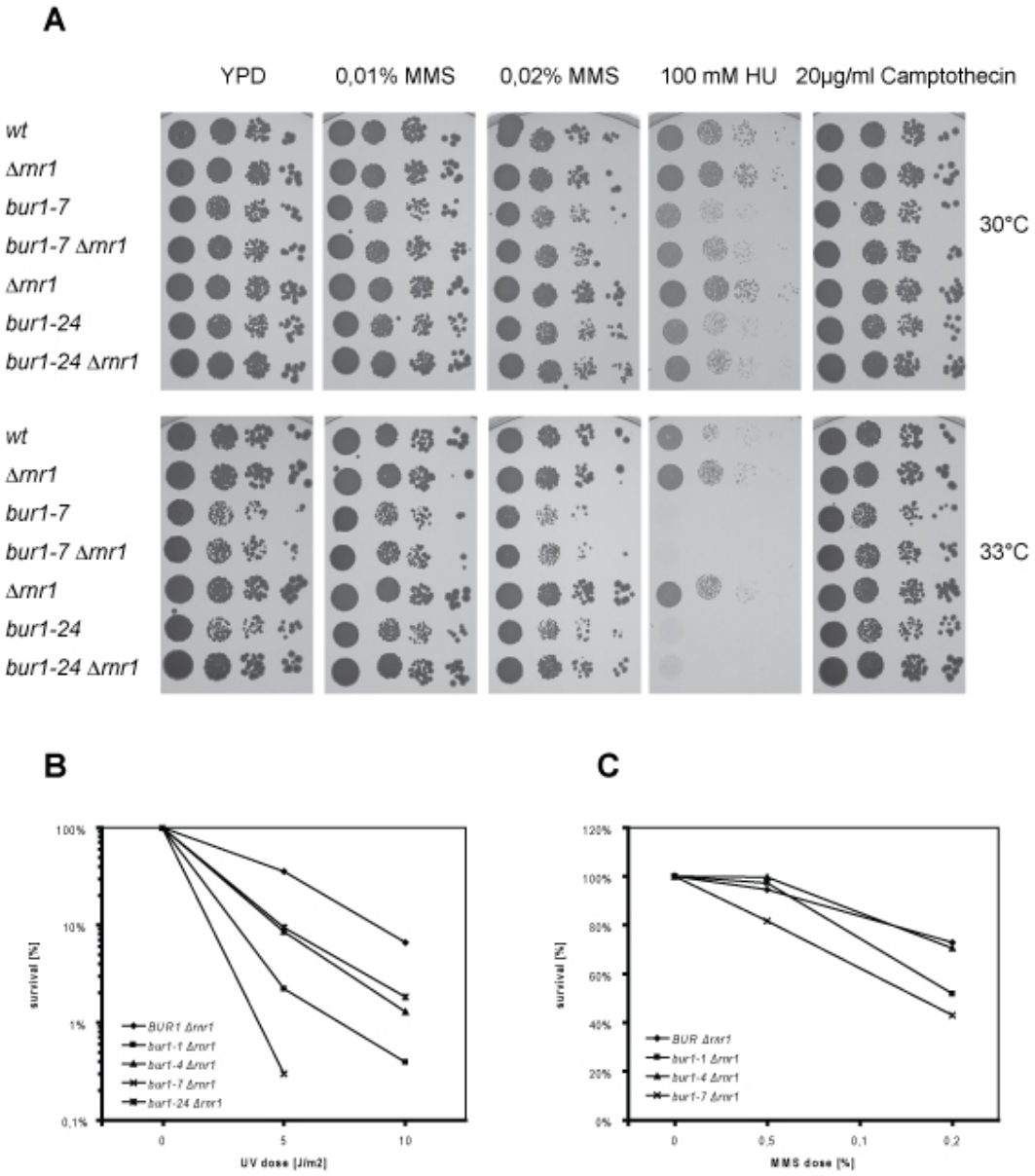

Figure 33: *BUR1* is not epistatic with *RNR1*

(A) Ten-fold serial dilutions of strains carrying *bur1* mutants and a deletion of *RNR1* that were transformed either with a plasmid containing the wild type gene or an empty plasmid were spotted on plates containing different concentrations of MMS, HU or Camptothecin. Only the *bur1-7* and *bur1-24* alleles were tested because they show the strongest sensitivity. After induction of damage the *bur1-7* and *bur1-7 Δrnr1* as well as the *bur1-24* and *bur1-24 Δrnr1* double mutants are sicker than the deletion of *RNR1* alone on MMS and HU. This phenotype is stronger at 33°C. Thus, *BUR1* mutants are more sensitive to DNA damage than the deletion of *RNR1*, excluding a function of *BUR1* in DNA replication. (B) Quantification of the UV sensitivity. The *bur1 Δrnr1* double mutants are more sensitive to UV irradiation than the deletion of *RNR1* alone showing that there is another pathway affected besides DNA replication and indicating that *BUR1* functions in a different pathway. (C) Quantification of the MMS sensitivity. Mutation of *BUR1* in addition to the deletion of *RNR1* leads to stronger sensitivity and thus to an additive effect.

2.6. Screening for high-copy suppressors of *bur1 ts* mutants

In order to find genes that have a similar function as *BUR1,* a high copy suppressor screen was performed. The principle is depicted in Fig. 34 A. Cells carrying a mutation that leads to a lethal phenotype, here the *bur1-1* and *bur1-7* temperature sensitive mutations grown at 37°C, are transformed with a library containing each yeast gene on a high copy plasmid. Genes that have a similar function as the mutated one compensate its function when highly expressed and therefore lead to growth of the cells. Transformants were grown for ten days at 37°C and the plasmids in the colonies that were able to grow again were isolated, checked for *BUR1* or *BUR2* as insert by restriction digest and retransformed into the *bur1-7* or *bur1-1* strain to verify the suppression phenotype. If it showed the suppression again the plasmid was sequenced. Both, *BUR1* and *BUR2* were identified in the screens showing that the screen worked. The new high copy suppressors identified were involved either in cell cycle regulation, *PKC1* signalling or cell wall integrity.

The cell cycle regulatory genes are *CLN2*, a G1 cyclin that activates Cdc28 and regulates the transition from G1 to S phase (Nasmyth, 1996) and *WHI3*, a RNA binding protein that sequesters the *CLN3* mRNA, which was published to suppress the deletion of *BUR1* when hyperactive (Irie *et al.*, 1991) and may be a upstream regulator of *CLN1* and *CLN2* (Tyers *et al.*, 1993). It can also retain *CDC28* to the cytoplasm and thus negatively regulates the cell cycle for the fulfilment of the critical cell size before transition of G1 to S phase (Wang *et al.*, 2004). *HSL1* is a protein kinase needed for the phosphorylation and degradation of *SWE1* (McMillan *et al.*, 1999), a kinase that regulates G2/M transition and inhibits *CDC28,* was also found among the cell cycle regulatory suppressors.

The second group of genes is involved in *PKC1* signalling. First of all, *PKC1*, a protein kinase involved in cell wall integrity, cell cycle and cytoskeleton dynamics (Heinisch *et al.*, 1999) was discovered. The other identified candidates, that are involved in this pathway are *WCS2*, a sensor of cell wall integrity and activator of the stress induced *PKC1* pathway (Verna *et al.*, 1997) as well as *SLG1* also acting upstream of *PKC1* (Jacoby *et al.*, 1998). Two other suppressors, *RHO2*, a GTPase that negatively regulates *ROM1*, and *ROM1* that is SL with ROM2, a GDP/GTP exchange factor could be found. *RHO1* and *ROM2* are also needed upstream of *PKC1* in cell wall integrity signalling (Philip and Levin, 2001). *SIA1* is an unassigned gene that is described to be an activator of the H+-ATPase on glucose and thus also

is needed for osmotic regulation (de la Fuente *et al.*, 1997) and *SKT5*, an activator for chitin synthase III (Trilla *et al.*, 1997).

An involvement of *BUR1* in *PKC1* signalling and cell wall integrity is further strengthened by two observations: First, *bur1-1* and *bur1-4* temperature sensitivity can be rescued when the cells were grown on plates containing 1M sorbitol as an osmotic stabilizer (data not shown). Second, Bur1 might phosphorylate Ste20, a MAP kinase kinase kinase that is acting in Pkc1 signalling (see Bur1 substrate finding).

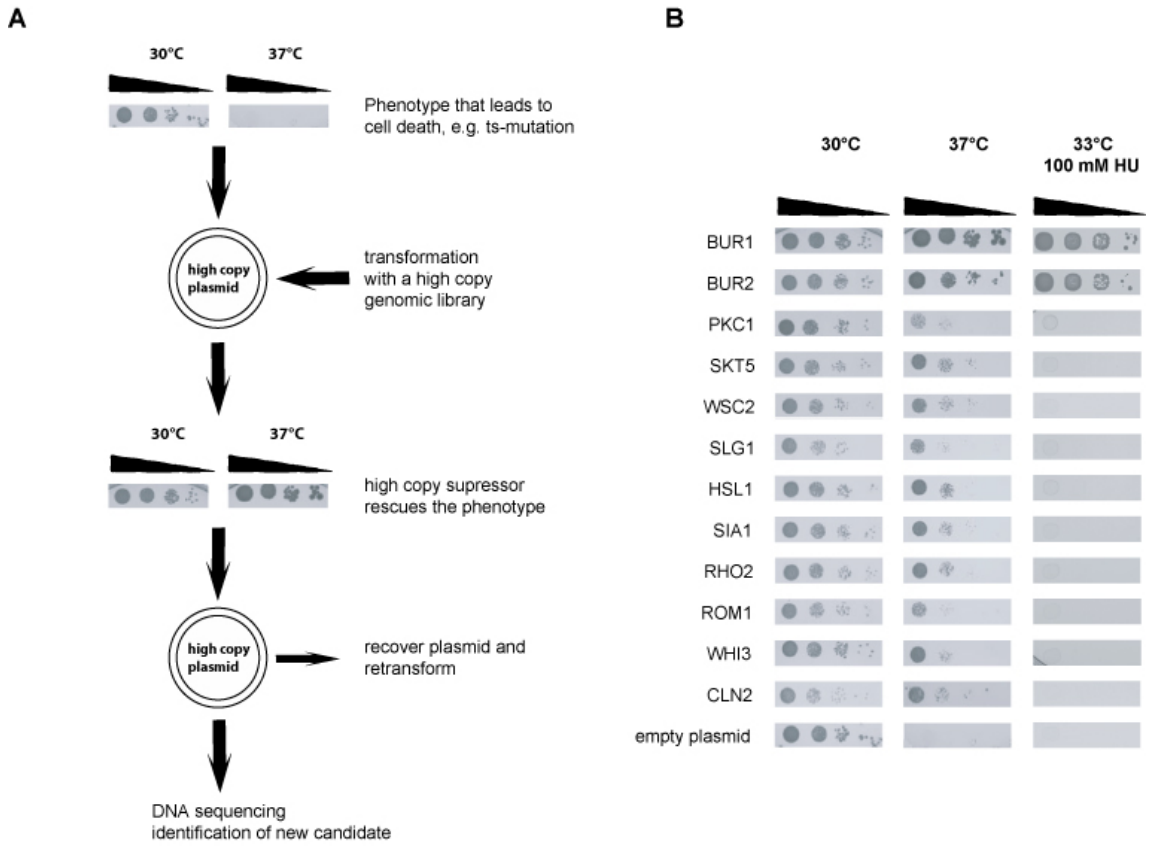

Figure 34: High copy suppressor screen of *bur1-7* temperature sensitive mutant

(A) Schematic showing the principle and workflow of a high copy suppressor screen.

(B) Overview of the suppressors found in the *bur1-7* screen at 37°C. Most of the suppressors act either in cell cycle, *PKC1* signalling or the cell wall integrity pathway. Noteworthy, those suppressors can not rescue the sensitivity to HU and thus might not be applicable to explain the function of *BUR1* in DNA damage or replication stress.

The high copy suppressor candidates from both screens, from *bur1-1* and *bur1-7* could also suppress the other mutation, respectively. Non of them was able to suppress the deletion of *BUR1* (not shown).

Other cell cycle regulatory genes, like *CDC28*, *CLB1*, *CLB6* and *CLN3* were also tested in a defined way but did not suppress the *bur1* mutants (data not shown).
Screens on MMS and HU were also performed to identify DNA damage or replication suppressors of *BUR1* mutants but did not lead to the identification of candidates.

2.7. Screening for *in vitro* substrates of Bur1 kinase

To identify the substrate of Bur1 kinase assays were performed. Two approaches were chosen (Fig. 35).
In the first one, putative substrates were tested in a defined manner by TAP purifying them and testing with an *in vitro* kinase assay.
The second one was a whole proteome approach using Protoarrays, protein arrays carrying 4088 yeast ORFs expressed as GST-6xHIS fusion proteins (Kung and Snyder, 2006) that can serve as substrates for phosphorylation.

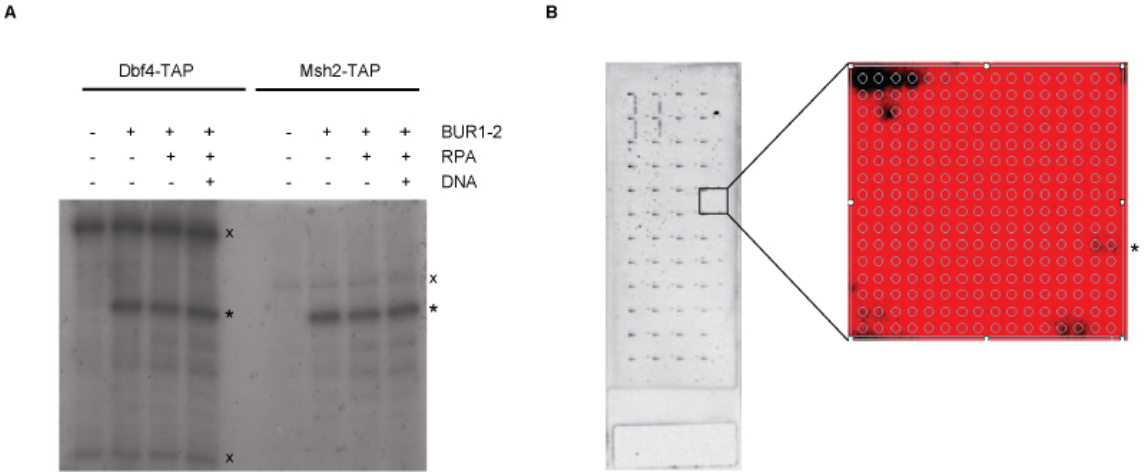

Figure 35: Two approaches for identifying substrates for Bur1 kinase
(A) An example of an *in vitro* kinase assay is shown. The putative substrates, Dbf4 and Msh2 were TAP purified and incubated either with a mock purification, BUR, BUR and RPA or BUR, RPA and activated DNA. Bands marked with (x) are an example for an unspecific phosphorylation as they are also detectable in the first lane that was just incubated with a mock purification. Bands marked with (*) show the auto-phosphorylation of Bur1.
(B) Identification of Bur1 substrates using Protoarrays. Phosphoimager scan of a Protoarray incubated with Bur1 and a representative cut-out from the analysis using GenePix Pro 6.0. Shown here is the identification of Ste20 (*) to depict the principle.

2.7.1 Substrate finding using an *in vitro* kinase assay

Putative substrates for Bur1 kinase were purified by TAP purification. Four different experiments were performed. First, just the substrate was incubated with a mock purification from an untagged wild type strain to see either auto- or unspecific

phosphorylation. In the second test, the possible substrate was incubated with Bur1 kinase, prepared by a high salt wash during the purification, to wash off RPA. The third trial was incubated with TAP purified Bur1 bound to RPA to see if the substrate specificity changes when the BUR complex is bound to RPA. The fourth setup was incubated with BUR, RPA and activated DNA because the binding of the BUR and RPA complex to the substrate might be mediated via DNA. The kinase and substrate preparations were incubated with radioactive γ-32P-ATP, separated by SDS-PAGE and phosphorylation was detected by autoradiography (Fig. 35 A).

Several possible substrates from different processes like cell cycle, checkpoint regulation, chromatin remodelling, DNA repair and transcription associated processes were tested: RPA, Rad3, Htz1, Ddc2, Dbf4, Cdh1, Ioc3, Dbp2, Dpb4, Msh2, Mph1, Snd1, Snf2, Mre11, Rnh1, Spt4, Hmo1, Ela1, Pho23, Cps60, Rad52, Rad9, Rsp5, Sir2, Sir3, Swi6 and Thp1. No substrate could be identified using this approach.

2.7.2 Substrate finding using Protoarrays

Additionally, a whole proteome approach was performed using Protoarrays. These arrays were incubated with TAP purified Bur1 kinase in the presence of γ-33P-labelled ATP in TAP buffer, because Bur1 was inactive in the buffer originally coming with the Protoarrays. The arrays were subsequently incubated on a Phosphoimager and analyzed using GenePix Pro 6.0 (Fig. 35 B).

Four putative substrates were identified using this assay:

Ste20, a serine threonine kinase involved in MAP kinase signalling in response to pheromone or high osmolarity (Drogen *et al.*, 2000) and histone H2B Ser10 phosphorylation (Ahn *et al.*, 2005). Ste20 can be phosphorylated by Cln2-Cdc28 (Wu *et al.*, 1998). Thus, it might also just be a good substrate for cyclin dependent kinases and the phosphorylation could be unspecific. Furthermore, Ste20 auto-phosphorylates (Leberer *et al.*, 1997) which also raises the possibility for an unspecific phosphorylation which has to be further investigated.

Additionally, Ptk2, a putative serine/threonine kinase with a function in ion homeostasis (Erez and Kahana, 2002), together with Sky1, was identified.

The third substrate identified is Rim11, a kinase needed for entry into meiosis (Mitchell and Bowdish, 1992) which could also explain the synthetic sick phenotype of *BUR1* with *RAD52* without the induction of DNA damage because *RAD52* is also needed for meiosis. Rim11 is also important for the phosphorylation of Ume6 and the

complex formation of Ume6 and Ume1 (Malathi *et al.*, 1997), a protein complex also needed for meiosis. Interestingly, Ume6 is also crucial for binding the URS1 upstream regulatory sequence and recruitment of RPA to it (Luche *et al.*, 1993). Additionally, Ume6 recruits the Rpb3-Sin3 histone deacetylase complex to promoters (Kadosh and Struhl, 1997). This complex counteracts Bur1 (Keogh *et al.*, 2005). Hence, the phosphorylation by Bur1 might offer a mechanism for regulating the recruitment of these factors.

The last substrate identified is Bcy1, a regulatory subunit of the cyclic AMP-dependent protein kinase (PKA) that is important for the cellular response to stress like heat shock or starvation and for sporulation (Toda *et al.*, 1987).

2.9 Mutation of *BUR1* causes genomic instability

We were particularly interested if the number of Rfa1 and Rad52 containing replication or repair foci changes depending on the *bur1* mutants. For this, Bur1-GFP and Rfa1-RFP tagged strains were created and investigated by fluorescence microscopy.

To make sure that the GFP and RFP tagged proteins still interact biochemically, a pulldown assay was performed. Bur1-GFP was purified and a subsequently tested for the interaction with RPA in a Western blot using an antibody against RFP. Untagged Bur1 was used as a negative control (Fig. 36).

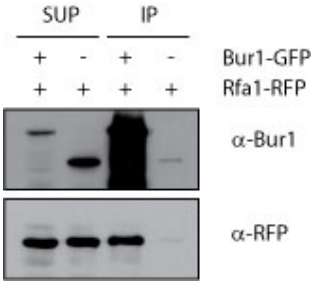

Figure 36: Bur1-GFP and Rfa1-RFP interact biochemically

Bur1-GFP was purified using GFP-binder coupled beads. Western blotting shows an enrichment of Bur1-GFP in the purification. There was no unspecific binding to the resin when untagged Bur1 was used as a negative control. Rfa1-RFP was detected using an antibody directed against RPF. The tagged proteins still copurify.

The whole cell extracts of the corresponding strains contained the proteins as expected. Detection of Bur1 in the extract of the GFP tagged strain lead to an upshift of the protein due to the GFP. In the IP, a lot of degraded protein is detected by the Bur1 antibody which is not seen in TAP purifications. Thus, this is most likely due to

the GFP based protein purification and degradation of the GFP tag. Rfa1-RFP can be detected in the IP together with Bur1-GFP but not in the control purification showing that the tagged proteins are still able to interact (Fig. 36).

In collaboration with Susanne German and Michal Lisby the influence on genome stability of *bur1* mutants was investigated by looking at the appearance of nuclear foci, DNA damage and replication factories that contain, among others, RPA (Lisby *et al.*, 2004) (Fig. 37 A). The fist observation is, that in the bur1-*7, bur1-24* and *bur1-ΔC* mutants, the overall levels of foci is increased (Fig. 37 B), hinting to more DNA repair or replication ongoing in these cells, which corresponds to the sensitivity of those cells to DNA damage inducing agents. To further investigate if these foci are involved in DNA replication or repair, additionally the co-localisation of Rad52-YFP with those foci was examined. Foci, that contain Rad52 show ongoing homologous recombination, indicating that they are involved in DNA repair. The *bur1-7, bur1-24* and *bur1-ΔC* clearly have increased levels of ongoing homologous recombination, indicating genome instability. Moreover, some of them also fail to suppress Rad52 foci upon addition of hydroxyurea, which is normally seen for the wildtype. This mutant phenotype may be due to slow disassembly (DNA repair) of existing Rad52 foci or a failure to suppress de novo recruitment of Rad52 to sites of DNA damage in the presence of HU. The first possibility is favoured because the Rad52 foci are very bright indicating slow repair, but further experiments are needed to un-ambiguously distinguish between these possibilities. Additionally, the overall percentage of cells containing Rad52 foci was determined in the *bur1-7* mutant after prolonged HU treatment. This mutant shows strongly elevated levels of Rad52 foci after one to three hours of HU incubation. Again, this shows that in these cells more homologous recombination is going on (Fig. 37 C). These results show that *bur1* mutant cells are impaired in genome maintenance.

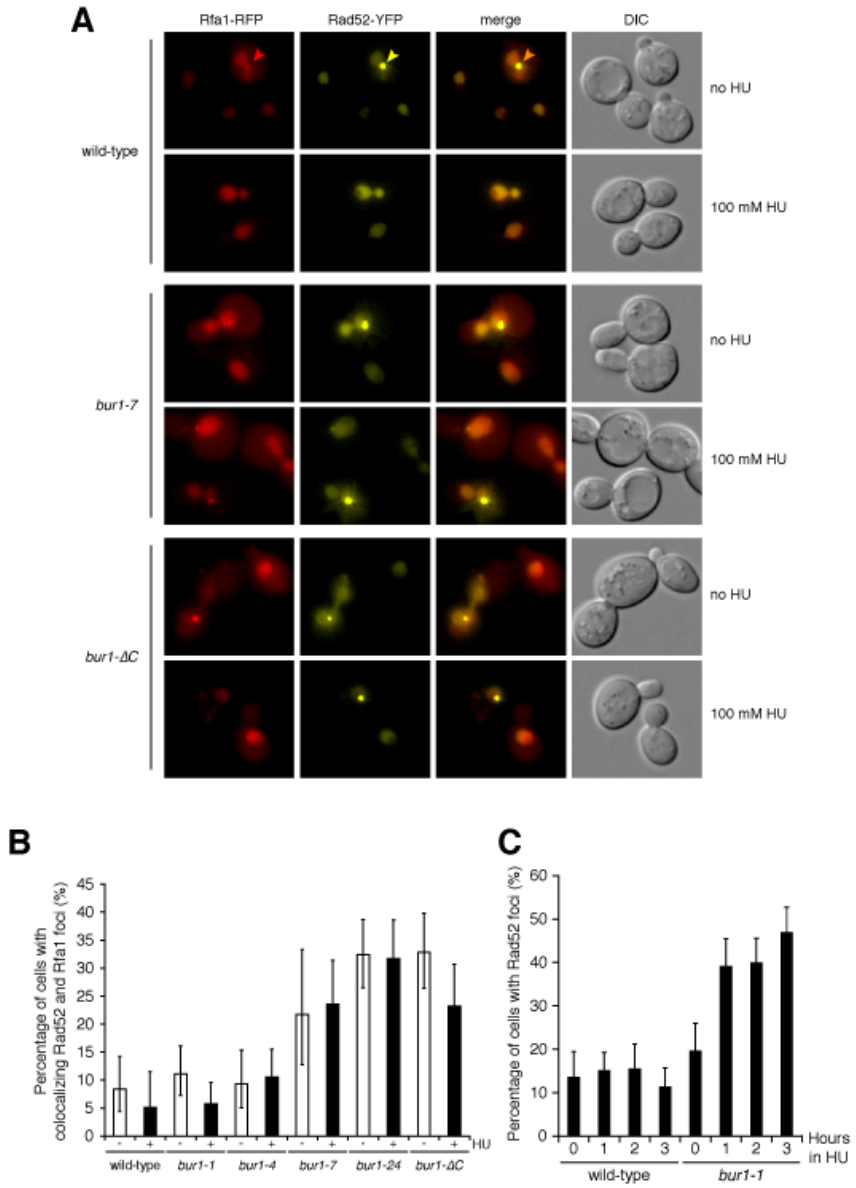

Figure 37: Increased formation of Rad52 foci in bur1 mutants.

(A) Colocalizing Rfa1-RFP and Rad52-YFP foci in *bur1* mutants. Wild-type and *bur1* (*bur1-1*, *bur1-4*, *bur1-7, bur1-24* and *bur1-ΔC*) mutant strains expressing Rfa1-RFP and Rad52-YFP ectopically (pWJ1213) were grown in SC-His at 30 °C. The occurrence of Rfa1-RFP and Rad52-YFP was determined by fluorescence microscopy before and after exposure to 100 mM hydroxyurea (HU) for 1 hour. Representative cells are shown. Selected foci are indicated by arrowheads. (B) Quantification of Rfa1 and Rad52 foci. For each genotype, 100-200 cells were inspected. Error-bars indicate 95% confidence intervals. In the absence of HU, the percentage of cells with colocalizing Rfa1 and Rad52 foci is significantly higher than wild-type in the *bur1-7*, *bur1-24* and *bur1-ΔC* mutants (P=0.007, P=1.63×10-8, P=2.59×10-8, respectively, by Fisher's exact test (one tailed)). The *bur1-1* and *bur1-4* mutants display focus levels similar to wild-type (P=0.26 and P=0.48, respectively). (C) Rad52 foci accumulate in HU-treated *bur1-7* cells. The experiment was performed as described for panel B, except that cells were examined for Rad52 foci at 0, 1,2, and 3 hours after addition of 100 mM HU.

2.10. Role of RPA in transcription

2.10.1 *RFA1* and TREX do not interact genetically

Bur1 was found in our lab to be synthetic lethal with TREX. This points to a functional overlap between the BUR and the TREX complex. BUR copurifies with RPA, a protein complex essential for DNA repair and replication. As TREX also has subunits, *HPR1* and *THO2,* that are important for DNA repair (Gonzalez-Barrera *et al.*, 2002) synthetic lethality was also tested between TREX and RPA. No genetic interaction could be detected with the RPA mutants that were generated (Fig. 38). (*rfa1-249*, *rfa1-6*, *rfa2-1-4*, *rfa2-26-2*, *rfa3-6-2*, *rfa3-8-2*, *rfa3-16-1*, Clausing and Winkler, unpublished data)

TREX subunit	RPA subunit	SL
HPR1	*RFA1*	-
MFT1	*RFA1*	-
HPR1	*RFA2*	-
MFT1	*RFA2*	-
HPR1	*RFA3*	-
MFT1	*RFA3*	-
THO2	*RFA3*	-
THP2	*RFA3*	-

Figure 38: TREX and RPA do not interact genetically

Double mutant strains carrying deletions of TREX components and RPA subunits were tested for a synthetic lethal phenotype. No interaction was detected using *rfa1*, *rfa2* or *rfa3* mutants with the TREX deletions tested (*HPR1, MFT1, THO2, THP2*).

2.10.2 A *rfa1* mutant shows synthetic sickness with *DST1* and *RTF1*

The sensitivity of the *rfa1-249* mutant to 6'-AU suggests a function of RPA in transcription elongation. This mutation also suppresses mutations in *BUR1*, which is crucial for efficient transcription elongation. Genetic interactions of the *rfa1* mutant were tested with *RTF1*, a component of the PAF transcription elongation complex and thus closely related to *BUR1* function, and *DST1*, coding for TFIIS. Interestingly *rfa1-249* is synthetic sick with *Δrtf1* as well as *Δdst1*. This phenotype can be

enhanced by growing the cells on media containing 6'-AU (Fig. 39). The genetic interaction points to a function for RPA in transcription elongation.

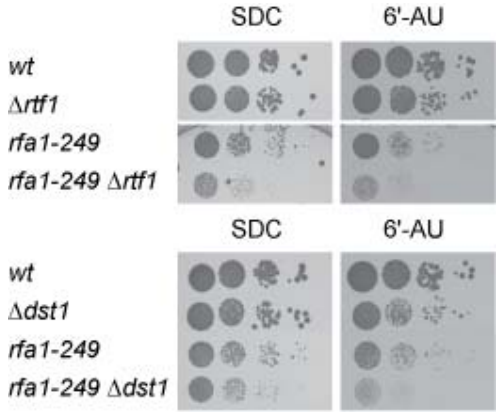

Figure 39: *RFA1* is synthetic sick with *RTF1* and *DST1*

RFA1 RTF1 and *RFA1 DST1* double shuffle strains were transformed with *RFA1, rfa1-249* and *RTF1, DST1* or an empty plasmid, shuffled and spotted on plates selective for the plasmids and containing either no drug or 6'-AU. Already without the drug the *rfa1-249* mutant shows a synthetic growth defect with deletions of *RTF1* or *DST1* indicating a function of *RFA1* in transcription elongation.

2.10.3 A *rfa1* mutant has lower levels of histone H3

The BUR complex was described to have a function in histone methylation and *Δbur2* strains were shown to have lowered amounts of histone H3 (Laribee *et al.*, 2005). The impact of the *bur1-7* and *rfa1-249* mutants on histone H3 levels and histone modifications was tested. Cells were grown at different conditions. Control experiments were performed at 30°C and the influence of the temperature sensitive mutants was directly tested by shifting cells to 37°C for 3 hours. DNA damage was induced by growing the cells in 0,1% MMS for 2h, replication stress was induced by 50 mM HU for 2 hours and transcription stress by 100 µg/ml 6'-AU for 2 hours. Cells were harvested, lysed and subjected to SDS-PAGE and Western blot analysis. First, the amount of total histone H3 in the extracts in comparison to Pgk1 was tested to achieve equal loading for further analysis. Interestingly, lowered levels of histone H3 were detectable in the *rfa1-249* mutant strains whereas this effect was rather low in the *bur1-7* mutant. An impact of the mutants is not visible at 30°C. At 37°C and upon treatment with MMS the *rfa1* mutant shows a significant lower amount of histone H3 compared to Pgk1, used as loading control. This is not visible in the *bur1-7 rfa1-249* double mutant which might explain the suppression of their phenotypes. It is also possible that the histone H3 levels are simply a secondary effect of the impaired cellular growth. The slowest growing cells might have the lowest levels of histone H3

(this might also be the case for *Δbur2* in the literature as it is also impaired in growth). Upon treatment with HU lowered histone H3 levels can be seen in both, the *rfa1-249* mutant alone as well as in the *bur1-7 rfa1-249* double mutant. The same phenotype, even though to a lower extent, can be detected upon treatment with 6'-AU (Fig. 40).

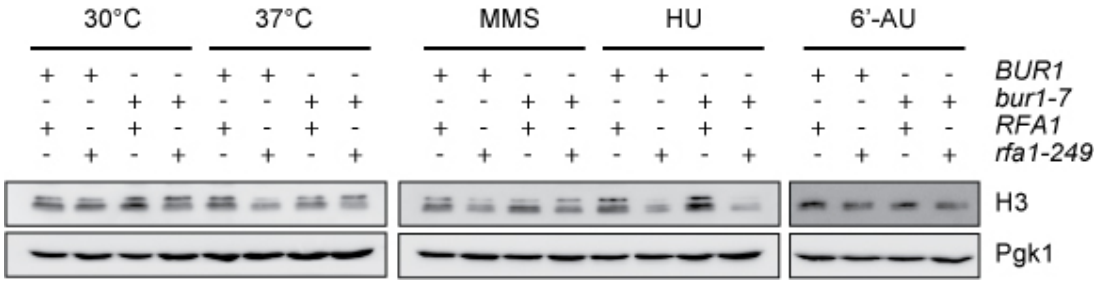

Figure 40: The *rfa1-249* mutant has lower levels of histone H3 upon stress

BUR1 RFA1 double shuffle strains were transformed with *BUR1*, *bur1-7* and *RFA1* or *rfa1-249*. The cells were grown under different conditions, 30°C as control, 37°C to see the effect of the ts mutants, MMS to induce DNA damage, HU to induce replication stress and 6'-AU to induce transcription stress. Whole cell extracts of these strains were analyzed by Western Blot using an antibody directed against unmodified histone H3. The overall cellular levels of histone H3 are significantly lowered in cells containing the *rfa1-249* mutation after stress. Pgk1 serves as a loading control.

2.10.4 The rfa*1-249* mutant has lower levels of histone H3 Lysine 4 trimethylation but is not impaired in H2B ubiquitination

The impact of the *bur1* and *rfa1* mutants on the methylation of histone H3K4 trimethylation was investigated. Again the cells were grown under different conditions and the cell extracts were subjected to SDS-PAGE and Western blotting. Equal loading of histone H3 was achieved by loading three two-fold serial dilutions of every extract and quantification of the Western blots afterwards. For the following blots equal amounts of histone H3 were loaded for every sample and tested for several transcription associated histone modifications. Differences in methylation were detectable in the H3K4me3. At 30°C only a very slight defect is visible. Both the *rfa1-249* and the *bur1-7* mutant are slightly impaired and the double mutant a slightly more (Fig. 41 A). When the cells were shifted to 37°C the *rfa1* mutant alone again showed only a slight defect whereas the *bur1-7* mutant shows a strong decrease in H3K4me3, which is also published for the deletion of *BUR2* (Laribee *et al.*, 2005). The *rfa1-249 bur1-7* double mutant shows the same phenotype as the *bur1-7* mutant (Fig. 41 B). When the cells were challenged with either 6'-AU, MMS or HU (Fig. 41 C, D, E) the single mutants alone were still almost unaffected whereas the double

mutant cells show a lower level of H3K4me3. The H3K4me and H3K4me2 were unaffected as well as H3K36me3 and H3K79me2 under all conditions examined. Detection of histone H4 Lysine 12 acetylation serves as a second loading control, using a different histone subunit, in addition to unmodified histone H3 (Fig. 41).

As the H3K4me3 is dependent on the ubiquitination of histone H2B (H2Bub) (Sun and Allis, 2002) and *Δbur2* cells are impaired in H2Bub (Laribee *et al.*, 2005), the impact of the *rfa1* mutation on H2Bub was also tested. Comparison of cell extracts from cells carrying the *rfa1-249* mutation grown either at 30°C or shifted to 37°C showed no significant difference in the ubiquitination of histone H2B (Fig. 41 F).

These results show a specific impairment on H3K4me3 in the *bur1-7 rfa1-249* double mutant strains, most likely without an impairment in H2Bub. This indicates a lowered level of transcription elongation, which is surprising, because these strains grow better than the *rfa1-249* single mutant. Hence, the suppression does not depend on the methylation of histone H3.

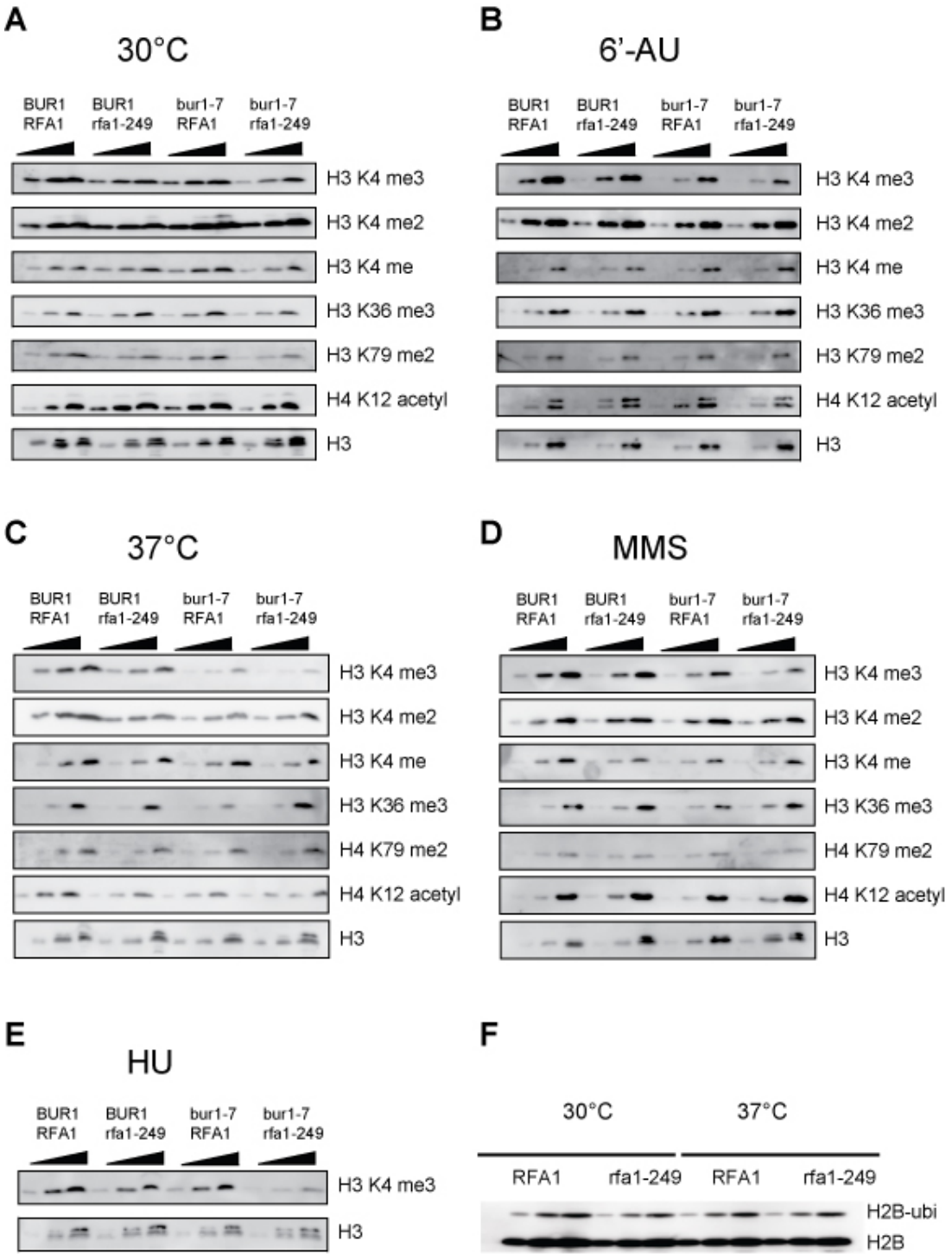

Figure 41: *bur1* and *rfa1* mutants are impaired in histone H3 lysine 4 trimethylation

BUR1 RFA1 double shuffle strains were transformed with *BUR1*, *bur1-7* and *RFA1 or rfa1-249*. The cells were grown under different conditions, (A) 30°C as control, (B) 6'-AU to induce transcription stress , (C) 37°C to see the effect of the ts mutants, (D) MMS to induce DNA damage and (E) HU to induce replication stress. (A-E) Whole cell extracts of these cells were analyzed by Western Blot using antibodies directed against histone H3K4me3, H3K4me2, H3K4me, H3K36me3, H3K79me2 and

H4K12 acetylation as well as unmodified histone H3 as loading controls. The protein amount was calibrated to the same amount of histone H3. Three two-fold dilutions of every extract were analyzed. The *rfa-249* mutant alone shows no or only slight impairment of H3K4me3. When grown at 37°C the *bur1-7* mutants show lowered levels of H3K4me3 which is consistent with the literature. Interestingly, *bur1-7 rfa1-249* double mutants show a stronger impairment in the trimethylation than the single mutants. This indicates a function for both proteins in histone H3 Lys4 trimethylation. (F) The *rfa1-249* mutant is not impaired in histone H2B ubiquitination.

2.10.5 *RFA1* mutants are impaired in a LacZ reporter gene expression

The influence of mutations in either *BUR1* or the *RFA1* on gene expression was examined using a β-galactosidase reporter gene assay. This gene is rather long and GC rich and its activity and amount can be easily detected by measuring the absorbance of a ortho-nitrophenyl-β-D-galactopyranoside (ONPG) catabolization at 420 nm (Miller, 1972). Yeast cells impaired in transcription elongation or a later step in gene expression might show an impairment in expressing this bacterial gene stronger than with a yeast gene. The *bur1-1, bur1-4, bur1-7* and *bur1-24* mutations were genomically integrated into a wild type strain, transformed with a plasmid containing the β-galactosidase reporter under control of the *GAL1* promoter. The *rfa1-249* mutant was tested in a *Δrfa1* strain covered with either a wild type *RFA1* or a plasmid coding for *rfa1-249* (Fig. 42).

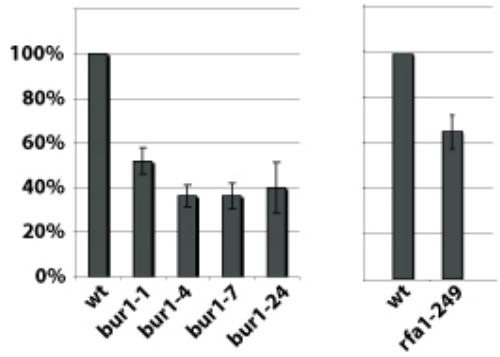

Figure 42: *bur1* and *rfa1* mutants show a decrease in β-galactosidase expression

(A) *bur1* temperature sensitive mutations were genomically integrated in a wild type strain. These strains were transformed with a plasmid containing a galactose inducible β-galactosidase gene. The reporter gene expression is decreased in *bur1* mutant strains.

(B) A *RFA1* shuffle strain was transformed with *RFA1* or *rfa1-249*, shuffled on 5'-FOA containing plates and transformed with the β-galactosidase reporter. The expression is also lowered in the *rfa1-249* mutant strain.

Cells were grown using raffinose as the carbon source, which does not affect the *GAL1* promoter. The expression of the reporter construct was induced adding galactose and letting the cells grow for eight hours logarithmically. The cells were harvested, lysed by three freeze and thaw cycles and the β-galactosidase expression was tested by measuring the absorbance of ortho-nitrophenyl-β-D-galactopyranoside (ONPG) at 420 nm in an ELISA reader. Mutations in the *BUR1* gene lead to a reduction to 40-50% in expression. Noteworthy, also the *RFA1* mutant is impaired and shows a reduction to 70% showing a direct influence of *RFA1* on gene expression (Fig. 42).

2.10.6 Influence of the *bur1-7* and *rfa1-249* mutation on Rad53 phosphorylation, RNApolII and Ctk1 levels

To get further molecular insight into the cellular changes of strains carrying the *bur1-7* or *rfa1-249* mutation or both cells were grown at 30°C or 37°C and subjected to DNA damage by MMS or not. First phosphorylation of the DNA damage effector kinase Rad53 was examined. Rad53 is not phosphorylated under normal conditions but when DNA damage is induced, *e.g.* by MMS, it becomes phosphorylated which can be seen by an upshift of the protein in Western analysis. No difference in Rad53 phosphorylation is detectable when the cells were grown at permissive temperature. There might be a slight impairment in the phosphorylation upon shift to 37°C indicating a problem in checkpoint signalling dependent on the *bur1* and *rfa1* mutation and strengthening the point for a function in DNA repair. The overall levels of RNApolII (8WG16) are reduced upon DNA damage, probably due to degradation of the enzyme. Phosphorylation on Serine 2 (H5) goes down in the wild type strain upon MMS treatment and seems to be higher when *BUR1*, *RFA1* or both are mutated. The pool of RNApolII is thus shifted to the elongating form instead of the initiating one to avoid recruitment of additional RNApolII to the damaged DNA and subsequently allow DNA repair. The level of Bur1 is slightly elevated in the *bur1-7* mutant strain and does not show the higher molecular weight band that is most likely due to the phosphorylation by Cak1. In the strains carrying the *bur1-7* mutation also Ctk1 is more expressed than in the strains without the mutation, indicating that Ctk1 might take over some of the functions of Bur1. Pgk1 serves as loading control. The same experiments were performed with a strain carrying the *BUR1* mutation and additionally a deletion of *RAD16*, needed for efficient nucleotide excision repair, as a

control for the specificity of the effects due to *RFA1*. Despite a small reduction in the overall levels of RNApolII (8WG16) there is no change in the protein levels examined (Fig. 43).

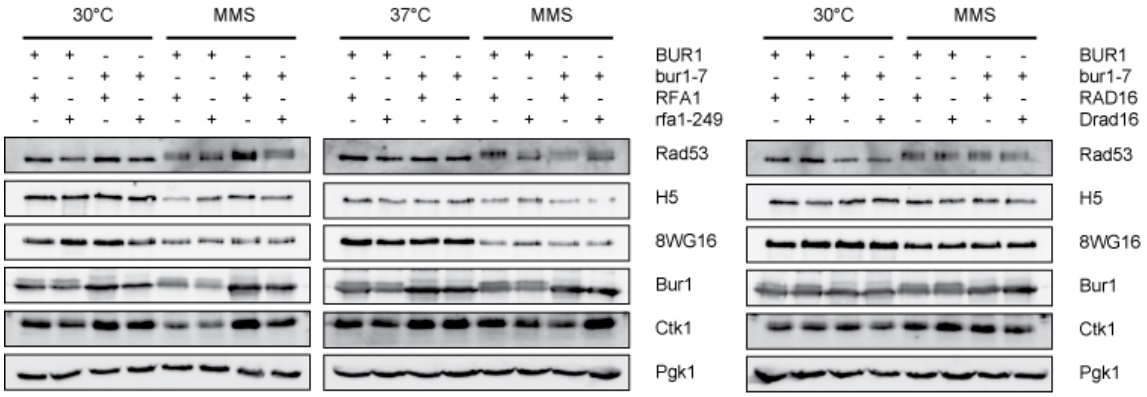

Figure 43: Expression analysis of checkpoint and transcription associated proteins in *bur1-7* and *rfa1-249* strains upon DNA damage

BUR1 RFA1 double shuffle strains were transformed with *BUR1*, *bur1-7* or *RFA1* and *rfa1-249* and shuffled on 5'FOA. Cells were grown at 30°C or 37°C and DNA damage was induced with 0.2% MMS for one hour. Afterwards, they were lysed by alkaline lysis and subjected to SDS-PAGE and Western blotting. Rad53 is a checkpoint effector kinase that becomes phosphorylated upon DNA damage. At 30°C there is no impairment in Rad53 phosphorylation but upon DNA damage at 37°C there might be a minor impairment in the *bur1-7* and *rfa1-249* strains. The levels of RNApolII (8WG16) are lowered upon DNA damage but the level of S2 phosphorylation (H5) is higher compared to the wild type in relation to the RNApolII levels. This indicates less transcription initiation upon DNA damage in the *bur1-7* and *rfa1-249* mutants. The levels of Bur1 might be elevated in strains carrying the *bur1-7* mutation and loose the second higher molecular weight band. Noteworthy, also Ctk1 expression goes up in these strains indicating that Ctk1 might take over part of the function of Bur1. Pgk1 serves as a loading control. Rad16 serves as a control for an independent DNA damage protein. Here the phenotypes described before are not visible, showing specificity for BUR and RPA.

2.11 Genome wide expression analysis *bur1* and *rfa1* mutants upon DNA damage

To investigate the expression of the whole yeast genome dependent on the *bur1-7* and *rfa1-249* single and double mutants upon DNA damage, microarray experiments were performed. Cells were grown logarithmically over night at 30°C before the addition of 0.1 % MMS for one hour, which was shown to have the most comprehensive effects on gene expression (Jelinsky and Samson, 1999). RNA was isolated and subjected to Affymetrix GeneChip Yeast Genome 2.0 arrays in collaboration with Andreas Mayer from Patrick Cramer's laboratory and Achim

Tresch. Experiments were performed in triplicates with a high level of reproducibility which depicted in the PCA mapping, showing that the experiments with the corresponding strains cluster with each other (Fig.43 A) after removal of a batch effect due to different days of RNA extraction. One of the experiments with the double mutant strains was left out from the data analysis due to problems with the array hybridisation. However, due to the high reproducibility of the experiments this still lead to significant expression data.

Compared to an isogenic wild-type strain, 41, 60 and 54 genes out of 5665 genes that were present on the array showed significantly altered mRNA levels in the *rfa1-249*, *bur1-7* and *bur1-7 rfa1-249* mutant strains, respectively (Fig. 44 B). Thus, the regulation of only a small subset of genes was affected by the different mutations (0.7% in *rfa1-249* and 1% in *bur1-7*). Although several genes were differentially expressed in at least two mutants the analysis revealed also genes affected in only one of the respective mutants. The largest overlap of significantly altered genes could be detected for *bur1-7* and the *bur1-7 rfa1-249* double mutant (22 genes), the smallest overlap was between *bur1-7* and *rfa1-249* single mutants (11 genes) (Fig. 44 B).

Hierarchical clustering of the expression profiles shows that the *bur1-7* and the *bur1-7 rfa1-246* double mutant strain cluster together whereas the single mutant *rfa1-249* does not. Mutation of *RFA1* and *BUR1* results in distinct changes of the transcriptome whereas the double mutation gives rise to a gene expression profile that is more similar to that of the *bur1* mutant (Fig.43 C). This result might explain the suppression of these strains seen in the sensitivity to DNA damage.

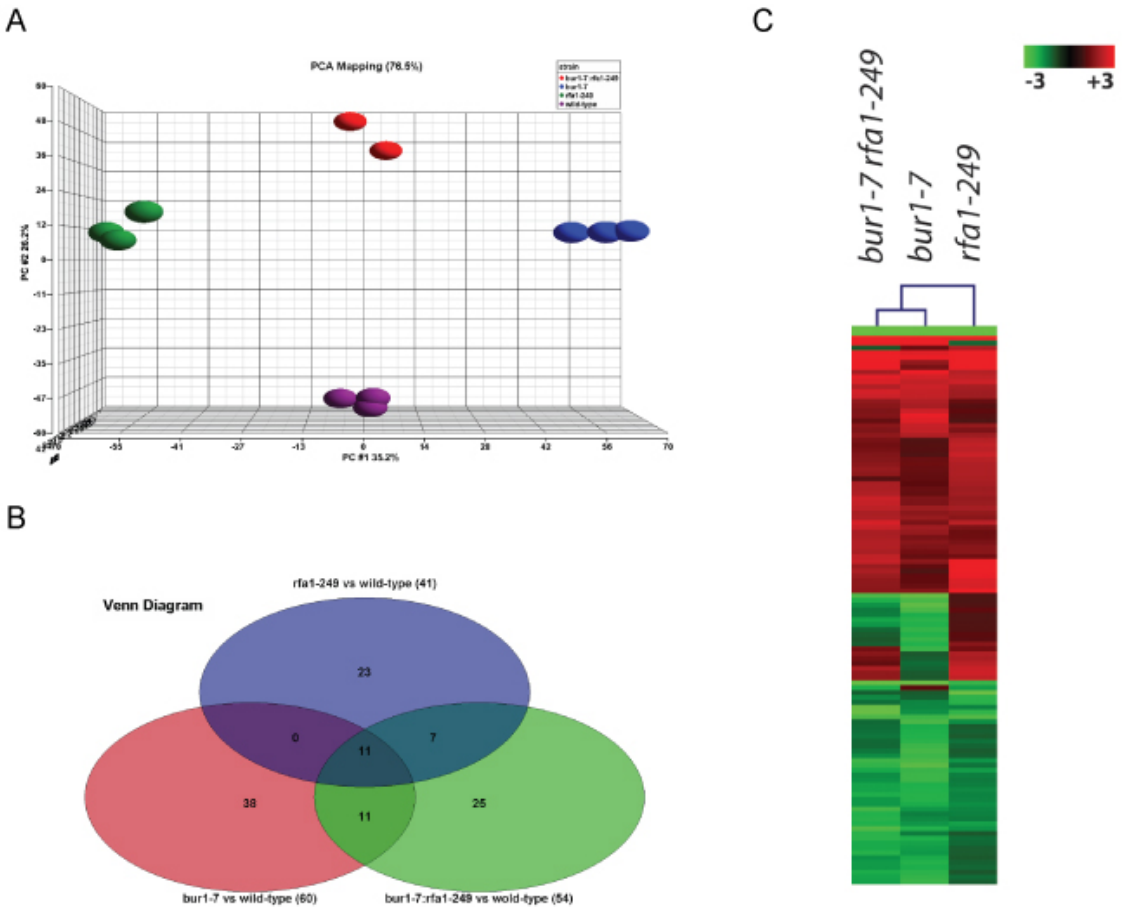

Figure 44: Whole genome expression analysis of bur1-7 and rfa1-249 single and double mutant strains upon DNA damage

(A) PCA Mapping of microarray experiments done independently in triplicates after removal of the batch effect. The different colours correspond to the different strains. The wild type strain is shown in purple, *bur1-7* in blue, *rfa1-249* in green and the *bur1-7 rfa1-249* double mutant in red. (B) Venn diagram showing the numbers of differentially regulated genes in the mutants strains compared to the wild type. Intersections show the number of genes that are similar in the respective mutants. (C) Hierarchical clustering of the expression data shows that *bur1-7* and the *bur1-7 rfa1-249* double mutant cluster together whereas the *rfa1-249* mutant is more distinct from these strains, which is depicted in the dendrogram.

To investigate if overlapping or distinct biological networks are affected by either the *rfa1* or the *bur1* mutation, a combined approach of both explorative analysis of microarray data and promoter analysis was performed.

In the case of *rfa1-249* the strong transcriptional activator Swi5 was discovered to be the mutant-specific transcription factor (TF) that targets the largest fraction of significantly changed genes (20%, Fig. 45 A). All three Swi5 target genes are up-regulated in the *rfa1-249* mutant. Swi5 represents a well-studied transcription factor that activates transcription of target genes at the M/G1 phase boundary of the mitotic

cell cycle (Breeden, 2003). Additionally, expression of known Swi5 target genes was analyzed. Strikingly, most of the known Swi5 target genes are at least slightly up-regulated. Since the mRNA level of *SWI5* in *rfa1-249* compared to wild-type yeast strain is not significantly changed, a post-transcriptional regulatory mechanism of Swi5 is most likely responsible for altered gene expression of most Swi5 target genes.

In case of *bur1-7*, all significantly changed genes are down-regulated. Ste12 turned out to be the mutant-specific TF that targets the largest fraction of significantly changed genes (28.6%, Fig. 45 B). All four Ste12 target genes were down-regulated in the *bur1-7* mutant. Ste12 activates genes involved in mating or pseudohyphal/invasive growth pathways (Herskowitz, 1995).

Taken together, mutation of either *RFA1* or *BUR1* affects both overlapping as well as distinct potential transcription regulatory networks. In the case of *rfa1-249* especially Swi5 target genes were at least slightly up-regulated. In the *bur1-7* mutant, all significantly changed genes are down-regulated. Ste12 is a kind of master regulator targeting not only the largest fraction of differentially expressed genes but also genes of other transcription factors which in turn regulate other significantly changed genes in the *bur1-7* expression profile.

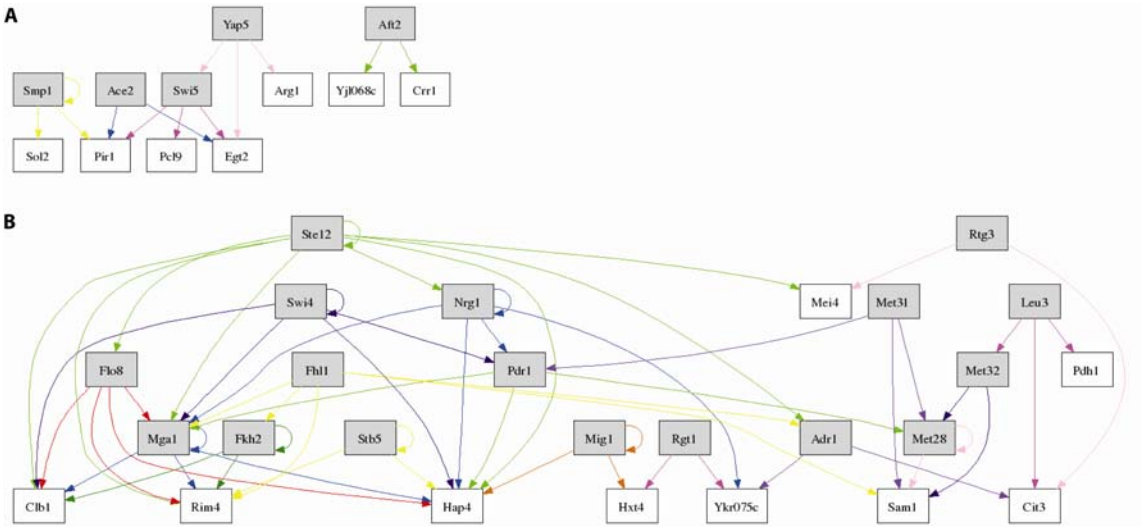

Figure 45: Possible transcription regulatory networks affected in *rfa1-249* (A) and *bur1-7* (B)

Transcription factors and target genes are indicated as grey and white boxes, respectively. Genes regulated by the particular transcription factor are symbolized by an arrow. Autoregulation is symbolized by a curved arrow. Only transcription factors regulating at least two differentially expressed target genes are shown in the diagram. The regulatory diagrams were generated with YEASTRACT.

3. Discussion

3.1 Bur1-2 and RPA interaction

In order go gain further insight into the function of the Bur1-2 complex, needed for efficient transcription elongation, tandem affinity purifications were performed to purify native *in vivo* complexes. Interestingly, the major proteins co-purifying with Bur1 and Bur2 were Rfa1, Rfa2 and Rfa3, components of a well studied protein complex, RPA, with functions in DNA repair, replication and recombination (Iftode *et al.*, 1999; Wold, 1997).

The N-terminus of Bur1 is homologous to cyclin dependent kinase domains. The C-terminus does not show any significant homology to known protein domains. Being interested in the function of those parts, truncations of Bur1 carrying just the kinase domain or the C-terminus were expressed in yeast cells. The kinase domain is sufficient for complementation of a *Δbur1* strain showing that the essential part is the kinase domain. The C-terminus could not complement a *BUR1* deletion. However, tandem affinity purification of the C-terminus showed that it is sufficient for the binding to RPA. Other tries to express the kinase domain or C-terminal truncations of the full length proteins lead to low expression levels and made it impossible to purify. Interestingly, it was also not possible to express full length Bur1 in *E. coli* or a Baculo expression system (data not shown). These approaches lead to either insolubility or degradation of the protein indicating that the kinase might take over unwanted functions in these cells and thus has to be inactivated.

Additionally, it was also not possible to over-express Bur1 in yeast cells showing that a deregulation of Bur1 kinase expression is fatal for the cell.

Depletion experiments showed that the amount of Bur1 can be depleted to a level that can not be detected by Western blot anymore but gave no impairment in growth (data not shown). Hence, only a very small amount of protein is needed to fulfil its function *in vivo*.

The interest was subsequently focused on the interaction of Bur1's C-terminus and RPA, with the initial aim to generate a full length protein fulfilling all other functions like protein-protein interactions and correct folding. Just the interaction with RPA should be disrupted to study specifically the function of the interaction of BUR and RPA *in vivo*.

First, the secondary structure of the C-terminus of Bur1 was examined by computer predictions using PSIPRED. The C-terminal part did not show any predictable folding. As there was no way of guessing where the interaction with RPA might take place, truncations of 50 amino acids were expressed in *E. coli*, as the C-terminus alone turned out to be soluble, and were tested for their binding abilities in a GST pulldown experiment. Two possible binding sites could be found using this strategy but when they were deleted from constructs coding for C-terminal fragments the protein was still able to bind to RPA, suggesting that there might be more, maybe weaker sites in this domain that cooperate in binding. Unstructured domains having a function in protein-protein interactions are known to have linear motifs, small interaction sites that are especially found in transient and regulatory interaction domains (Fuxreiter *et al.*, 2007). Additionally, this point is also strengthened by the finding that the BUR/RPA complex is already disrupted by 250 mM NaCl in TAP purifications (data not shown).

In order to have an alternative approach for the detection of the interaction site a peptide mapping approach was performed in collaboration with Georg Arnold. It has the advantage to detect also weaker interaction sites and smaller fragments of the C-terminus that might be important for binding of Bur1 to RPA.

These experiments showed that many of the 15 amino acid long peptides of the C-terminus had the ability to bind to RPA. It was thus not possible to indentify just a small number of residues needed for binding and to create a full length non-binding *BUR1* mutant. Instead, a mutant carrying a deletion of the whole C-terminus was used. The possibility that the natively disordered domain folds upon binding to RPA could possibility be characterized by a structural biology approach. Binding of the two protein complexes via linear motifs might also explain why the human homolog, Cdk9, is not able to bind to RPA as these kind of interaction domains are not evolutionary conserved.

The interaction of the Bur1-2 complex with RPA might provide insight into a new level of interconnection between transcription, chromatin modification and genome stability.

3.2 Function of Bur1 in Pkc1 signalling

Screening for high copy suppressors of *BUR1* mutations resulted in the identification of several genes involved in Pkc1 signalling. Pkc1 acts as a kinase upstream of the MAP kinase signalling pathway needed to regulate mating, sporulation and maintenance of cellular integrity upon response to stress due to low osmolarity as well as cell cycle and cytosketetal dynamics. Among the genes identified were *PKC1* as well as upstream regulators like *WSC2* or *SLG1* and genes needed for the signalling in this pathway like *RHO2* or *ROM1*. Another group of genes identified in the screen is involved in cell cycle regulation, *e.g. WHI3* which regulates *CLN3*. *CLN3* is acting upstream of *CLN1* and *CLN2* in G1 phase. Hyperactive *CLN3* was described to suppress deletion of *BUR1,* which was also initially indentified as a gene having an unspecific function in the response to mating pheromone (Irie *et al.*, 1991). Another cell cycle regulator that was found to suppress the mutation of *BUR1* was *CLN2*. It was originally argued that the suppression by Cln3 is based on the continuous expression of Cln3 whereas Cln2 (and Cln1) are expressed in waves in the cell cycle. In our screen Cln2 was expressed from a high copy plasmid and thus might also show continuous expression and could in turn suppress the *bur1* mutation like Cln3. Interestingly, GO analysis of microarray experiments performed with *bur1-7* mutant strains upon the addition of MMS showed enrichment of genes involved in mating. Additionally, Ste20, a serine threonine kinase involved in MAP kinase signalling in response to pheromone or high osmolarity (Drogen *et al.*, 2000) could be identified as a putative substrate of Bur1 by a whole proteome approach. These data point to a function of Bur1 in cell cycle regulation and Pkc1 signalling.

It is thus also possible that the sensitivity to drugs inducing DNA damage or replication or transcription stress of the *bur1* mutants is a secondary effect of the impairment in cell wall integrity. However, this is considered to be unlikely because we could observe a role of the *bur1* mutants in the formation of DNA repair foci making it unlikely that the damage sensitivity is simply a secondary effect of the impairment in cell wall integrity. This and the interaction with RPA agues for a specific role in DNA repair.

The identification of the high copy suppressor genes of two *bur1* mutants with roles in cell cycle and Pkc1 signalling suggests an additional function of Bur1 kinase in these processes. This might be uncoupled of the interaction with RPA and thus provides insight into another process Bur1 might me involved in.

3.3 Function of RPA in transcription

The *in vivo* interaction of BUR and RPA could also suggest a function of RPA in transcription and chromatin modification. Sensitivity of *rfa1-249* mutants to 6'AU was observed, arguing for a role of RPA in transcription. Additionally, the *rfa1-249* mutant shows a genetic interaction (synthetic sickness) with *DST1* and *RTF1* which are both needed for efficient transcription elongation, by backtracking of RNA PolII or by facilitating histone H3 Lysine 4 trimethylation (H3K4me3), respectively. The combination of the *bur1-7* mutant with *rfa1-249* also shows impairment in H3K4me3. As the single mutants showed only a slight impairment in the methylation it could be possible that BUR and RPA act on a different pool of histones. This could be examined using a ChIP on Chip approach to see on a whole genome basis the levels of this histone modification in *bur1* and *rfa1* mutants. Besides the modification of histone H3K4me3, the overall level of histone H3 is lower in the *rfa1* mutant.

Additionally, impairment in the expression of a β-galactosidase reporter gene could be observed in *bur1*, but surprisingly also in an *rfa1* mutant. This result hints to a more direct effect of RPA in gene expression in accordance with other studies. The Cooper lab showed that RPA binds specifically to regulatory sequences, *e.g.* URS1 (Luche *et al.*, 1993), needed for transcription regulation. A direct effect of RPA on transcription could also be observed at the metallothionein promoter in human cells (Tang *et al.*, 1996). Despite this, two recent publications on Arabidopsis RPA showed that rfa2 mutants show a missregulation in transcriptional silencing (Elmayan *et al.*, 2005; Kapoor *et al.*, 2005).

Until today it remains elusive what the specific function of RPA on gene expression is. Possibly, RPA regulates transcription by binding to regulatory elements like promoters or upstream regulatory sequences. There, it might either recruit other factors needed for transcription, like Bur1-2, or prevent binding by blocking their binding sites. A mechanism like this could explain the suppression of the *bur1* and *rfa1* mutants, pointing to antagonistic roles of both proteins.

One could also suspect a function RPA in the inheritance of regulatory histone modifications during S-phase of the cell cycle.

Another possibility is that after mutation of *BUR1* R-loops, DNA-RNA hybrids that often form upon impaired transcription, might occur behind the transcription bubble. It was shown that in a strain carrying a deletion of *HPR1*, a component of the TREX complex, R-Loops are formed co-transcriptionally (Huertas and Aguilera, 2003). Bur1

kinase is synthetic lethal with TREX components and might thus lead to similar phenotypes. The R-loops would lead to patches of ssDNA behind the transcribing polymerase because of the pairing of the transcribed mRNA with DNA. These ssDNA patches could then serve as a substrate for RPA to bind. This binding of RPA might even stabilize those areas and as the *rfa1-249* mutant also has mutations in the DNA binding sites of RPA there might be a lower affinity of our mutant to ssDNA than in the wild type protein. This weaker binding could in turn lead to a faster dissociation of RPA from the DNA and the R-loop can be resolved faster. A mechanism like this could also explain the suppression seen in *BUR1* and *RFA1* double mutants. In the *bur1* mutant the occurrence of R-Loops is possibly higher and lower in the *rfa1* mutant. Hence, the negative effect of the *bur1* mutant can be suppressed by the *rfa1* mutant. However, this mechanism can not explain why the *rfa1* mutant itself is extremely sick. To gain a deeper insight into a possible role of *RFA1* in R-loop formation or resolution one would need to further characterize more defined mutations in the DNA binding domains of *RFA1* in this process.

Another result explaining the suppression is gene expression on a whole genome basis. Analysis of microarray experiments performed with the *bur1-7* and *rfa1-249* single and double mutants shows that the double mutant clusters together with the *bur1-7* mutant whereas the *rfa1-249* mutant does not. Thus even though the *rfa1-249* mutant is also present in the double mutant strain gene expression seems to be closer to wild-type or *bur1-7* and this might lead to the better growth of the double mutant.

The interaction of BUR and RPA provides the possibility for a role of RPA in transcription elongation. Results of this study, like impaired reporter gene expression and impairment in H3K4me3 strengthen the idea, even though the exact mechanism has to be investigated in future studies.

3.4 Function of Bur1 in genome stability

The observation that the BUR complex bind to RPA, which has functions in DNA replication, recombination and repair lead to the idea that BUR could also be involved in one of these processes. To test this possibility, temperature sensitive mutants of *BUR1* were generated and subjected to phenotypic and genetic analysis. Mutations in *BUR1* lead to sensitivity of the cells to MMS, UV irradiation and Hydroxyurea, agents that induce DNA damage or replication stress, respectively. Interestingly,

these sensitivities were even stronger than the sensitivity to 6'-AU which impairs transcription elongation. To elucidate the pathway Bur1 plays a role in, the mutant alleles were analysed for their epistatic behaviour with non essential deletions of genes involved in specific DNA repair pathways. No epistatic behaviour with any of these candidate genes was observed, showing that *BUR1* is not a component of any of these pathways and most likely has a higher order role in regulating genome maintenance.

Mutation of Bur1 also did not lead to a drastic reduction in Rad53 phosphorylation excluding a function in checkpoint signalling.

The possibility of Bur1 having a function in post-replication repair could not be excluded because it was not possible to generate a *BUR1 RAD6* double mutant strain.

A function of Bur1 in genome stability was further investigated in collaboration with the Lisby lab. Using fluorescence microscopy it could be shown that some mutations in *BUR1* lead to increased levels of homologous recombination, indicating genome instability. This was investigated by examining the co-localisation of the homologous recombination factor Rad52 with nuclear foci that form upon induction of DNA damage or replication. The phenotype is strong in the *bur1-7*, *bur1-24* and *bur1-ΔC* mutants, which are the most sensitive alleles to MMS, UV irradiation and Hydroxyurea. These mutants were also unable to suppress Rad52 foci upon addition of Hydroxyurea. This is normally seen in wild type cells due to the impairment on DNA replication (Lisby *et al.*, 2004). This could be due to slow disassembly of existing Rad52 foci due to DNA repair or due to a failure to suppress *de novo* recruitment of Rad52 to sites of DNA damage. This slowing down might be a consequence of slow DNA repair. Furthermore, upon longer treatment with HU the number of cells with Rad52 foci in the *bur1-7* mutant strain is significantly higher than in wild type cells also pointing to an impairment in genome stability due to the mutation of *BUR1*.

In summary, a function of *BUR1* in genome stability could be established, first by interaction with RPA, second due to sensitivity of *bur1* mutants to DNA damage and third by the impact of *bur1* mutants on the amount and persistence of DNA repair foci. A simple secondary effect on DNA repair due to impaired transcription could be excluded because the level of DNA repair annotated genes does not change in whole genome expression experiments.

4. Materials

4.1 Consumables and chemicals

Consumables and chemicals were purchased from the following companies:
Acros Organics (Geel, Belgium), Applichem (Darmstadt), Applied Biosciences (Darmstadt), Apollo Scientific Limited (Bredbury, UK), Axon (Kaiserslautern), Becton Dickinson, (Heidelberg), Beckman Coulter (Krefeld), Biaffin (Kassel), Biomol (Hamburg), Biorad (Munich), Biozym (Hess. Oldendorf), Chemicon (Temecula, Canada), Fermentas (St. Leon-Rot), Formedium (Norwich, UK), GE Healthcare (München), Gilson (Bad Camberg), Invitrogen (Karlsruhe), Lake Placid Biologicals (Lake Placid, USA), Macherey & Nagel (Düren), Medac (Hamburg), Medigenomix (München), Membra Pure (Bodenheim), Merck Biosciences (Darmstadt), Millipore (Molsheim, France), Mobitec (Göttingen), MP Biomedical (Illkirch, France), NEB (Frankfurt), Neolab (Heidelberg), Nunc (Wiesbaden), Peske (Aindling-Arnhofen), Promega (Mannheim), Qiagen (Hilden), Roche (Mannheim), Roth (Karlsruhe), Santa Cruz (Santa Cruz, USA), Sarstedt (Nümbrecht), Semadeni (Düsseldorf), Serva (Heidelberg), Sigma (Taufkirchen), Stratagene (Amsterdam, The Netherlands), VWR (Ismaning).

4.2 Commercially available kits

DC Protein Assay (Biorad, München), ECL kit (Applichem, Darmstadt), Nucleobond AX PC100, Nucleospin Mini, Nucleospin extract (all Macherey & Nagel, Düren), RNeasy MinElute Cleanup Kit (Quiagen, Hilden), Protoarray Yeast PPI (Invitrogen, USA)

4.3 Equipment

Beckman DU650 spectrophotometer, L80 Ultracentrifuge, SW32 rotor (Beckman Coulter, Krefeld), T3 Thermocycler (Biometra, Goettingen), Gel dryer model 583, Mini-Protean II system (Biorad, München), DNA engine (Biozym, Hess Oldendorf), Lumat LB9507 (EG&G Berthold), bead mill (Fritsch, Idar-Oberstein), Thermomixer compact, Eppendorf centrifuge 5415D, 5415R (Eppendorf, Wesseling-Berzdorf), Äkta Basic System (GE Healthcare, München), Rotanda, 46R (Hettich, Tuttlingen), Ika Vibrax VXR basic (Ika, Staufen), Heraeus Hera Freeze (Kendro, Langenselbold), Kodak X-omat M35 (Kodak), Kühner ISF-1-V (Kühner AG, Switzerland),

Elektrophoresis Power Supply Consort E835, Heidolph shaker duomax 1030, Rotator, Thermostatcabinet Aqualytic, Vortex Genie (Neolab, Heidelberg), Innova 44 shaking incubator (New Brunswick Scientific, Nürtingen), Semi-dry blotting device (Peqlab, Erlangen), Dissection microscope manual MSM (Singer, Somerset, UK), RP80AT-364, Sorvall Evolution, Sorvall RCM120Ex, SLC6000, SS34 rotor (Thermo Fisher Scientific), Image reader LAS-3000 (Fujifilm),
ELISA reader

4.4 Radioactivity

Radioactivity was obtained from GE healthcare:
[γ-32P]-ATP (370 MBq/ml, 10 mCi/ml), [γ-33P]-ATP (3000Ci/mmol, 10 mCi/ml)

4.5 Enzymes

Calf Intestine Alkaline Phosphatase (1U/µl), restriction endonucleases (*Bam*HI, *Bgl*II, *Bsr*BI, *Cla*I, *Dpn*I, *Eco*RV, *Eco*RI, *Hind*III, *Hpa*I, *Kpn*I, *Nsi*I, *Nco*I, *Nde*I, *Nhe*I, *Not*I, *Sph*I, *Pst*I, *Pvu*II, *Sac*I, *Sal*I, *Sma*I, *Spe*I, *Sph*I, *Xba*I, *Xho*I), Pfu and Pfu Turbo Polymerases (Stratagene, La Jolla, USA), T4-DNA Ligase, *Taq*-Polymerase for colony PCR and KNOP PCR, CIAP Phosphatase (all Fermentas, St. Leon-Rot), Micrococcal Nuclease (Roche, Mannheim), *Taq* Polymerase for RT-PCR (Axon, Kaiserslautern) TEV protease, Vent-Polymerase for KNOP-PCR (NEB, Frankfurt), Zymolyase 20000T / 100000T (Medac, Hamburg)

4.6 Antibodies

	Source	**Dilution**	**Company**
Primary antibodies			
anti-actin	mouse	1:1000	Chemicon
anti-CDK9	rabbit	1:200	Santa Cruz
anti-Cdk9-55	rabbit	1:2500	Price lab
PAP	rabbit	1:5000	Sigma
anti-Pgk1	mouse	1:10000	Molecular Probes
anti-H3	rabbit	1:2500	Lake Placid Biologicals

anti-H3K4me	rabbit	1:500	Upstate
anti-H3K4me2	rabbit	1:1000	Upstate
anti-H3K4me3	rabbit	1:2500	Upstate
anti-H3K36me3	rabbit	1:1000	Abcam
anit-H3K79me2	rabbit	1:500	Upstate
anti-H4K12 acetyl	rabbit	1:1000	Upstate
anti-Rfa1	rabbit	1:2000	Brill lab
anti-Rfa2	rabbit	2:2000	Brill lab
anti-Bur1	rabbit	1:5000	Sträßer lab
anti-Rpb1 CTD	mouse	1:500	Covance
anti-Rpb1 S2 P	mouse	1:500	Covance
anti-Rpb1 S5 P	mouse	1:500	Covance
anti-Flag	mouse	1:5000	Sigma
anti-RFP	goat	1:500	Leonhardt lab
anti-RPA32	mouse	1:1000	Abcam
anti-Ctk1	rabbit	1:5000	Sträßer lab
anti Rad53	goat	1:100	Santa Cruz
Secondary antibodies			
anti mouse IgG HRPO	goat	1:3000	Biorad
anti rabbit IgG HRPO	goat	1:3000	Biorad
anti goat IgG-HRPO	goat	1:5000	Sigma

4.7 Oligonucleotides

Name	Sequence	Purpose
5'-BamHI-*BUR1* aa365-ATG	GGGGGATCCATGTGGTTTAAAGAGGACCC TTTACA	Bur1-Cterm constructs starting from aa365
5'-BamHI-*BUR1*	GGGGGATCCATGGAAAAGGGTGAATCAC	Bur1-Cterm constructs starting

aa413-ATG	CTGTCGTG	from aa413
5'-BamHI-*BUR1* aa390-ATG	GGGGGATCCATGATTAAGAGGTACAAGGA AGAAATGC	Bur1-Cterm constructs starting from aa390
5'-BamHI-*BUR1* aa450-ATG	GGGGGATCCATGTCGAAAATAAGAGAACT ACATCAAA	Bur1-Cterm constructs starting from aa450
5'-BamHI-*BUR1* aa500-ATG	GGGGGATCCATGAGCACTGCACCCAACA ACAGCAG	Bur1-Cterm constructs starting from aa500
5'-BamHI-*BUR1* aa510-ATG	GGGGGATCCATGGTAAATCGATTTCATCC TGAGACA	Bur1-Cterm constructs starting from aa510
5'-BamHI-*BUR1* aa520-ATG	GGGGGATCCATGAGCTCTAAATATAATAA AGTACCTT	Bur1-Cterm constructs starting from aa520
5'-BamHI-*BUR1* aa540-ATG	GGGGGATCCATGTCAAATGAGTCCCGGTA CAAAAAC	Bur1-Cterm constructs starting from aa540
5'-BamHI-*BUR1* aa560-ATG	GGGGGATCCATGGTGAACAAGCCGGAAA CCAACTTC	Bur1-Cterm constructs starting from aa560
5'-BamHI-*BUR1* aa580-ATG	GGGGGATCCATGAATGCGCCAATCAATAA AAATTATAA	Bur1-Cterm constructs starting from aa580
5'-BamHI-*BUR1* aa600-ATG	GGGGGATCCATGCATCATCAAGGCTCGA GACCTTC	Bur1-Cterm constructs starting from aa600
5'-BamHI-*BUR1* aa470-ATG	GGGGGATCCATGAAAACTGCGATTCCACC GCCAGC	Bur1-Cterm constructs starting from aa470
5'-BamHI-*BUR1* aa480-ATG	GGGGGATCCATGGCAGGAGTTAATAGATA CCGACCC	Bur1-Cterm constructs starting from aa480
5'-BamHI-*BUR1* aa490-ATG	GGGGGATCCATGAGTTCCAGAAATAATCG CTTCAGC	Bur1-Cterm constructs starting from aa490
3'-SalI-STOP-*BUR1* cterm	GGGGTCGACTTAATATAGATCTGCAATAT CACTATTTT	Bur1-Cterm constructs ending at aa657 inlcluding STOP
3'-SalI-*BUR1* aa650-STOP	GGGGTCGACTTAATTTTGGAACTCCTTAG ACTCATCT	Bur1-Cterm constructs ending at aa650 inlcluding STOP
3'-SalI-*BUR1* aa630-STOP	GGGGTCGACTTATTCTCTATTGGTTTACTC GTAAGCT	Bur1-Cterm constructs ending at aa630 inlcluding STOP
3'-SalI-*BUR1* aa610-STOP	GGGGTCGACTTATGGATGAGAAGGTCTCG AGCCTT	Bur1-Cterm constructs ending at aa610 inlcluding STOP
3'-SalI-*BUR1* aa598-STOP	GGGGTCGACTTAAGCCATATTGCGAGAAC CGTTTG	Bur1-Cterm constructs ending at aa598 inlcluding STOP
3'-SalI-*BUR1* aa590-STOP	GGGGTCGACTTAAGGATTATAATTTTTATT GATTGGCG	Bur1-Cterm constructs ending at aa590 inlcluding STOP
3'-SalI-*BUR1* aa570-STOP	GGGGTCGACTTACCTATTGAAGTTGGTTT CCGGCTT	Bur1-Cterm constructs ending at aa570 inlcluding STOP
3'-SalI-*BUR1* aa550-STOP	GGGGTCGACTTATGGCGAGTTTTTGTACC GGGACTC	Bur1-Cterm constructs ending at aa550 inlcluding STOP
3'-SalI-*BUR1* aa 530-STOP	GGGGTCGACTTATGGCAAAGGTACTTTAT TATATTTAG	Bur1-Cterm constructs ending at aa530 inlcluding STOP
3'-SalI-*BUR1* aa500-STOP	GGGGTCGACTTAGCTGAAGCGATTATTTC TGGAACT	Bur1-Cterm constructs ending at aa500 inlcluding STOP
3'-SalI-*BUR1*	GGGGTCGACTTAATTGTTGGGTCCGTATC	Bur1-Cterm constructs ending

aa490-STOP	TATTAACT	at aa 490 inlcluding STOP
3'-SalI-*BUR1* aa480-STOP	GGGGTCGACTTAAGGGGCTGCTGGCGGT GGAATC	Bur1-Cterm constructs ending at aa480 inlcluding STOP
3'-SalI-*BUR1* aa470-STOP	GGGGTCGACTTAAGCATATCCGCTGTTCA CATGATA	Bur1-Cterm constructs ending at aa470 inlcluding STOP
3'-SalI-*BUR1* aa460-STOP	GGGGTCGACTTAAGGATTTTGATGTAGTT CTCTTATTT	Bur1-Cterm constructs ending at aa460 inlcluding STOP
3'-SalI-*BUR1* aa450-STOP	GGGGTCGACTTACGGCTTAGCCAATACGT TCTTTGATG	Bur1-Cterm constructs ending at aa450 inlcluding STOP
3'-SalI-*BUR1* aa400-STOP	GGGGTCGACTTATGATTGGTGCATTTCTT CCTTGTAC	Bur1-Cterm constructs ending at aa400 inlcluding STOP
3'- Bur1 Del 490-500	GCTGTTGTTGGGTGCAGTGCTATTGTTGG GTCCGTATCTATTAACTCC	Deletion of aa490 bis 500 in Bur1-Cterm construct
5'- Bur1 Del 490-500	AATAGATACGGACCCAACAATAGCACTGC ACCCAACAACAGCAGGA	
3'- Bur1 Del 480-490	GCTGAAGCGATTATTTCTGGAAGGGGCTG CTGGCGGTGGAATCGCAGT	Deletion of aa480 bis 490 in Bur1-Cterm constructs
5'- Bur1 Del 480-490	ATTCCACCGCCAGCAGCCCCTAGTTCCAG AAATAATCGCTTCAGCG	
3'- Bur1 Del 540-550	TATGATATCTAGAGTCATTATTACCCTGGT ATCTTGACTGAGGCCC	Deletion of aa540 bis 550 in Bur1-Cterm constructs
5'- Bur1 Del 540-550	CAGTCAAGATACCAGGGTAATAATGACTC TAGATATCATAACCCTA	
3'- Bur1 Del 550-560	GGTTTCCGGCTTGTTCACTGGCGAGTTTT TGTACCGGGACTCATT	Deletion of aa550 bis 560 in Bur1-Cterm constructs
5'- Bur1 Del 550-560	TCCCGGTACAAAAACTCGCCAGTGAACAA GCCGGAAACCAACTTC	
3'-BUR1 Del 560-570	GGCGACTATATTTCTGTGGTTGTGGCGAG TTTTTGTACCGGGACTCA	Deletion of aa560 bis 570 in Bur1-Cterm constructs
5'-BUR1 Del 560-570	GATATCATAACCCTAGGTACCAACCACAG AAATATAGTCGCCAAGAA	
5'-NotI-*BUR1* Prom	GGGGCGGCCGCTTTTTACCGAGAAATCAG CCGTTGG	cloning of the BUR1 promoter
3'-BamHI-*BUR1* Prom	GGGGGATCCATTATTTTACTGTTATTCTGC TTGACC	cloning of the BUR1 promoter
5'-BamHI-*BUR1* – ATG	GGGGGATCCATGAGTGATAATGGTTCCCC CG	cloning of Bur1 for expression and complementation studies
3'- SalI-STOP-*BUR1* kinase aa372	GGGGTCGACTTATGGTAAAGGGTCCTCTT TAAACC	cloning of Bur1 kinase domain for complementation studies
3'- SalI-noSTOP-*BUR1* kinase aa372	GGGGTCGACTGGTAAAGGGTCCTCTTTAA ACC	cloning of Bur1 kinase domain for expression studies
5'-BamHI-*BUR1* aa365-ATG	GGGGGATCCATGTGGTTTAAAGAGGACCC TTTACCA	cloning of Bur1 C-terminus for expression and complementation studies

3'-SalI-STOP-*BUR1* cterm	GGGGTCGACTTATATAGATCTGCAATATC ACTATTTTG	cloning of Bur1 C-terminus complementation studies
3'-SalI-noSTOP-*BUR1* cterm	GGGGTCGACTATAGATCTGCAATATCACT ATTTTG	cloning of Bur1 C-terminus for expression studies
5'-NcoI-Oligo1-Flag-TAP	GGGTCCATGGAAAAGAGAAGAATGGACTA CAAGGACGACGATGACAAGGATTATGATA TTCCAACTACTGCTAGC	cloning of pBS1479-Flag-TEV-ProtA
3'-KpnI-TAP	GGGGGTACCGGGCCCATGTTTGATACATG	cloning of pBS1479-Flag-TEV-ProtA
5'-XhoI-*MSH6*	GGGCTCGAGAGTTTTCTGAATGGCCAACT TTCC	Cloning of *MSH6*
3'-BamHI-*MSH6*	GGGGGATCCACCCCATTCTTGCCCAAGAT GCG	Cloning of *MSH6*
5'-XhoI-*POL4*	GGGCTCGAGTGATAATGGTCCAGCGTGG TTACA	Cloning of *POL4*
3'-BamHI-*POL4*	GGGGGATCCTCATTGGTGGTGGTGACACT GCC	Cloning of *POL4*
5'-XhoI-*RAD16*	GGGCTCGAGGTTTTAAAGTTCGTCAGTTG TTCC	Cloning of *RAD16*
3'-BamHI-*RAD16*	GGGGGATCCGACAGGTGTTGATTGGTCTA ATGG	Cloning of *RAD16*
5'-SalI-*RAD26*	GGGGTCGACGATCAACAGTACGAAAACTT GTGC	Cloning of *RAD26*
3'-BamHI-*RAD26*	GGGGGATCCACAAAGTATGTAGGTGGCTT CTCC	Cloning of *RAD26*
5'-BamHI-*XRS2*	GGGGGATCCCTAGACATTCAATGGTACTC AAGG	Cloning of *XRS2*
3'-SmaI-*XRS2*	GGGCCCGGGTATCAGTTGGAGTATTCAAA GAGG	Cloning of *XRS2*
5'-XhoI-*APN1*	GGGCTCGAGATGGTCGCCACCAAAGGAG AAGG	Cloning of *APN1*
3'-BamHI-*APN1*	GGGGGATCCAAACTTTCTATGCTTAGGAA TAACG	Cloning of *APN1*
5' XhoI-*MAG1*	GGGCTCGAGCCCTAATCAATAATAAGTCA TCGG	Cloning of *MAG1*
3'-BamHI-*MAG1*	GGGGGATCCGCCAAGAGCTCCGATGAGA AACG	Cloning of *MAG1*
5'-XhoI-*RNR1*	GGGCTCGAGTACGCGTTTTATCCCATTAT ATGG	Cloning of *RNR1*
3'-BamHI-*RNR1*	GGGGGATCCGTGCTATTTAATTACAATTCT TTGG	Cloning of *RNR1*
5'-SalI-*CDC28*	GGGGTCGACGTTTACTCTAAGATTGTTAA CTCC	Cloning of *CDC28*
3'-BamHI-*CDC28*	GGGGGATCCACTTTCGCGTATAACTGAAT	Cloning of *CDC28*

	GTTCC	
5'-SalI-*CLN3*	GGGGTCGACCTACTGAGTCTGCCAGTCAA ATGG	Cloning of *CLN3*
3'-BamHI-*CLN3*	GGGGGATCCTATAATGTGACTAGAGGAAG TAAGG	Cloning of *CLN3*
5'-SalI-*CLB1*	GGGGTCGACACTTCAATTTGCGTTCCGCA TACG	Cloning of *CLN3*
3'-BamHI-*CLB1*	GGGGGATCCCGTGTGATAATATATATGAG ATAACC	Cloning of *CLN3*
5'-SalI-*CLB6*	GGGGTCGACCCAAATAGCAGTTTTACGCG TACC	Cloning of *CLB6*
3'-BamHI-*CLB6*	GGGGGATCCATCAGGCATTCATTATTCAT ATAACG	Cloning of *CLB6*

4.8 Plasmids

pRS313-*BUR1* pRS314-*BUR1* pRS315-*BUR1* pRS316-*BUR1*	Sträßer
pRS313-*bur1-1* pRS314-*bur1-1* pRS315-*bur1-1*	Sträßer
pRS313-*bur1-4* pRS314-*bur1-4* pRS315-*bur1-4*	Sträßer
pRS313-*bur1-7* pRS314-*bur1-7* pRS315-*bur1-7*	Sträßer
pRS313-*bur1-24* pRS314-*bur1-24* pRS315-*bur1-24*	Sträßer
pRS314-*RFA1* pRS315-*RFA1* pRS316-*RFA1*	Winkler
pRS313-*RFA1*	*RFA1* was cut out BamHI, XhoI from pRS314-*RFA1* and cloned into the same sites of pRS313
pRS315-*rfa1-6* pRS315-*rfa2-1-4* pRS315-*rfa2-26-2* pRS315-*rfa3-6-1* pRS315-*rfa3-8-1* pRS315-*rfa3-16-1*	Winkler
pRS314-*rfa1-249*	plasmid pRS314-*RFA1* was mutagenized in vitro using hydroxylamine, transformed into the *RFA1* shuffle strain and ts phenotypes selected after shuffling
pRS313-*rfa1-249* pRS315-*rfa1-249*	*rfa1-249* was cut out BamHI, XhoI from pRS314-*rfa1-249* and cloned into the same sites of pRS313 or pRS315

pGEX-4T-3	GE Healthcare
pGEX-4T-3-*BUR1* truncations	Müller
pRS314-*RAD52* pRS316-*RAD52*	Winkler
pRS315-*MSH6* pRS316-*MSH6*	*MSH6* was PCR amplified form genomic DNA using primers 5'-XhoI-*MSH6* ca. 500 bp upstream of *MSH6* and 3'-BamHI-*MSH6* ca. 300 bp downstream of *MSH6* and cloned into the same sites of pRS315 or pRS316
pRS315-*POL4* pRS316-*POL4*	*POL4* was PCR amplified from genomic DNA using primers 5'-XhoI-*POL4* ca. 500 bp upstream of *POL4* and 3'-BamHI-*POL4* ca. 300 bp downstream of *POL4* and cloned into the same sites of pRS315 or pRS316
pRS315-*RAD16* pRS316-*RAD16*	*RAD16* was PCR amplified from genomic DNA using primers 5'-XhoI-*RAD16* ca. 500 bp upstream of *RAD16* and 3'-BamHI-*RAD16* ca. 300 bp downstream of *RAD16* and cloned into the same sites of pRS315 or pRS316
pRS315-*RAD26* pRS316-*RAD26*	*RAD26* was PCR amplified from genomic DNA using primers 5'-SalI-*RAD26* ca. 500 bp upstream of *RAD26* and 3'-BamHI-*RAD26* ca. 300 bp downstream of *RAD26* and cloned into the same sites of pRS315 or pRS316
pRS313-*XRS2* pRS316-*XRS2*	*XRS2* was PCR amplified from genomic DNA using primers 5'-BamHI-XRS2 ca. 500 bp upstream of *XRS2* and 3'-SmaI-*XRS2* ca. 300 bp downstream of *XRS2* and cloned into the blunted BamHI site of pRS313 or pRS316
pRS313-*APN1* pRS316-*APN1*	*APN1* was PCR amplified from genomic DNA using primers 5'-XhoI-*APN1* ca. 500 bp upstream of APN1 and 3'-BamHI-*APN1* ca. 300 bp downstream of *APN1* and cloned into the same sites of pRS313 or pRS316
pRS315-*MAG1* pRS316-*MAG1*	*MAG1* was PCR amplified from genomic DNA using primers 5' XhoI-*MAG1* ca. 500 bp upstream of *MAG1* and 3'-BamHI-*MAG1* ca. 300 bp downstream of *MAG1* and cloned into the same sties of pRS315 or pRS316
pRS315-*RNR1*	*RNR1* was PCR amplified from genomic DNA using primers 5'-XhoI-*RNR1* ca. 500 bp upstream of *RNR1* and 3'-BamHI-*RNR1* ca. 300 bp downstream of *RNR1* and cloned into the same sites of pRS315
pRS315-*DST1* pRS316-*DST1*	Sträßer
pRS315-*RTF1* pRS316-*RTF1*	Sträßer
YEplac181-*CDC28*	*CDC28* was PCR amplified from genomic DNA using primers 5'-SalI-*CDC28* and 3'-BamHI-*CDC28* and cloned into the same sites of YEplac181
YEplac181-*CLN3*	*CLN3* was PCR amplified from genomic DNA using primers 5'-SalI-*CLN3* and 3'-BamHI-*CLN3* and cloned into the same sites of YEplac181
YEplac181-*CLB1*	*CLB1* was PCR amplified from genomic DNA using primers 5'-SalI-*CLB1* and 3'-BamHI-*CLB1* and cloned into the same sites of YEplac181
YEplac181-*CLB6*	*CLB6* was PCR amplified from genomic DNA using primers 5'-SalI-CLB6 and 3'-BamHI-*CLB6* and cloned into the same sites of YEplac181

pBS1479-Flag-TEV-ProtA	Flag-TEV-ProteinA was PCR amplified from pBS1479, adding the Flag epitope instead of CBP using primers 5'-NcoI-Oligo1-Flag-TAP and 3'-KpnI-TAP and cloned into the same sites of pBS1479 after cutting the standard TAP tag using these enzymes, respectively.
pBS-*bur1-1* pBS-*bur1-4* pBS-*bur1-7* pBS-*bur1-24*	Hiechinger
pBS-*bur1-1::LEU2*	The *LEU2* marker was cut out of YDp-L with BamHI, blunt-ended and cloned in the Eco47III site of pBS-*bur1-1*
pBS-*bur1-4::LEU2*	The *LEU2* marker was cut out of YDp-L with BamHI, blunt-ended and cloned in the Eco47III site of pBS-*bur1-4*
pBS-*bur1-7::LEU2*	The *LEU2* marker was cut out of YDp-L with BamHI, blunt-ended and cloned in the Eco47III site of pBS-*bur1-7*
pBS-*bur1-24::LEU2*	The *LEU2* marker was cut out of YDp-L with BamHI, blunt-ended and cloned in the Eco47III site of pBS-*bur1-24*
pRS315-TADH1	Röther
pRS315-TAP-TADH1	Röther
pRS315-*BUR1* Prom-TADH1	*BUR1* Promoter was PCR amplified from genomic DNA using primers adding NotI and BamHI sites and was cloned into the same sites of pRS315-TADH1
pRS315-*BUR1* Prom-TAP-TADH1	*BUR1* Promoter was PCR amplified from genomic DNA using primers adding NotI and BamHI sites and was cloned into the same sites of pRS315-TAP-TADH1
pRS315-*BUR1*-FL-TAP-TADH1	The *BUR1* ORF was PCR amplified from genomic DNA using primers adding a 5'-BamHI site and a 3'- XhoI site and a deletion of the STOP codon. This PCR product was subsequently cloned into the BamHI and XhoI sites of pRS315-*BUR1* Prom-TAP-TADH1
pRS315-*BUR1* C-terminus-TAP-TADH1	The *BUR1* C-Terminus starting from amino acid 365 was PCR amplified from genomic DNA using primers adding a 5'-BamHI site, a 3'-XhoI site, an ATG and a mutation of the STOP codon. This PCR product was subsequently cloned into the BamHI and XhoI sites of pRS315-*BUR1* Prom-TAP-TADH1.
pRS315- *BUR1*-FL-TADH1	The *BUR1* ORF was PCR amplified from genomic DNA using primers adding a 5'-BamHI site and a 3' XhoI site. This PCR product was subsequently cloned into the BamHI and XhoI sites of pRS315-*BUR1* Prom-TAP-TADH1
pRS315-*bur1ΔC*-TADH1	The *BUR1* kinase domain from amino acid 1 until 372 was PCR amplified from genomic DNA using primers adding a 5'-BamHI site, a 3'-XhoI site and an ATG. This PCR product was subsequently cloned into the BamHI and XhoI sites of pRS315-*BUR1* Prom-TADH1
pRS315-*BUR1* C-Terminus-TADH1	The *BUR1* C-Terminus starting from amino acid 365 was PCR amplified from genomic DNA using primers adding a 5'-BamHI site, a 3'-XhoI site and an ATG. This PCR product was subsequently cloned into the BamHI and XhoI sites of pRS315-*BUR1* Prom-TAP-TADH1
RPA32-GFP	Leonhadt lab
pRS313-GAL1::LacZ	Breuning lab

The following previously described plasmids were used:
pRS314-*YRA1*, pRS314-*yra1-451*, pRS314-*yra1-635*, pRS314-*yra1-667* = *yra1-1*, pRS315-*MFT1* (Strasser et al. 2000; Strasser and Hurt 2000; Hurt et al. 2004), pRS315-*THO2* (A. Aguilera), pUN100-*HPR1* (Joris Braspening / Jochen Baßler), pRS313, pRS314, pRS315, pRS316 (Sikorski and Hieter, 1989), pBSKS (+) (Alting-Mees *et al.*, 1992), pBS1479, pBS1539 (Puig *et al.*, 2001).

4.9 Strains

E. coli strains

DH5α	F^-, φ80d*lacZ*ΔM15, Δ(*lacZYA-argF*)U169, *deoR*, *recA*1, *endA*1, *hsdR*17(rk^-, mk^+), *phoA*, *supE*44, λ^-, *thi*-1, *gyrA*96, *relA*1
BL21 DE3	F–, *omp*T, *hsd*S_B(r_B-, m_B-), *dcm*, *gal*, λ(DE3)

S. cerevisiae stains

RS453	MAT a; *ade2-1; his3-11,15; ura3-52; leu2-3,112; trp1-1; can1-100; GAL+*	
BUR1 YRA1 double shuffle	MAT a; *his3; leu2; ura3; trp1; ade2; YPR161c::kanMX4; YJL173c::kanMX4* pRS316-*BUR1*; pRS316-*YRA1*	*BUR1* shuffle (spore IIIa) was mated *YRA1* shuffle (sporeIb), spore Ib
Bur1-TAP	as RS453; MAT a; *BUR1-CBP-TEV-protA::TRP1-KL;*	Sträßer
Bur2-TAP	as RS453; MAT a; *BUR2-CBP-TEV-protA::TRP1-KL;*	Sträßer
Rfa1-TAP	RS453; MAT a; *RFA1-CBP-TEV-protA::TRP1-KL;*	Sträßer
Prt1-TAP	as RS453; MAT a; *PRT1-CBP-TEV-protA::TRP1-KL;*	Röther
BUR1 shuffle	BY and RS; MAT a; *his3; leu2; ura3; trp1; ade2; YPR161c::kanMX4*	Hiechinger
RFA1 shuffle	BY and RS; MAT a; *ade2; his3; ura3; leu2; trp1; can1-100; GAL+;YAR007c::kanMX4*	Winkler
BUR1 RFA1 double shuffle	BY and RS; MAT α; *his3; leu2; ura3; trp1; YPR161c::kanMX4YAR007c::kanMX4* pRS316-*BUR1*; pRS316-*RFA1*	*BUR1* shuffle was mated to *RFA1* shuffle, spore Ia
BUR1 MSH6 double shuffle	BY and RS; MAT α; *his3*; *leu2*; *ura3*; *trp1*; *ade2*; *YPR161c::kanMX4*; *YDR097c::kanMX4* pRS316-*BUR1*; pRS316-*MSH6*	*BUR1* shuffle was mated to *Δmsh6* (spore IVc), spore Vb
BUR1 POL4 double shuffle	BY and RS; MAT a; *his3; leu2; ura3; trp1; ade2; YPR161c::kanMX4; YCR014c::kanMX4* pRS316-*BUR1*; pRS316-*POL4*	BUR1 shuffle was mated to *Δpol4* (spore IId), spore Ia

BUR1 RAD16 double shuffle	BY and RS; MAT α; *his3; leu2; ura3; trp1; ade2; YPR161c::kanMX4; YBR114w::kanMX4* pRS316-*BUR1*; pRS316-*RAD16*	*BUR1* shuffle was mated to *Δrad16* (spore Id), spore VIb
BUR1 RAD26 double shuffle	BY and RS453; MAT α; *his3; leu2; ura3; trp1 YJR035w::kanMX4; YPR161c::kanMX4* pRS316-*BUR1*; pRS316-*RAD26*	*BUR1* shuffle (spore Ia) was mated to *Δrad26* (spore IId), spore Ia
BUR1 RAD16 suffle *Δrad26*	BY and RS453; MAT α*; his3; leu2; ura3; trp1 YJR035w::kanMX4; YPR161c::kanMX4; YBR114w::HIS3* pRS316-*BUR1*; pRS316-*RAD16*	*rad26 KO::HIS3* (Chanarat) was integrated into *BUR1 Δrad16*
bur1-7 XRS2 shuffle	BY; MAT a; *his3; leu2; ura3; TPR1+; YDR369c::kanMX4; bur1-7::LEU2 pRS316-XRS2*	*bur1-7::LEU2* was integrated into *XRS2* shuffle (spore Ia)
BUR1 APN1 double shuffle	BY and RS; MAT a; *his3; leu2; ura3; TRP1+; YPR161c::kanMX4; YKL114c::kanMX4* pRS316-*BUR1*; pRS316-*APN1*	*BUR1* shuffle was mated to *Δapn1* (spore Ib), spore Ia
BUR1 MAG1 double shuffle	BY and RS;MAT α; *his3; leu2; ura3; trp1; YPR161c::kanMX4; YER142c::kanMX4* pRS316-*BUR1*; pRS316-*MAG1*	*BUR1* shuffle was mated to *Δmag1* (spore Id), spore VIII b
BUR1 RNR1 double shuffle	BY and RS; MAT a; *his3; leu2; ura3; trp1; ade2; YPR161c::kanMX4; YER070w::kanMX4* pRS316-*BUR1*; pRS316-*RNR1*	*BUR1* shuffle was mated to *Δrnr1* (spore IIa),spore IVb
RFA1 DST1 double shuffle	BY and RS; MAT a; *his3; leu2; ura3; trp1; YAR007c::kanMX4; YGL043w::kanMX4* pRS316-*RFA1*; pRS316-*DST1*	*RFA1* shuffle was mated to *Δdst1* (Y136), spore IVb
RFA1 RTF1 double shuffle	BY and RS; MAT a; *his3; leu2; ura3; TRP1+; YAR007c::kanMX4; YGL244w::kanMX4* pRS316-*RFA1*; pRS316-*RTF1*	*RFA1* shuffle (spore aIb) was mated to *Δrtf1* (Y110), spore IVa
HPR1 RFA1 double shuffle	W303, RS453, BY; MAT a; *ade2; his3; ura3; leu2; trp1; YAR007c::kanMX4; hpr1::HIS3* pRS316-*RFA1*; pRS316-*HPR1*	*Δhpr1* (spore VId) was mated to *RFA1* shuffle, spore IIId
MFT1 RFA1 double shuffle	W303, RS453, BY; MAT α; *ade2; his3; ura3; leu2; trp1; can1-100; mft1::kanMX4; YAR007c::kanMX4* pRS316-*RFA1*; pRS316-*MFT1*	*Δmft1* (spore Ia) was mated to *RFA1* shuffle, spore Ib
HPR1 RFA2 double shuffle	W303, RS453, BY; MAT a; *ade2; his3; ura3; leu2; trp1; can1-100; YNL312w::kanMX4; hpr1::HIS3* pRS316-*RFA2*; pRS316-*HPR1*	*Δhpr1* (spore VId) was mated to *RFA2* shuffle (spore dId), spore Id
MFT1 RFA2 double shuffle	W303, RS453, BY; MAT a; *ade2; his3; ura3; leu2; trp1; can1-100; YNL312w::kanMX; mft1::kanMX4* pRS316-*RFA2*; pRS316-*MFT1*	Sträßer
HPR1 RFA3 double shuffle	W303, RS453, BY; MAT α; *ade2; his3; ura3; leu2; trp1; can1-100; YJL173c::kanMX4; hpr1::HIS3* pRS316-*RFA3*; pRS316-*HPR1*	*Δhpr1* (spore VId) was mated to *RFA3* shuffle (spore IVb), spore Id
MFT1 RFA3 double shuffle	W303, RS453, BY; MAT α; *ade2; his3; ura3; leu2; trp1; can1-100; YJL173c::kanMX4; mft1::kanMX4* pRS316-*RFA3*; pRS316-*MFT1*	*Δmft1* (spore Ia) was mated to *RFA3* shuffle (spore IVb), spore Vb

THO2 RFA3 double shuffle	W303, RS453, BY; MAT a; *ade2; his3; ura3; leu2; trp1; can1-100; YJL173c::kanMX4; tho2::kanMX4* pRS316-*RFA3*; pRS316-*THO2*	Sträßer
THP2 RFA3 double shuffle	RS and BY; MAT a; *his3; leu2; ura3; trp1; ADE2; YJL173c::kanMX4; thp2::kanMX4* pRS316-*RFA3*; pRS316-*THP2*	Sträßer
bur1-1::LEU2	MAT a; *ade2-1; his3-11,15; ura3-52; 3,112; trp1-1; can1-100; GAL+; bur1-1::LEU2*	*bur1-1* was integrated into RS453 using the NotI, SalI fragment from pBS-*bur1-1::LEU2*
bur1-4::LEU2	MAT a; *ade2-1; his3-11,15; ura3-52; 3,112; trp1-1; can1-100; GAL+; bur1-4::LEU2*	*bur1-4* was integrated into RS453 using the NotI, SalI fragment from pBS-*bur1-4::LEU2*
bur1-7::LEU2	MAT a; *ade2-1; his3-11,15; ura3-52; 3,112; trp1-1; can1-100; GAL+; bur1-7::LEU2*	*bur1-7* was integrated into RS453 using the NotI, SalI fragment from pBS-*bur1-7::LEU2*
bur1-24::LEU2	MAT a; *ade2-1; his3-11,15; ura3-52; 3,112; trp1-1; can1-100; GAL+; bur1-7::LEU2*	*bur1-24* was integrated into RS453 using the NotI, SalI fragment from *pBS-bur1-24::LEU2*

5. Methods

5.1 Standard methods

Cloning procedures such as restriction digest, dephosphorylation of fragments, ligations, and transformation of newly generated vectors in *Escherichia coli* and separation of DNA in agarose gels were done according to Sambrook and Russell, CSHL Press, 2001. Commercial available kits were used according to manufacturer's instructions.

Amplification of yeast genes or TAP-tags was usually done in a 50-100 µl KNOP-PCR reaction using 0.5 µM primer1, 0.5 µM primer2, 0.2 mM of each dNTP, 1 x KNOP buffer (50 mM Tris-HCl, pH 9.2, 16 mM (NH4)2SO4, 2.25 mM MgCl2), 0.3 µl genomic DNA or 1 µl 1:20 diluted plasmid Midi prep and 1 µl KNOP polymerase (2U *Taq*, 0.56 U Vent). In general, the following amplification protocol was used: 2 min 94°C, [1 min 94°C, 30 s at the respective °C, 1 min / 1000 bp 68°C], 35 cycles, 10 min 68°C.

To check for the correct integration of the disruption cassette, colony PCR was performed. A 25 µl reaction was assembled, containing 1 µM primer1, 1 µM primer2, 62.5 µM of each dNTP, 750 µM MgCl2 and 1x Taq buffer (Fermentas, St. Leon-Rot). Freshly growing cells were picked with a yellow tip and added to the reaction. The PCR reaction was boiled for 15 min, before 1.5 U *Taq* polymerase (Fermentas, St. Leon-Rot) were added. Amplification was performed using the following protocol: [30 s 95°C, 30 s 45°C, 60 s 72°C] 25 cycles, 2 min 72°C.

Point mutations were inserted by quick change mutagenesis using Pfu or Pfu Turbo polymerase (Stratagene). The PCR product was then digested with 10 U *Dpn*I for 2 hours at 37°C. 50 µl of the reaction were then transformed into *E. coli* DH5α. Point mutations or plasmids were sent for sequencing to Medigenomix (Munich).

Fusion PCR for deletion mutants were also perfomed using Pfu polymerse.

5.2 Yeast-specific techniques

5.2.1 Culture of *S. cerevisiae*

Yeast strains were cultured in either full-medium or synthetic complete (SC) medium. Full-medium contained 1% yeast extract (Becton Dickinson, Heidelberg), 2% Bacto-Peptone (Becton Dickinson, Heidelberg) and either 2% glucose (YPD) or 2% galactose (YPG). Synthetic complete media contained 0.67% yeast nitrogen base

(Formedium, Norwich, UK), 0.06% complete synthetic mix (including all essential amino acids except the four amino acids used as auxotrophy markers, *i.e.* leucine, tryptophane, histidine, uracil and adenine) and either 2% glucose (SDC) or 2% galactose (SGC). 5-FOA was added to a final concentration of 0.1%.

5.2.2 Transformation of yeast cells

50 ml of yeast were grown to an optical density of 0.5 to 0.8 and harvested by centrifugation for 3 min at 3600 rpm using a Rotanda 46R centrifuge. After washing with 10 ml H2O, the pellet was resuspended in 500 µl of solution I (10 mM Tris-HCl, pH 7.5, 1 mM EDTA, 100 mM Li-acetate). After centrifugation, the pellet was resuspended in 250 µl solution I. 1 µl of Midi-prep DNA or 5 µl of Mini-Prep DNA was provided in a tube, 5 µl of single strand carrier DNA (DNA of salmon or herring testis, 2 mg/ml), 50 µl of cells in solution I and 300 µl of solution II (10 mM Tris-HCl, pH 7.5, 1 mM EDTA, 100 mM Li-acetate, 40% PEG-4000) was added and the mixture was incubated for 30 min on a turning wheel at room temperature. Transformations were then heat-shocked for 10 min at 42°C, followed by 3 min incubation on ice. 1 ml of H2O was added and centrifuged. The pellet was resuspended in 50-µl H2O and plated on selective plates. For genomic integrations of a galactose promoter, a TAP-tag or a disruption cassette, the pellets were resuspended in 1 ml YPD or YPG and incubated for 1 h at room temperature on a turning wheel prior to plating. To transform yeast cells grown on plate, 1 loop of freshly restreaked yeast cells was resuspended in 100 mM Li-acetate and vortexed. DNA, carrier DNA and solution II were added as described above. After incubation for 30 min on a turning wheel at RT, 35 µl DMSO were added prior to heat shock and transformations were then treated as described above.

5.2.3 Preparation of genomic DNA

10 ml of an overnight RS453 culture with an OD600nm > 1 were centrifuged (3 min, 3600 rpm) and washed with 10 ml H2O. The cells were resuspended in 500 µl H2O and 200 µl lysis buffer (2% Triton X-100, 1% SDS, 100 mM NaCl, 10 mM Tris-HCl, pH 8.0, 1 mM EDTA). 300 µl glass beads and 300 µl phenol:chloroform:isoamylalcohol (25:24:1) were added and the mixture was vortexed for 3 min. After a centrifugation for 10 min at 16,000 g the upper phase was removed and extracted with an equal volume of chloroform. Genomic DNA was precipitated using 1.2 ml 100% ethanol and incubation of the solution for 10 min at -

20°C. After a centrifugation for 30 min at 4°C and 16,000 g, the pellet was dried and resuspended in 400 µl TE (10 mM Tris-HCl, pH 8.0, 1 mM EDTA, pH 8.0). To destroy RNA, 20 µl RNaseA (10 mg/ml) were added and incubated for 40 min at 37°C. Genomic DNA was precipitated by addition of 40 µl 3 M Na-acetate, pH 5.2 and 800 µl 100% ethanol and incubation of the mixture for 10 min at – 20°C. After centrifugation (16,000 g, 4°C, 30 min) the pellet was washed with 80% ethanol, dried and resuspended in 30 µl TE.

5.2.4 Genomic integration of a TAP (tandem-affinity-purification) tag

The genomic integration of the TAP-tag is achieved by homologous recombination of the C-terminal region of the respective gene with a transformed PCR-product containing the TAP-tag and an auxotrophy marker. For C-terminal tagging, the 5' primer consisted of 50 nucleotides of yeast genomic sequence flanking the integration site before the stop codon plus 5'-tccatggaaaagagaag-3' (*YXZ*-oligo1), which hybridizes at the 5' end of the CBP coding sequence. The 3' primer consisted of 50 nucleotides in the 3' UTR region, 30 nt downstream of the stop codon (-30 to -80) plus 5'-tacgactcactataggg-3', which anneals downstream of the selection marker (*XYZ*-oligo2). These primers were used to amplify the TAP-tag using pBS1539 (*URA3*) or pBS1479 (*TRP1*) as template (Puig et al. 2001), following the Knop-PCR protocol. The PCR-product was then purified via phenol chloroform extraction. 100 µl PCR-product was mixed with 60 µl phenol:chloroform:isoamylalcohol (25:24:1). After 10 min centrifugation at 16,000 g, the upper phase was removed, mixed with an equal volume of chloroform and centrifuged for 5 min at 16,000 g. The upper phase was removed, mixed with 1 / 10 volume of 3 M Na-acetate and 2 volumes of 100% ethanol. After incubation for 1 h at -20°C, the DNA was precipitated and washed with 70% ethanol. The pellet was dried and resuspended in 10 µl TE. The DNA was then transformed into the yeast cells (5.2.2) to achieve integration into the genome by homologous recombination. Transformants were then tested for the presence of the tag by Western Blotting (5.13).

5.2.5 Crossings of yeast strains to test for synthetic lethality and Epistasis

Synthetic lethality can be assessed by either combining the deletion of two non-essential genes or by analyzing combinations between different allelic mutations in case of essential genes. Thus, double knockout shuffle strains of the genes of

interest needed to be created. Haploid parental strains carrying opposite mating types were mixed onto YPD plates. After several hours, the characteristic diploid cells were selected using a dissection microscope onto YPD plates. As soon as these cells formed colonies, they were first transferred to the respective plates (either YPD or SDC-ura) and on the following day transferred to a sporulation plate. On these plates, the diploid cells undergo meiosis and the genetic information is divided in four haploid spores, enclosed in a tetrad. The outer cell wall of the tetrad was destroyed by incubating 1 loop of cells in 10 µl Zymolyase 20 T (50 mg/ml, 1.2 M sorbitol, 10 mM Tris-HCl, pH 8.0, 1 mM EDTA, pH 8.0). The destruction was stopped by addition of 30 µl of 10 mM Tris-HCl, pH 8.0, 0.5 mM EDTA, and the spores could be dissected using the dissection microscope. Tetrads with 4 growing spores were then restreaked onto YPD and the respective drop-out plates. Correct double knockout strains were selected by checking for the correct 2:2 auxotrophy marker distribution. Two spores with the opposite mating type were chosen to test for synthetic lethality.

5.2.6 Dot spots and drug sensitivity

1 loop of freshly growing cells was resuspended in 1 ml water. After performing five 10-fold serial dilutions, 10-15 µl of the cell suspensions were spotted onto the corresponding plate (YPD, SDC-X with or without the addition of drugs). Plates with dot spots that were treated with DNA damage inducing agents were incubated in the dark to prevent photorepair.

5.2.7 Quantification of MMS and UV survival

Quantification of MMS and UV survival rates was tested by growing yeast cells to logarithmic phase in selective liquid medium (SDC-X), counting them and plating defined amounts onto plates. For the MMS survival rates, the liquid cultures were treated with different amounts of MMS for 30 minutes, the MMS was neutralized with sodiumthiolulfate and defined amounts of cells were plated out. For the UV survival rates, defined amounts of cells were first plated out, the plates were dried by waiting for 30-60 minutes and subsequently irradiated with defined doses of UV irradiation using a Spectroline UV crosslinker. Plates were immediately wrapped with aluminium foil and incubated in the dark for 3-4 days before counting the surviving colonies.

5.2.8 Generation of temperature sensitive alleles

20 µg of pLEU2-*RFA1* plasmid DNA was incubated in 500 µl of 2 M hydroxylamine buffer for 20 h at 55 °C. The *RFA1* shuffle strain was transformed with the mutagenized plasmid and cells were streaked on plates containing selection medium lacking leucine for 3 days at 30 °C in the dark. About 3800 single colonies were picked and streaked on 5-fluoroorotic acid-containing plates at 30 °C.
Those plates were replica plated onto YPD plates and incubated at 30°C and 37°C. One *rfa1-ts* mutant (*rfa1-249*) was derived from this screen, recovered and reintroduced into *RFA1* shuffle to verify the ts phenotype.

5.2.9 β-galactosidase reporter gene expression

Cells were grown in synthetic medium containing 2% raffinose before either 2% galactose or 2% glucose were added. Cells were harvested after 8 h of logarithmic growth, washed twice with Z-buffer, and frozen in liquid nitrogen. Cells were lysed in Z-buffer by three freeze and thaw cycles, and the hydrolysis of Onitrophenyl-galactopyranoside was assayed as described (Miller, 1972). β-galactosidase activity was calculated from six independent experiments and glucose values were substracted from the galactose values.

5.3 Cell culture

HeLa cells were maintained in DMEM high glucose (Invitrogen, Karlsruhe), supplemented with 10% fetal calf serum, 2 mM L-glutamine, 100 U/ml penicilline, 100 µg/ml streptomycine (all Invitrogen, Karlsruhe). Cells were splitted every other day to maintain a proliferating culture.
Transfections were performed using Lipofectamine 2000 as in the manufacturer's protocol.

5.4 Tandem affinity purification (TAP)

TAP allows a rapid and clean purification of native protein complexes using a combination of two different tags, Protein A and calmodulin binding protein (CBP), separated by a TEV-cleavage site.

5.4.1 Cell harvest and lysis

For purification of native protein complexes of *S. cerevisiae* (Puig et al. 2001), a 2 l culture of an optical density of 3-4 was harvested (2 min, 5000 rpm). Cells were first

washed with water, followed by a second washing step with 25 ml TAP-buffer (100 mM NaCl, 50 mM Tris-HCl, pH 7.5, 1.5 mM MgCl2, 0.15% NP-40) plus protease inhibitors (1.3 µg/ml pepstatin A, 0.28 µg/ml leupeptin, 170 µg/ml PMSF, 330 µg/ml benzamidine). Cells were then flash-frozen in liquid nitrogen. An equal volume of TAP-Buffer (containing 1 mM DTT, protease inhibitors) and a double volume of glass beads were mixed with the cells in a bead mill (Fritsch, Idar-Oberstein), and lysed by the following milling protocol: 3 x [4 min, 500 rpm, 2 min break]. The glass beads were removed and washed once with buffer, so that the lysate comprised 25 ml. After centrifugation for 10 min at 4°C and 4000 rpm (Hettich Rotanda, Germany), the supernatant was subjected to a 1 h 100,000 g ultracentrifugation at 4°C using an SW32 rotor.

The top fatty phase was removed by aspiration and the clear lysate was collected. For storage, glycerol was added to the lysate up to a final concentration of 5% and the lysate was flash-frozen in liquid nitrogen.

5.4.2 Purification and TCA precipitation

0.4 ml IgG-sepharose were washed 3 x in TAP-buffer (2 min, 1800 rpm, 4°C) and added to the lysate. After incubation for 1 h on a turning wheel at 4°C, the beads were centrifuged down and transferred to a mobicol column, containing a 35 µm filter. The beads were washed with 10 ml TAP-Buffer containing 0.5 mM DTT by gravity flow.

To cleave-off the protein complex 6 µl TEV protease were added in 150 µl TAP-buffer plus 0.5 mM DTT and incubated for 1 h 20 min on a turning wheel at 19°C. For elution, the mobicol was centrifuged in a table top centrifuge for 1 min at 2000 rpm.

During the TEV cleavage, 0.5 ml calmodulin beads were washed 3 x with TAP-buffer containing 1 mM DTT and 2 mM CaCl2. After removal of surplus buffer, the beads were incubated with 150 µl TAP-buffer containing 1 mM DTT and 2 mM $CaCl_2$ on ice. For calmodulin binding the 150 µl TEV eluate were added, incubated for 1 h on a turning wheel at 4°C and washed with 7.5 ml of TAP-buffer plus 1 mM DTT and 2 mM $CaCl_2$.

To elute the protein complex, the beads were incubated in a thermomixer at 37°C for 2 x 7.5 min in 10 mM Tris-HCl, pH 8.0 and 5 mM EGTA. The eluate was obtained by centrifugation for 1 min at 2000 rpm.

To concentrate the samples, TCA was added to a final concentration of 10% and the samples were incubated for 20 min on ice. After 20 min centrifugation at 16,000 g

and 4°C, the pellet was resuspended in 60 µl 1 x SB (62.5 mM Tris-HCl, pH 6.8, 2.3% SDS, 10% glycerol, 0.05% bromophenolblue, 25 mM DTT), the resulting solution neutralized by the addition of Tris-Base, denatured and subjected to SDS-PAGE.

5.4.3 Purification of proteins for *in vitro* kinase assays

For *in vitro* kinase assays cells from 2 l cultures of either wt or Bur1-TAP cells were lysed and the tagged protein was purified. After the IgG binding step the beads were washed with 10 ml TAP-buffer containing 1 M NaCl for the purification of the BUR complex without RPA, followed by a 5 ml wash with TAP-buffer. The BUR/RPA complex was purified as in the normal protocol. For the subsequent assays TEV eluates were used.

5.4.4 Purification of Rfa1-Flag-TEV-ProtA for peptide mapping

For peptide mapping a 2 l culture of Rfa1-Flag-TEV-ProtA cells was lysed and the tagged protein was purified in three TAP purifications (one purification according to 666 ml of cell suspension). After the IgG binding step the beads were washed with 10 ml TAP-buffer containing 1 M NaCl, followed by a 5 ml wash with standard TAP-buffer. For the assay the TEV eluate was used.

5.4.4 Purification of proteins using GFP binder

Protein purifications using GFP binder were done as described in the manufacturer's protocol, except for using TAP buffer after establishing the method.

5.5 *In vitro* kinase assay

For in vitro kinase assays 5 µl of each kinase and/or substrate were incubated in the presence of 0.5 mM ATP, 1 mM DTT, 100 mM Tris-HCl, pH 7.5, 1 mM MgCl2, 1 mM EGTA and 1 Ci [γ-32P]-ATP at 30°C for 30 min. Reactions were separated by 15% SDS-PAGE, followed by autoradiography.

5.6 Protoarrays

The Protoarray Yeast PPI Kit (Invitrogen, USA) was used as in the manufacturer's protocol except for exchanging the buffer for TAP buffer (see 5.4.1) (Bur1 kinase was inactive in the buffer coming with the kit.)

5.7 Whole cell extracts (WCE)

Analytical WCE were used to test for the correct integration of the TAP-tag. A 2 ml culture was inoculated with one loop of freshly grown cells and grown over night to saturation. Cells were harvested (3 min 3600 rpm), resuspended in 96°C 100 µl 1 x SB and vortexed with 100-µl glass beads as following: 3 x [1 min vortexing, 3 min 96°C]. After 5 min 16,000 g, 5-µl of this extract were subjected to SDS-PAGE and Western blotting and the presence of the TAP-tag was assessed using the PAP antibody.

For native WCE, cells were grown to mid-log phase and 10 OD600nm were harvested and washed with 1 ml TAP-buffer. The pellet was resuspended in an equal volume of TAP-buffer and lysed with the double volume of glass beads (4 x 2 min vortex, 2 min ice). After a low spin (3 min 1500 g, 4°C), the supernatant was centrifuged for 30 min at 16,000 g, 4°C. The protein concentration was determined using the DC Protein Assay kit (Biorad, München) and 0.2 A750 were loaded onto SDS-PAGE and subsequent Western blotting.

5.8 SDS-PAGE and Western Blotting

SDS-PAGE was performed according to Laemmli using the Mini-Protean II system (Biorad, München). Proteins were transferred onto nitrocellulose membrane using a semi-dry blotting machine (Peqlab, Erlangen). After transfer, the membrane was blocked with blocking buffer (2% milk-powder in PBS) and incubated overnight at 4°C with the first antibody dissolved in blocking buffer. Excess of first antibody was removed by washing the membrane 3 times for 15 min with blocking buffer at RT. The membrane was incubated with secondary antibodies diluted in blocking buffer for 2 h at RT. Visualization of immunodecorated proteins was performed using either an ECL-Kit (Applichem), followed by exposure of the membrane to light-sensitive films and subsequent developing using a Kodak X omat M35 developing machine, or by incubating the membrane with 0.3 mg/ml chloronaphthol, 10% methanol, 0.03% H_2O_2 in PBS. For quantification of the signal, the intensity was measured using a Fujifilm Image Reader LAS-3000 system.

5.9 Cell extracts and blots for the detection of histone modifications

Cells were inoculated from a saturated pre-cultures in the evening to have them growing logarithmically in the morning. They were at least grown from an OD_{600} of 0.1

to 0.8-1.0. Cells were harvested by centrifugation, washed with 10 ml of water, washed with water containing protease inhibitors once and transferred to a reaction tube and frozen in liquid nitrogen. The cell pellets were kept at -80°C until use. For the extracts the cell pellets were resuspended in lysis buffer (200 mM Tris-HCl pH 8.0, 320 mM ammonium-sulphate, 5 mM $MgCl_2$, 10 mM EGTA pH 8.0, 20 mM EDTA pH 8.0, 20% glycerol and freshly added 1mM DTT, 10 mM NaF, 5 mM sodium-phosphate and protease inhibitors). Lysis was performed by vortexing with 200 µl acid washed glass beads four times 2 minutes with 2 minutes breaks on ice in between. The lysate was spun down in a tabletop centrifuge for 20 min at 13000 rpm at 4°C. The supernatant was transferred to a new tube and mixed with sample buffer (62.5 mM Tris-HCl, pH 6.8, 2.3% SDS, 10% Glycerin, 0.05% bromophenol-blue, 25 mM DTT). The amount of protein was adjusted either using A280 measurement or if the mutant used had an impact on the overall levels of histone H3 by quantification of the H3 intensities by quantitative western blotting. Two fold dilutions of every sample were loaded on a 15% PAA gel with 1 mm spacer plates. Gels were run at 120 V for approximately 2 hours in SDS running buffer (15.1 g/l Tris, 72 g/l Glycin, 3.72 g/l EDTA, 5 g/l SDS) and blotted on PVDF membranes in semidry blotting buffer (5.85 g/l Tris, 9.92 g/l Glycin, 0.37 g/l SDS, 10% Methanol) at 1.5 V/cm2 for 90 minutes and blocked in 5% milk in TBS for at least one hour. Antibodies detecting histone modifications were incubated in 2.5% milk-TBS over night. Blots were then washed three times with 5% milk-TBS and the secondary antibody was incubated for 2h at RT and the membrane was washed three times for 5 min with TBST (Kizer *et al.*, 2006) before detection by X-ray film or quantification.

5.10 GST pulldown and binding assay

5.10.1 Expression and purification of Bur1 C-terminal fragments

Fragments of the Bur1 C-terminus were PCR amplified from a plasmid containing the *BUR1* ORF adding a 5' BamHI site and a 3' SalI site. The PCR products were cloned into the same sites of pGEX-4T3 to express them with a N-terminal GST tag. Those constructs were transformed into BL21 *E. coli* strains. Those strains were inoculated in 20 ml LB media and grown at 37°C until an OD_{600} of 0.5 was reached. Expression of the protein was induced by adding 0.5 mM IPTG for 4 hours at 37°C. Cells were harvested and washed once in TAP buffer with the addition of protease inhibitors and frozen in liquid nitrogen. For lysis the cells were thawed and resuspended in TAP

buffer with 0,5 mM DTT and protease inhibitors and sonified for 6 min (30% duty cycle, 10% output). The lysate was centrifuged in a SS34 rotor for 15 min at 15000 rpm. The supernatant was transferred to a 15 ml tube and incubated with 400 µl of slurry buffer equilibrated Glutathione sepharose. After an incubation of 1h at 4°C, the beads were transferred to a mobicol and washed with 50 ml TAP buffer containing 1 M NaCl and 0,5 mM DTT and with 3ml TAP buffer containing 100 mM NaCl. The settled beads were resuspended in 300 µl TAP buffer and 10 µl of those beads containing the immobilized GST-Bur1-C-terminus fragments were subjected to the binding reaction with TAP purified Rfa1.

5.10.2 Bur1-Rfa1 binding assay

The immobilized Bur1 fragments served as bait proteins for the binding assay with TAP purified Rfa1. For the assay 10 µl of slurry Glutatione beads were mixed with 50 µl of 1 M NaCl washed Rfa1-TEV eluates and 140 µl of TAP buffer. The negative controls contained either no Rfa1-TEV eluate or just expressed and immobilized GST. Binding was performed for 1 h at 4°C followed by 3 washing steps with 500 µl TAP buffer with 0.5 mM DTT and protease inhibitors. Elution was performed with 45 µl TAP buffer and 15 µl 4 x SB, boiling for 2 min at 96°C. Of this eluate 17 µl were subjected to SDS-PAGE analysis.

5.11 Genome-wide expression profiling

5.11.1 RNA isolation

For genome-wide gene expression profiling, cells were inoculated from a saturated pre-culture and grown logarithmically over night at 30°C without diluting them. MMS was added to a concentration of 0,1% for one hour to the logarithmically growing cells. For the isolation of RNA, fifteen OD_{600} of cells were harvested, washed in 1 ml of ice cold TE buffer, and resuspended in 500 µl RNA cross buffer 1 (0.3 M NaCl, 10 mM Tris pH 7.5, 1 mM EDTA, 0.2% SDS). Cells were lysed using 200 µl of acid washed glass beads, 400 µl phenole-chloroforme for RNA isolation (Roth) on a Vibrax, for 10 minutes at 4°C. The lysate was spun down 5 min at 13000 rpm at 4°C in a tabletop centrifuge. From the supernatant 400 µl were taken off and mixed with 1 ml of cold 100% ethanol. The RNA was precipitated at -20°C for 1 hour with subsequent centrifugation (15 min, 13000 rpm, 4°C). The pellet was dried for 3 minutes at 65°C and resuspended in 78 µl of DEPC-treated water with heating at

65°C for 5 minutes. The solubilised RNA was incubated with 10 µl DNaseI buffer and 10 µl DNaseI (Fermentas) and 2 µl RNasin (Promega) for 15 minutes at room temperature. The reaction was stopped by adding 11 µl 25 mM EDTA and heat inactivation of the DNaseI at 65°C for 10 minutes. The RNA concentration was determined (2 µl RNA in 98 µl water). Afterwards 45 µg of the RNA were loaded onto a Quiagen RNeasy MinElute coloumn and cleaned up according to the manufacturer's protocol. The quality of the RNA was determined by agarose gel electrophoresis and staining with ethidium bromide.

5.11.2 Microarray hybridization

Yeast RNA was hybridized to Affymetrix GeneChipYeast Genome 2.0 Arrays (Affymetrix, Santa Clara, CA) as described in the users manual (Affymetrix GeneChip Expression Analysis Technical Manual, 2005), using the GeneChip Expression 3' Amplification One-Cycle Target Labeling and Control Reagents kit. Briefly, 700 ng total RNA was reverse transcribed to cDNA using a T7-oligo (dt) primer. Following second-strand cDNA synthesis, the double-stranded cDNA was purified as a template for the subsequent in vitro transcription (IVT) reaction. Linearly amplified biotin-labeled complementary RNA (cRNA) was synthesized in the presence of a biotinylated nucleotide analogue. The labelled cRNA was purified and the quantity of each cRNA sample measured via a ND-1000 Spectrophotometer (NanoDrop Technologies). Yields were above 50 µg for all samples. 15 µg of each cRNA sample were fragmented by metal-ion catalyzed hydrolysis. cRNA fragmentation was evaluated by 4% agarose gel electrophoresis (ready-to-use gels from Invitrogen). 5 µg of the labelled and fragmented cRNA was then hybridized to the arrays at 45°C for 16 hours with constant rotational mixing at 60 rpm in a GeneChip Hybridization Oven 640 (Affymetrix, Santa Clara, CA). Washing and staining of the arrays was performed using the FS450_0003 script of the Affymetrix GeneChip Fluidics Station 450. The arrays were scanned using an Affymetrix GeneChip Scanner 3000 7G.
Biological triplicate measurements were performed for the wild-type strain, *bur1-7* and *rfa1-249*. Biological duplicate measurements were done for the *bur1-7 rfa1-249* double mutant strain, since one sample was identified to be an outlier (see below).

5.11.3 Data analysis

Raw signal intensities for each probe set as they are contained in the *.CEL* files were analyzed using PARTEK GENOMICS SUITE version 6.3 software (Partek Inc., St

Louis, MO). As part of the import process of all *.CEL* files into the software package, data was filtered by application of a modified mask-file that was based on the *s_cerevisiae.msk* file of Affymetrix. This allowed us not only to mask all the *S. pombe* probe sets that are also part of the Affymetrix GeneChipYeast Genome 2.0 Array but also to mask unspecific probe sets as well as outdated replicate probe sets of *S. cerevisiae*. The RMA (robust multiarray average) normalization method (Irizarry *et al.*, 2003) was used for RMA background correction, quantile normalization and medianpolish probe set summarization. Expression values were $\log_2$ transformed before statistical analysis.

During analysis, one *bur1-7 rfa1-249* sample was identified to be an outlier showing an unusual expression pattern with respect to all other samples. This sample was therefore excluded from the analysis. Since the microarray experiments were performed on different days, a batch effect ("scan day") could be observed via principal components analysis (PCA). This batch effect was removed by application of the "Remove Batch Effect" tool that is part of the PARTEK GENOMICS SUITE software package.

After exclusion of the outlier sample and batch-remove a 1-way ANOVA was performed, to detect genes that were differentially expressed between wild-type and mutant yeast strains. Within the ANOVA model, a linear contrast was used to compare mutant samples with baseline wild-type samples (mutant versus wild-type). The P-values of the mutant versus wild-type comparison were then corrected using a step-up false discovery rate (FDR) value of 5% (Benjamini *et al.*, 2001) to produce a list of significantly differentially expressed genes. This list of statistically significant genes was further filtered to include only genes that demonstrated two fold or greater up- or downregulation.

5.11.4 Hierarchical cluster and correlation analysis

Hierarchical cluster analysis was performed with microarray data of *bur1-7*, *rfa1-249* and *bur1-7 rfa1-249* mutant yeast strains. In total the hierarchical cluster analysis was performed for 115 significantly altered genes. Hierarchical cluster analysis was calculated using TIGR MeV application (Saeed *et al.*, 2003), choosing average linkage as the linkage method and Euclidean distance as distance metric.

Pearson's correlation was calculated in Microsoft Excel. The respective correlation coefficient (r-value) was calculated for each pair of mutant strains and was based on the respective lists of significantly altered genes.

5.11.5 Gene Ontology (GO) analysis.

Overrepresented biological processes for genes with significant expression changes were determined using the Gene Ontology Enrichment Analysis Software Toolkit (Zheng and Wang, 2008) that is based on GO database (Ashburner *et al.*, 2000) and annotation files of Affymetrix GeneChip system. Affymetrix probe set IDs served as gene identifiers. Therefore a list of Affymetrix probe set IDs of differentially expressed genes could be directly uploaded into GOEAST. Additionally this provided a list of all genes present on the Affymetrix GeneChipYeast Genome 2.0 Array as the corresponding genomic background. The statistical method used by GOEAST to identify significantly enriched GO terms (p-value < 0.05) among the given list of genes was hypergeometric test.

5.11.6 Explorative and promoter analysis

Explorative data analysis was performed with PARTEK GENOMICS SUITE software package. Genes with a fold change > 1.7 or < -1.7 and a p-value ≤ 0.05 were considered to be significantly changed. Genes with a fold change between -1.3 and 1.3 were regarded as not changed. In the resulting final gene lists, open-reading-frames (ORFs) with the associated gene title “putative protein of unknown function” were not considered in further analysis.

Promoter analysis was conducted with YEASTRACT (Yeast **S**earch for Transcriptional Regulators And Consensus Tracking; www.yeastract.com), an open-source and web-based database of regulatory associations between transcription factors (TFs) and target genes in *Saccharomyces cerevisiae (Teixeira et al., 2006)*. The “Group Genes by TF”-tool was used to reveal transcription factors that target the corresponding genes in the lists. Only documented associations with direct evidence code (most stringent search query available in that database) were considered. The “Search for Potential Transcription Factors (TFs)”-tool was applied to detect potential binding sites of Swi5 in the promoter region of the genes of interest.

6. References

Ahn, S.H., Kim, M., and Buratowski, S. (2004) Phosphorylation of serine 2 within the RNA polymerase II C-terminal domain couples transcription and 3' end processing. *Mol Cell* **13**: 67-76.

Ahn, S.H., Cheung, W.L., Hsu, J.Y., Diaz, R.L., Smith, M.M., and Allis, C.D. (2005) Sterile 20 kinase phosphorylates histone H2B at serine 10 during hydrogen peroxide-induced apoptosis in S. cerevisiae. *Cell* **120**: 25-36.

Alting-Mees, M.A., Sorge, J.A., and Short, J.M. (1992) pBluescriptII: multifunctional cloning and mapping vectors. *Methods Enzymol* **216**: 483-495.

Ashburner, M., Ball, C.A., Blake, J.A., Botstein, D., Butler, H., Cherry, J.M., Davis, A.P., Dolinski, K., Dwight, S.S., Eppig, J.T., Harris, M.A., Hill, D.P., Issel-Tarver, L., Kasarskis, A., Lewis, S., Matese, J.C., Richardson, J.E., Ringwald, M., Rubin, G.M., and Sherlock, G. (2000) Gene ontology: tool for the unification of biology. The Gene Ontology Consortium. *Nat Genet* **25**: 25-29.

Assenmacher, N., and Hopfner, K.P. (2004) MRE11/RAD50/NBS1: complex activities. *Chromosoma* **113**: 157-166.

Baumli, S., Lolli, G., Lowe, E.D., Troiani, S., Rusconi, L., Bullock, A.N., Debreczeni, J.E., Knapp, S., and Johnson, L.N. (2008) The structure of P-TEFb (CDK9/cyclin T1), its complex with flavopiridol and regulation by phosphorylation. *EMBO J* **27**: 1907-1918.

Benjamini, Y., Drai, D., Elmer, G., Kafkafi, N., and Golani, I. (2001) Controlling the false discovery rate in behavior genetics research. *Behav Brain Res* **125**: 279-284.

Bowers, J., Sokolsky, T., Quach, T., and Alani, E. (1999) A mutation in the MSH6 subunit of the Saccharomyces cerevisiae MSH2-MSH6 complex disrupts mismatch recognition. *J Biol Chem* **274**: 16115-16125.

Breeden, L.L. (2003) Periodic transcription: a cycle within a cycle. *Curr Biol* **13**: R31-38.

Briggs, S.D., Xiao, T., Sun, Z.W., Caldwell, J.A., Shabanowitz, J., Hunt, D.F., Allis, C.D., and Strahl, B.D. (2002) Gene silencing: trans-histone regulatory pathway in chromatin. *Nature* **418**: 498.

Brill, S.J., and Stillman, B. (1991) Replication factor-A from Saccharomyces cerevisiae is encoded by three essential genes coordinately expressed at S phase. *Genes Dev* **5**: 1589-1600.

Chavez, S., and Aguilera, A. (1997) The yeast HPR1 gene has a functional role in transcriptional elongation that uncovers a novel source of genome instability. *Genes Dev* **11**: 3459-3470.

Chavez, S., Beilharz, T., Rondon, A.G., Erdjument-Bromage, H., Tempst, P., Svejstrup, J.Q., Lithgow, T., and Aguilera, A. (2000) A protein complex containing Tho2, Hpr1, Mft1 and a novel protein, Thp2, connects transcription elongation with mitotic recombination in Saccharomyces cerevisiae. *EMBO J* **19**: 5824-5834.

Cho, E.J., Kobor, M.S., Kim, M., Greenblatt, J., and Buratowski, S. (2001) Opposing effects of Ctk1 kinase and Fcp1 phosphatase at Ser 2 of the RNA polymerase II C-terminal domain. *Genes Dev* **15**: 3319-3329.

Chu, Y., Sutton, A., Sternglanz, R., and Prelich, G. (2006) The BUR1 cyclin-dependent protein kinase is required for the normal pattern of histone methylation by SET2. *Mol Cell Biol* **26**: 3029-3038.

Corden, J.L. (1990) Tails of RNA polymerase II. *Trends Biochem Sci* **15**: 383-387.

Coverley, D., and Laskey, R.A. (1994) Regulation of eukaryotic DNA replication. *Annu Rev Biochem* **63**: 745-776.

Daniel, J.A., Torok, M.S., Sun, Z.W., Schieltz, D., Allis, C.D., Yates, J.R., 3rd, and Grant, P.A. (2004) Deubiquitination of histone H2B by a yeast acetyltransferase complex regulates transcription. *J Biol Chem* **279**: 1867-1871.

de la Fuente, N., Maldonado, A.M., and Portillo, F. (1997) Yeast gene YOR137c is involved in the activation of the yeast plasma membrane H+-ATPase by glucose. *FEBS Lett* **420**: 17-19.

Dehe, P.M., Pamblanco, M., Luciano, P., Lebrun, R., Moinier, D., Sendra, R., Verreault, A., Tordera, V., and Geli, V. (2005) Histone H3 lysine 4 mono-methylation does not require ubiquitination of histone H2B. *J Mol Biol* **353**: 477-484.

DeMott, M.S., Zigman, S., and Bambara, R.A. (1998) Replication protein A stimulates long patch DNA base excision repair. *J Biol Chem* **273**: 27492-27498.

Dichtl, B., Blank, D., Ohnacker, M., Friedlein, A., Roeder, D., Langen, H., and Keller, W. (2002) A role for SSU72 in balancing RNA polymerase II transcription elongation and termination. *Mol Cell* **10**: 1139-1150.

Drogen, F., O'Rourke, S.M., Stucke, V.M., Jaquenoud, M., Neiman, A.M., and Peter, M. (2000) Phosphorylation of the MEKK Ste11p by the PAK-like kinase Ste20p is required for MAP kinase signaling in vivo. *Curr Biol* **10**: 630-639.

Egloff, S., and Murphy, S. (2008) Cracking the RNA polymerase II CTD code. *Trends Genet* **24**: 280-288.

Elmayan, T., Proux, F., and Vaucheret, H. (2005) Arabidopsis RPA2: a genetic link among transcriptional gene silencing, DNA repair, and DNA replication. *Curr Biol* **15**: 1919-1925.

Erez, O., and Kahana, C. (2002) Deletions of SKY1 or PTK2 in the Saccharomyces cerevisiae trk1Deltatrk2Delta mutant cells exert dual effect on ion homeostasis. *Biochem Biophys Res Commun* **295**: 1142-1149.

Espinoza, F.H., Farrell, A., Nourse, J.L., Chamberlin, H.M., Gileadi, O., and Morgan, D.O. (1998) Cak1 is required for Kin28 phosphorylation and activation in vivo. *Mol Cell Biol* **18**: 6365-6373.

Fillingham, J., Keogh, M.C., and Krogan, N.J. (2006) GammaH2AX and its role in DNA double-strand break repair. *Biochem Cell Biol* **84**: 568-577.

Fong, N., and Bentley, D.L. (2001) Capping, splicing, and 3' processing are independently stimulated by RNA polymerase II: different functions for different segments of the CTD. *Genes Dev* **15**: 1783-1795.

Frank, R. (2002) The SPOT-synthesis technique. Synthetic peptide arrays on membrane supports--principles and applications. *J Immunol Methods* **267**: 13-26.

Fuxreiter, M., Tompa, P., and Simon, I. (2007) Local structural disorder imparts plasticity on linear motifs. *Bioinformatics* **23**: 950-956.

Gaillard, H., Wellinger, R.E., and Aguilera, A. (2007) A new connection of mRNP biogenesis and export with transcription-coupled repair. *Nucleic Acids Res* **35**: 3893-3906.

Gilmour, D.S., and Fan, R. (2008) Derailing the locomotive: transcription termination. *J Biol Chem* **283**: 661-664.

Gonzalez-Barrera, S., Prado, F., Verhage, R., Brouwer, J., and Aguilera, A. (2002) Defective nucleotide excision repair in yeast hpr1 and tho2 mutants. *Nucleic Acids Res* **30**: 2193-2201.

Guo, S., Zhang, Y., Yuan, F., Gao, Y., Gu, L., Wong, I., and Li, G.M. (2006) Regulation of replication protein A functions in DNA mismatch repair by phosphorylation. *J Biol Chem* **281**: 21607-21616.

Guzder, S.N., Sung, P., Prakash, L., and Prakash, S. (1997) Yeast Rad7-Rad16 complex, specific for the nucleotide excision repair of the nontranscribed DNA strand, is an ATP-dependent DNA damage sensor. *J Biol Chem* **272**: 21665-21668.

Hahn, S. (2004) Structure and mechanism of the RNA polymerase II transcription machinery. *Nat Struct Mol Biol* **11**: 394-403.

Hausmann, S., and Shuman, S. (2002) Characterization of the CTD phosphatase Fcp1 from fission yeast. Preferential dephosphorylation of serine 2 versus serine 5. *J Biol Chem* **277**: 21213-21220.

Heinisch, J.J., Lorberg, A., Schmitz, H.P., and Jacoby, J.J. (1999) The protein kinase C-mediated MAP kinase pathway involved in the maintenance of cellular integrity in Saccharomyces cerevisiae. *Mol Microbiol* **32**: 671-680.

Hengartner, C.J., Myer, V.E., Liao, S.M., Wilson, C.J., Koh, S.S., and Young, R.A. (1998) Temporal regulation of RNA polymerase II by Srb10 and Kin28 cyclin-dependent kinases. *Mol Cell* **2**: 43-53.

Herskowitz, I. (1995) MAP kinase pathways in yeast: for mating and more. *Cell* **80**: 187-197.

Hilpert, K., Winkler, D.F., and Hancock, R.E. (2007) Peptide arrays on cellulose support: SPOT synthesis, a time and cost efficient method for synthesis of large numbers of peptides in a parallel and addressable fashion. *Nat Protoc* **2**: 1333-1349.

Hsiang, Y.H., Hertzberg, R., Hecht, S., and Liu, L.F. (1985) Camptothecin induces protein-linked DNA breaks via mammalian DNA topoisomerase I. *J Biol Chem* **260**: 14873-14878.

Huertas, P., and Aguilera, A. (2003) Cotranscriptionally formed DNA:RNA hybrids mediate transcription elongation impairment and transcription-associated recombination. *Mol Cell* **12**: 711-721.

Iftode, C., Daniely, Y., and Borowiec, J.A. (1999) Replication protein A (RPA): the eukaryotic SSB. *Crit Rev Biochem Mol Biol* **34**: 141-180.

Irie, K., Nomoto, S., Miyajima, I., and Matsumoto, K. (1991) SGV1 encodes a CDC28/cdc2-related kinase required for a G alpha subunit-mediated adaptive response to pheromone in S. cerevisiae. *Cell* **65**: 785-795.

Irizarry, R.A., Hobbs, B., Collin, F., Beazer-Barclay, Y.D., Antonellis, K.J., Scherf, U., and Speed, T.P. (2003) Exploration, normalization, and summaries of high density oligonucleotide array probe level data. *Biostatistics* **4**: 249-264.

Jacoby, J.J., Nilius, S.M., and Heinisch, J.J. (1998) A screen for upstream components of the yeast protein kinase C signal transduction pathway identifies the product of the SLG1 gene. *Mol Gen Genet* **258**: 148-155.

Jelinsky, S.A., and Samson, L.D. (1999) Global response of Saccharomyces cerevisiae to an alkylating agent. *Proc Natl Acad Sci U S A* **96**: 1486-1491.

Jentsch, S., McGrath, J.P., and Varshavsky, A. (1987) The yeast DNA repair gene RAD6 encodes a ubiquitin-conjugating enzyme. *Nature* **329**: 131-134.

Jimeno, S., Rondon, A.G., Luna, R., and Aguilera, A. (2002) The yeast THO complex and mRNA export factors link RNA metabolism with transcription and genome instability. *EMBO J* **21**: 3526-3535.

Joshi, A.A., and Struhl, K. (2005) Eaf3 chromodomain interaction with methylated H3-K36 links histone deacetylation to Pol II elongation. *Mol Cell* **20**: 971-978.

Kadosh, D., and Struhl, K. (1997) Repression by Ume6 involves recruitment of a complex containing Sin3 corepressor and Rpd3 histone deacetylase to target promoters. *Cell* **89**: 365-371.

Kadosh, D., and Struhl, K. (1998) Targeted recruitment of the Sin3-Rpd3 histone deacetylase complex generates a highly localized domain of repressed chromatin in vivo. *Mol Cell Biol* **18**: 5121-5127.

Kapoor, A., Agarwal, M., Andreucci, A., Zheng, X., Gong, Z., Hasegawa, P.M., Bressan, R.A., and Zhu, J.K. (2005) Mutations in a conserved replication protein suppress transcriptional gene silencing in a DNA-methylation-independent manner in Arabidopsis. *Curr Biol* **15**: 1912-1918.

Keogh, M.C., Podolny, V., and Buratowski, S. (2003) Bur1 kinase is required for efficient transcription elongation by RNA polymerase II. *Mol Cell Biol* **23**: 7005-7018.

Keogh, M.C., Kurdistani, S.K., Morris, S.A., Ahn, S.H., Podolny, V., Collins, S.R., Schuldiner, M., Chin, K., Punna, T., Thompson, N.J., Boone, C., Emili, A., Weissman, J.S., Hughes, T.R., Strahl, B.D., Grunstein, M., Greenblatt, J.F., Buratowski, S., and Krogan, N.J. (2005) Cotranscriptional set2 methylation of histone H3 lysine 36 recruits a repressive Rpd3 complex. *Cell* **123**: 593-605.

Kim, E., Du, L., Bregman, D.B., and Warren, S.L. (1997) Splicing factors associate with hyperphosphorylated RNA polymerase II in the absence of pre-mRNA. *J Cell Biol* **136**: 19-28.

Kim, T., and Buratowski, S. (2007) Two Saccharomyces cerevisiae JmjC domain proteins demethylate histone H3 Lys36 in transcribed regions to promote elongation. *J Biol Chem* **282**: 20827-20835.

Kizer, K.O., Xiao, T., and Strahl, B.D. (2006) Accelerated nuclei preparation and methods for analysis of histone modifications in yeast. *Methods* **40**: 296-302.

Krishnamurthy, S., He, X., Reyes-Reyes, M., Moore, C., and Hampsey, M. (2004) Ssu72 Is an RNA polymerase II CTD phosphatase. *Mol Cell* **14**: 387-394.

Krogan, N.J., Dover, J., Wood, A., Schneider, J., Heidt, J., Boateng, M.A., Dean, K., Ryan, O.W., Golshani, A., Johnston, M., Greenblatt, J.F., and Shilatifard, A. (2003a) The Paf1 complex is required for histone H3 methylation by COMPASS and Dot1p: linking transcriptional elongation to histone methylation. *Mol Cell* **11**: 721-729.

Krogan, N.J., Kim, M., Tong, A., Golshani, A., Cagney, G., Canadien, V., Richards, D.P., Beattie, B.K., Emili, A., Boone, C., Shilatifard, A., Buratowski, S., and Greenblatt, J. (2003b) Methylation of histone H3 by Set2 in Saccharomyces cerevisiae is linked to transcriptional elongation by RNA polymerase II. *Mol Cell Biol* **23**: 4207-4218.

Krogh, B.O., and Symington, L.S. (2004) Recombination proteins in yeast. *Annu Rev Genet* **38**: 233-271.

Kung, L.A., and Snyder, M. (2006) Proteome chips for whole-organism assays. *Nat Rev Mol Cell Biol* **7**: 617-622.

Laribee, R.N., Krogan, N.J., Xiao, T., Shibata, Y., Hughes, T.R., Greenblatt, J.F., and Strahl, B.D. (2005) BUR kinase selectively regulates H3 K4 trimethylation and H2B ubiquitylation through recruitment of the PAF elongation complex. *Curr Biol* **15**: 1487-1493.

Laribee, R.N., Fuchs, S.M., and Strahl, B.D. (2007a) H2B ubiquitylation in transcriptional control: a FACT-finding mission. *Genes Dev* **21**: 737-743.

Laribee, R.N., Shibata, Y., Mersman, D.P., Collins, S.R., Kemmeren, P., Roguev, A., Weissman, J.S., Briggs, S.D., Krogan, N.J., and Strahl, B.D. (2007b)

CCR4/NOT complex associates with the proteasome and regulates histone methylation. *Proc Natl Acad Sci U S A* **104**: 5836-5841.

Leberer, E., Wu, C., Leeuw, T., Fourest-Lieuvin, A., Segall, J.E., and Thomas, D.Y. (1997) Functional characterization of the Cdc42p binding domain of yeast Ste20p protein kinase. *EMBO J* **16**: 83-97.

Li, B., Carey, M., and Workman, J.L. (2007) The role of chromatin during transcription. *Cell* **128**: 707-719.

Li, S., and Smerdon, M.J. (2002) Rpb4 and Rpb9 mediate subpathways of transcription-coupled DNA repair in Saccharomyces cerevisiae. *EMBO J* **21**: 5921-5929.

Lindstrom, D.L., and Hartzog, G.A. (2001) Genetic interactions of Spt4-Spt5 and TFIIS with the RNA polymerase II CTD and CTD modifying enzymes in Saccharomyces cerevisiae. *Genetics* **159**: 487-497.

Lisby, M., Barlow, J.H., Burgess, R.C., and Rothstein, R. (2004) Choreography of the DNA damage response: spatiotemporal relationships among checkpoint and repair proteins. *Cell* **118**: 699-713.

Luche, R.M., Smart, W.C., Marion, T., Tillman, M., Sumrada, R.A., and Cooper, T.G. (1993) Saccharomyces cerevisiae BUF protein binds to sequences participating in DNA replication in addition to those mediating transcriptional repression (URS1) and activation. *Mol Cell Biol* **13**: 5749-5761.

Malathi, K., Xiao, Y., and Mitchell, A.P. (1997) Interaction of yeast repressor-activator protein Ume6p with glycogen synthase kinase 3 homolog Rim11p. *Mol Cell Biol* **17**: 7230-7236.

Marra, G., and Schar, P. (1999) Recognition of DNA alterations by the mismatch repair system. *Biochem J* **338 (Pt 1)**: 1-13.

Marshall, N.F., Peng, J., Xie, Z., and Price, D.H. (1996) Control of RNA polymerase II elongation potential by a novel carboxyl-terminal domain kinase. *J Biol Chem* **271**: 27176-27183.

Max, T., Sogaard, M., and Svejstrup, J.Q. (2007) Hyperphosphorylation of the C-terminal repeat domain of RNA polymerase II facilitates dissociation of its complex with mediator. *J Biol Chem* **282**: 14113-14120.

McGuffin, L.J., Bryson, K., and Jones, D.T. (2000) The PSIPRED protein structure prediction server. *Bioinformatics* **16**: 404-405.

McMillan, J.N., Longtine, M.S., Sia, R.A., Theesfeld, C.L., Bardes, E.S., Pringle, J.R., and Lew, D.J. (1999) The morphogenesis checkpoint in Saccharomyces cerevisiae: cell cycle control of Swe1p degradation by Hsl1p and Hsl7p. *Mol Cell Biol* **19**: 6929-6939.

Memisoglu, A., and Samson, L. (2000) Base excision repair in yeast and mammals. *Mutat Res* **451**: 39-51.

Miller, J.H. (1972) Experiments in molecular genetics. *Cold Spring Harbor Laboratory, Cold Spring Harbor, NY,*: 352.

Mitchell, A.P., and Bowdish, K.S. (1992) Selection for early meiotic mutants in yeast. *Genetics* **131**: 65-72.

Murray, S., Udupa, R., Yao, S., Hartzog, G., and Prelich, G. (2001) Phosphorylation of the RNA polymerase II carboxy-terminal domain by the Bur1 cyclin-dependent kinase. *Mol Cell Biol* **21**: 4089-4096.

Nasmyth, K. (1996) At the heart of the budding yeast cell cycle. *Trends Genet* **12**: 405-412.

Ng, H.H., Feng, Q., Wang, H., Erdjument-Bromage, H., Tempst, P., Zhang, Y., and Struhl, K. (2002) Lysine methylation within the globular domain of histone H3

by Dot1 is important for telomeric silencing and Sir protein association. *Genes Dev* **16**: 1518-1527.

Ng, H.H., Dole, S., and Struhl, K. (2003) The Rtf1 component of the Paf1 transcriptional elongation complex is required for ubiquitination of histone H2B. *J Biol Chem* **278**: 33625-33628.

Orphanides, G., and Reinberg, D. (2002) A unified theory of gene expression. *Cell* **108**: 439-451.

Ostapenko, D., and Solomon, M.J. (2005) Phosphorylation by Cak1 regulates the C-terminal domain kinase Ctk1 in Saccharomyces cerevisiae. *Mol Cell Biol* **25**: 3906-3913.

Pei, Y., and Shuman, S. (2003) Characterization of the Schizosaccharomyces pombe Cdk9/Pch1 protein kinase: Spt5 phosphorylation, autophosphorylation, and mutational analysis. *J Biol Chem* **278**: 43346-43356.

Philip, B., and Levin, D.E. (2001) Wsc1 and Mid2 are cell surface sensors for cell wall integrity signaling that act through Rom2, a guanine nucleotide exchange factor for Rho1. *Mol Cell Biol* **21**: 271-280.

Piruat, J.I., and Aguilera, A. (1998) A novel yeast gene, THO2, is involved in RNA pol II transcription and provides new evidence for transcriptional elongation-associated recombination. *EMBO J* **17**: 4859-4872.

Pokholok, D.K., Hannett, N.M., and Young, R.A. (2002) Exchange of RNA polymerase II initiation and elongation factors during gene expression in vivo. *Mol Cell* **9**: 799-809.

Pokholok, D.K., Harbison, C.T., Levine, S., Cole, M., Hannett, N.M., Lee, T.I., Bell, G.W., Walker, K., Rolfe, P.A., Herbolsheimer, E., Zeitlinger, J., Lewitter, F., Gifford, D.K., and Young, R.A. (2005) Genome-wide map of nucleosome acetylation and methylation in yeast. *Cell* **122**: 517-527.

Prelich, G. (2002) RNA polymerase II carboxy-terminal domain kinases: emerging clues to their function. *Eukaryot Cell* **1**: 153-162.

Puig, O., Caspary, F., Rigaut, G., Rutz, B., Bouveret, E., Bragado-Nilsson, E., Wilm, M., and Seraphin, B. (2001) The tandem affinity purification (TAP) method: a general procedure of protein complex purification. *Methods* **24**: 218-229.

Robzyk, K., Recht, J., and Osley, M.A. (2000) Rad6-dependent ubiquitination of histone H2B in yeast. *Science* **287**: 501-504.

Rondon, A.G., Jimeno, S., Garcia-Rubio, M., and Aguilera, A. (2003) Molecular evidence that the eukaryotic THO/TREX complex is required for efficient transcription elongation. *J Biol Chem* **278**: 39037-39043.

Rothbauer, U., Zolghadr, K., Muyldermans, S., Schepers, A., Cardoso, M.C., and Leonhardt, H. (2008) A versatile nanotrap for biochemical and functional studies with fluorescent fusion proteins. *Mol Cell Proteomics* **7**: 282-289.

Saeed, A.I., Sharov, V., White, J., Li, J., Liang, W., Bhagabati, N., Braisted, J., Klapa, M., Currier, T., Thiagarajan, M., Sturn, A., Snuffin, M., Rezantsev, A., Popov, D., Ryltsov, A., Kostukovich, E., Borisovsky, I., Liu, Z., Vinsavich, A., Trush, V., and Quackenbush, J. (2003) TM4: a free, open-source system for microarray data management and analysis. *Biotechniques* **34**: 374-378.

Shore, S.M., Byers, S.A., Maury, W., and Price, D.H. (2003) Identification of a novel isoform of Cdk9. *Gene* **307**: 175-182.

Shrivastav, M., De Haro, L.P., and Nickoloff, J.A. (2008) Regulation of DNA double-strand break repair pathway choice. *Cell Res* **18**: 134-147.

Sikorski, R.S., and Hieter, P. (1989) A system of shuttle vectors and yeast host strains designed for efficient manipulation of DNA in Saccharomyces cerevisiae. *Genetics* **122**: 19-27.

Singh, K.K., and Samson, L. (1995) Replication protein A binds to regulatory elements in yeast DNA repair and DNA metabolism genes. *Proc Natl Acad Sci U S A* **92**: 4907-4911.

Smale, S.T., and Kadonaga, J.T. (2003) The RNA polymerase II core promoter. *Annu Rev Biochem* **72**: 449-479.

Strasser, K., and Hurt, E. (2000) Yra1p, a conserved nuclear RNA-binding protein, interacts directly with Mex67p and is required for mRNA export. *EMBO J* **19**: 410-420.

Strasser, K., Masuda, S., Mason, P., Pfannstiel, J., Oppizzi, M., Rodriguez-Navarro, S., Rondon, A.G., Aguilera, A., Struhl, K., Reed, R., and Hurt, E. (2002) TREX is a conserved complex coupling transcription with messenger RNA export. *Nature* **417**: 304-308.

Sun, Z.W., and Allis, C.D. (2002) Ubiquitination of histone H2B regulates H3 methylation and gene silencing in yeast. *Nature* **418**: 104-108.

Svejstrup, J.Q. (2004) The RNA polymerase II transcription cycle: cycling through chromatin. *Biochim Biophys Acta* **1677**: 64-73.

Swaminathan, S., Kile, A.C., MacDonald, E.M., and Koepp, D.M. (2007) Yra1 is required for S phase entry and affects Dia2 binding to replication origins. *Mol Cell Biol* **27**: 4674-4684.

Tang, C.M., Tomkinson, A.E., Lane, W.S., Wold, M.S., and Seto, E. (1996) Replication protein A is a component of a complex that binds the human metallothionein IIA gene transcription start site. *J Biol Chem* **271**: 21637-21644.

Teixeira, M.C., Monteiro, P., Jain, P., Tenreiro, S., Fernandes, A.R., Mira, N.P., Alenquer, M., Freitas, A.T., Oliveira, A.L., and Sa-Correia, I. (2006) The YEASTRACT database: a tool for the analysis of transcription regulatory associations in Saccharomyces cerevisiae. *Nucleic Acids Res* **34**: D446-451.

Teng, Y., Longhese, M., McDonough, G., and Waters, R. (1998) Mutants with changes in different domains of yeast replication protein A exhibit differences in repairing the control region, the transcribed strand and the non-transcribed strand of the Saccharomyces cerevisiae MFA2 gene. *J Mol Biol* **280**: 355-363.

Thoma, F. (1999) Light and dark in chromatin repair: repair of UV-induced DNA lesions by photolyase and nucleotide excision repair. *EMBO J* **18**: 6585-6598.

Toda, T., Cameron, S., Sass, P., Zoller, M., Scott, J.D., McMullen, B., Hurwitz, M., Krebs, E.G., and Wigler, M. (1987) Cloning and characterization of BCY1, a locus encoding a regulatory subunit of the cyclic AMP-dependent protein kinase in Saccharomyces cerevisiae. *Mol Cell Biol* **7**: 1371-1377.

Trilla, J.A., Cos, T., Duran, A., and Roncero, C. (1997) Characterization of CHS4 (CAL2), a gene of Saccharomyces cerevisiae involved in chitin biosynthesis and allelic to SKT5 and CSD4. *Yeast* **13**: 795-807.

Tseng, H.M., and Tomkinson, A.E. (2004) Processing and joining of DNA ends coordinated by interactions among Dnl4/Lif1, Pol4, and FEN-1. *J Biol Chem* **279**: 47580-47588.

Tyers, M., Tokiwa, G., and Futcher, B. (1993) Comparison of the Saccharomyces cerevisiae G1 cyclins: Cln3 may be an upstream activator of Cln1, Cln2 and other cyclins. *EMBO J* **12**: 1955-1968.

Van Dyke, M.W., Roeder, R.G., and Sawadogo, M. (1988) Physical analysis of transcription preinitiation complex assembly on a class II gene promoter. *Science* **241**: 1335-1338.

Verhage, R.A., van Gool, A.J., de Groot, N., Hoeijmakers, J.H., van de Putte, P., and Brouwer, J. (1996) Double mutants of Saccharomyces cerevisiae with

alterations in global genome and transcription-coupled repair. *Mol Cell Biol* **16**: 496-502.

Verna, J., Lodder, A., Lee, K., Vagts, A., and Ballester, R. (1997) A family of genes required for maintenance of cell wall integrity and for the stress response in Saccharomyces cerevisiae. *Proc Natl Acad Sci U S A* **94**: 13804-13809.

Wada, T., Takagi, T., Yamaguchi, Y., Watanabe, D., and Handa, H. (1998) Evidence that P-TEFb alleviates the negative effect of DSIF on RNA polymerase II-dependent transcription in vitro. *EMBO J* **17**: 7395-7403.

Wang, H., Gari, E., Verges, E., Gallego, C., and Aldea, M. (2004) Recruitment of Cdc28 by Whi3 restricts nuclear accumulation of the G1 cyclin-Cdk complex to late G1. *EMBO J* **23**: 180-190.

Weake, V.M., and Workman, J.L. (2008) Histone ubiquitination: triggering gene activity. *Mol Cell* **29**: 653-663.

Weisshart, K., Pestryakov, P., Smith, R.W., Hartmann, H., Kremmer, E., Lavrik, O., and Nasheuer, H.P. (2004) Coordinated regulation of replication protein A activities by its subunits p14 and p32. *J Biol Chem* **279**: 35368-35376.

Wold, M.S., and Kelly, T. (1988) Purification and characterization of replication protein A, a cellular protein required for in vitro replication of simian virus 40 DNA. *Proc Natl Acad Sci U S A* **85**: 2523-2527.

Wold, M.S. (1997) Replication protein A: a heterotrimeric, single-stranded DNA-binding protein required for eukaryotic DNA metabolism. *Annu Rev Biochem* **66**: 61-92.

Wood, A., Schneider, J., Dover, J., Johnston, M., and Shilatifard, A. (2003) The Paf1 complex is essential for histone monoubiquitination by the Rad6-Bre1 complex, which signals for histone methylation by COMPASS and Dot1p. *J Biol Chem* **278**: 34739-34742.

Wood, A., Schneider, J., Dover, J., Johnston, M., and Shilatifard, A. (2005) The Bur1/Bur2 complex is required for histone H2B monoubiquitination by Rad6/Bre1 and histone methylation by COMPASS. *Mol Cell* **20**: 589-599.

Woychik, N.A., and Hampsey, M. (2002) The RNA polymerase II machinery: structure illuminates function. *Cell* **108**: 453-463.

Wu, C., Leeuw, T., Leberer, E., Thomas, D.Y., and Whiteway, M. (1998) Cell cycle-and Cln2p-Cdc28p-dependent phosphorylation of the yeast Ste20p protein kinase. *J Biol Chem* **273**: 28107-28115.

Wyce, A., Xiao, T., Whelan, K.A., Kosman, C., Walter, W., Eick, D., Hughes, T.R., Krogan, N.J., Strahl, B.D., and Berger, S.L. (2007) H2B ubiquitylation acts as a barrier to Ctk1 nucleosomal recruitment prior to removal by Ubp8 within a SAGA-related complex. *Mol Cell* **27**: 275-288.

Yao, R., Zhang, Z., An, X., Bucci, B., Perlstein, D.L., Stubbe, J., and Huang, M. (2003) Subcellular localization of yeast ribonucleotide reductase regulated by the DNA replication and damage checkpoint pathways. *Proc Natl Acad Sci U S A* **100**: 6628-6633.

Yao, S., Neiman, A., and Prelich, G. (2000) BUR1 and BUR2 encode a divergent cyclin-dependent kinase-cyclin complex important for transcription in vivo. *Mol Cell Biol* **20**: 7080-7087.

Yao, S., and Prelich, G. (2002) Activation of the Bur1-Bur2 cyclin-dependent kinase complex by Cak1. *Mol Cell Biol* **22**: 6750-6758.

Yudkovsky, N., Ranish, J.A., and Hahn, S. (2000) A transcription reinitiation intermediate that is stabilized by activator. *Nature* **408**: 225-229.

Zhang, L., Schroeder, S., Fong, N., and Bentley, D.L. (2005) Altered nucleosome occupancy and histone H3K4 methylation in response to 'transcriptional stress'. *EMBO J* **24**: 2379-2390.

Zheng, Q., and Wang, X.J. (2008) GOEAST: a web-based software toolkit for Gene Ontology enrichment analysis. *Nucleic Acids Res* **36**: W358-363.

7. Abbreviations

°C	degree centigrade
5-FOA	5-Fluoroorotic acid
aa	amino acid
ATP	adenosine triphosphate
bp	basepair
d	day
Da	dalton
DNA	deoxyribonucleic acid
dNTP	deoxyribonucleosid triphosphate
E. coli	Escherichia coli
ECL	enhanced chemoluminiscence
g	gram
GFP	green fluorescence protein
GST	glutathione S-transferase
h	hours
HU	Hydroxyurea
l	litre
m	milli
M	molar
min	minute
mRNA	messenger ribonucleic acid
mRNP	messenger ribonucleoprotein
nt	nucleotide
OD	optical density
ORF	open reading frame
PAGE	polyacrylamide gelelectrophoresis
PCR	polymerase chain reaction
pH	potential of hydrogen
RNA	ribonucleic acid
rpm	revolutions per minute
RT	room temperature

SDS	sodium dodecyle sulphate
sec	second
ts	temperature sensitive
UV	ultraviolet
µ	micro

8. Acknowledgements

Many people were involved in the success of this project and I would like to thank especially…

…First of all, Katja, for giving me the opportunity to work on this challenging project, for her advice and constantly open door

…Ralf for being my “Doktorvater”, for his advises and for fruitful discussions in our seminars

…Karl-Peter for being the second examiner of my thesis and for the possibility to collaborate

…Andreas as well as Achim for their great effort in mining data in the whole genome hyperspace

… Oliver for microscopy of human cells

…Susanne und Michael for their work on the nuclear foci

…Georg Arnold for the peptide membrane

…The whole Sträßer lab, Susanne, Anja, Lina, Britta, Sittinan, Patricia, Ninda and Katharina for the nice working atmosphere and for being the best colleagues one can have.

…Susanne for her support, especially in my starting time as well as sharing “thingies”

…Anja for her help, especially teaching me the first TAP purification

…Silvia for sharing the work on Bur1 and always being in a positive and communicative mood

…Lina for her “big mouth” and constant willingness to discuss experiments and life

…Britta for her always good mood and positive approach towards life

…Sittinan for sharing scientific ideas, news about Thailand and constant sweets supply

…My students Karin, Xixi, Anian, Bijan and Barbara

…Anian for keeping me busy at Christmas time

...Barbara, for expressing vast amounts of Bur1 truncations, job opportunities and her positive and communicative mood

…The Jansen lab, Maria, Stephan, Goncalo, Tung, Heidrun, Susi, Birgit, Valerie and Hanna for being great neighbours and sharing ideas in our seminars

…Maria and Stephan for endless discussions about future careers “excellent networking skills”

…Gonçalo for his always good and funny mood and insights into the MBA world

…Christopher for his “schwummsschen” approach

…My brother Stefan for being the best brother in the world

…my beloved Katja and Julian, for their support, their patience and understanding, for simply being there, I love you.

…Finally, I want to thank my parents, for their constant help and support, especially for the time after Julian’s birth, without you this would not have been possible.

9. Publications

Röther, S.*, Clausing, E.*, Kieser, A. and Sträßer, K. (2006) Swt1, a novel yeast protein, functions in transcription, J Biol Chem **281**:36518-25
** equal contribution*

Clausing, E., Mayer, A., German, S., Lisby, M., Cramer, P., and Sträßer, K., The transcription elongation factor Bur1-2 interacts with RPA to maintain genome stability; *manuscript in preparation*

Bemeleit D., Lammens K., Clausing, E., Sträßer, K., Hopfner, KP., The structure of the Mre11-Rad50 complex;
manuscript in preparation

10. Curriculum vitae

Personal data:

Name:	Emanuel Nikolaus Clausing
Date of Birth:	March, 12th 1976
Place of Birth:	Munich, Germany
Citizenship:	German

Education

since 05/2004	Ph.D. student, Laboratory of Dr. Katja Sträßer, Gene Center, Faculty of Chemistry and Pharmacy, Ludwig-Maximilians University Munich
09/2002 – 06/2003	Diploma thesis, Laboratory of Prof. Dr. Harry MacWilliams, Department Biology II, Ludwig-Maximilians University Munich
03/2003 – 04/2003	Research stay, Laboratory of Prof. Dr. Adrian Tsang, Department of Biology, Concordia University Montréal
10/1996 – 08/2003	Study of Biology, Ludwig-Maximilians University Munich
09/1995 – 07/1996	Military service, Air Force, Germersheim and Erding
1995	„Abitur“
09/1986 – 07/1995	Gymnasium Ottobrunn